

AD

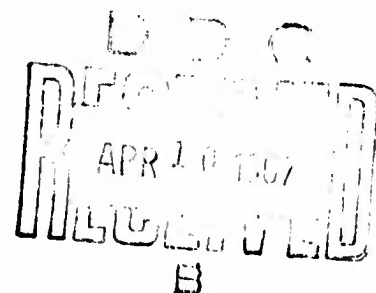
USAAVLABS TECHNICAL REPORT 66-65

AN EXPERIMENTAL INVESTIGATION OF THE EFFECT OF FORWARD AND REARWARD MOTION ON THE THRUST OF A SHROUDED PROPELLER

By

Joe F. Thompson, Jr.

September 1966



**U. S. ARMY AVIATION MATERIEL LABORATORIES
FORT EUSTIS, VIRGINIA**

**CONTRACT DA 44-177-AMC-892(T)
MISSISSIPPI STATE UNIVERSITY
STATE COLLEGE, MISSISSIPPI**

*Distribution of this
document is unlimited*



ARCHIVE COPY

Disclaimers

The findings in this report are not to be construed as an official Department of the Army position unless so designated by other authorized documents.

When Government drawings, specifications, or other data are used for any purpose other than in connection with a definitely related Government procurement operation, the United States Government thereby incurs no responsibility nor any obligation whatsoever; and the fact that the Government may have formulated, furnished, or in any way supplied the said drawings, specifications, or other data is not to be regarded by implication or otherwise as in any manner licensing the holder or any other person or corporation, or conveying any rights or permission, to manufacture, use, or sell any patented invention that may in any way be related thereto.

Disposition Instructions

Destroy this report when no longer needed. Do not return it to originator.

ACCESSION for	
CFSTI	WHITE SECTION <input checked="" type="checkbox"/>
DDC	BUFF SECTION <input type="checkbox"/>
UNANNOUNCED	<input type="checkbox"/>
JUSTIFICATION	
BY	
DISTRIBUTION/AVAILABILITY CODES	
DIST.	AVAIL. and/or SPECIAL
1	



DEPARTMENT OF THE ARMY
U S ARMY AVIATION MATERIEL LABORATORIES
FORT EUSTIS, VIRGINIA 23604

This report has been reviewed by this command and is considered to be technically sound. It is published for the exchange of information and the stimulation of ideas.

Task 1P125901A14203
Contract DA 44-177-AMC-892(T)
USAAVLABS Technical Report 66-65
September 1966

AN EXPERIMENTAL INVESTIGATION OF THE EFFECT
OF FORWARD AND REARWARD MOTION ON THE THRUST OF A SHROUDED PROPELLER

Aerophysics Research Report No. 65

by

Joe F. Thompson, Jr.

Prepared by

The Aerophysics Department
Mississippi State University
State College, Mississippi

for

U. S. ARMY AVIATION MATERIEL LABORATORIES
FORT EUSTIS, VIRGINIA

Distribution of this document is unlimited

ABSTRACT

Experimental evidence of the existence of a stagnation line between the leading and trailing edges on the outer surface of the shroud of a shrouded propeller in the static condition, in rearward motion, and in forward motion is presented. This stagnation line on the outer surface, which is a result of viscous interaction between the propeller slipstream and the external flow, causes a reduction in shroud circulation below that calculated by distributed singularities methods which assume a stagnation line at the trailing edge only. Shroud thrust decreases as the distance between this stagnation line and the trailing edge increases. It is shown that in rearward motion, such as is the case for a VTOL aircraft landing, the stagnation line moves forward from the vicinity of the trailing edge to the vicinity of the leading edge as vehicle speed increases. This forward movement of the stagnation line results in a significant loss in thrust, which can be correlated with the stagnation line location. Shroud pressure distribution, stagnation line location, and shroud thrust are presented for all three cases of motion at several propeller pitch angles, propeller rotational speeds, and vehicle linear speeds. It is shown that the flow pattern about the shroud is rather complicated in rearward motion, involving two coaxial ring-vortices surrounding the shroud.

CONTENTS

	<u>Page</u>
ABSTRACT -----	iii
LIST OF ILLUSTRATIONS -----	vi
LIST OF SYMBOLS -----	viii
INTRODUCTION -----	1
TEST PROCEDURE -----	2
STATIC -----	2
REARWARD MOTION -----	3
FORWARD MOTION -----	3
TEST RESULTS -----	4
STATIC -----	4
REARWARD MOTION -----	4
FORWARD MOTION -----	7
CONCLUSIONS -----	9
BIBLIOGRAPHY -----	84
DISTRIBUTION -----	85

ILLUSTRATIONS

<u>Figure</u>		<u>Page</u>
1	Inviscid Flow Pattern - Static Condition -----	11
2	Actual Flow Pattern - Static Condition -----	11
3	Static Test Apparatus -----	12
4	Shroud Coordinates -----	13
5	Rearward Motion Test Apparatus -----	14
6	Wire Tuft Assembly Used in Both Rearward and Forward Tests -----	15
7	Forward Motion Test Apparatus -----	15
8	Shroud Pressure Distributions - Static Condition ---	16
9	Static Thrust Division -----	21
10	Tuft Patterns - Static Condition -----	22
11	Stagnation Line Location - Static Condition -----	24
12	Shroud Pressure Distributions - Rearward Motion ----	25
13	Pressure Distribution Types - Rearward Motion -----	36
14	Tuft Patterns - Rearward Motion -----	37
15	Flow Patterns - Rearward Motion -----	53
16	Shroud Thrust - Rearward Motion -----	56
17	Stagnation Line Location - Rearward Motion -----	57
18	Relation of Shroud Thrust to Stagnation Line Location -----	58
19	Shroud Pressure Distributions - Forward Motion -----	59
20	Tuft Patterns - Forward Motion -----	65
21	Flow Patterns - Forward Motion -----	80

<u>Figure</u>		<u>Page</u>
22	Shroud Thrust - Forward Motion -----	81
23	Stagnation Line Location - Forward Motion -----	82

SYMBOLS

c	shroud chord
C_p	pressure coefficient, $P - P_o / \rho \omega^2 D^2$
C_T	thrust coefficient, $T / \rho \omega^2 D^4$
D	propeller diameter
J	advance ratio, $2V_o / \omega D$
p	static pressure
T	thrust
V	vehicle linear speed where $V_1 < V_2 < V_3 < V_4$, etc.
x	distance along chord from leading edge
$(\frac{x}{c})_{SL}$	stagnation line location
y	distance perpendicular to chord
ρ	air density
ω	propeller rotational speed

Subscripts

o	refers to free-stream conditions
s	refers to shroud
SL	refers to stagnation line

INTRODUCTION

The shrouded propeller has received much attention over the past few years and is now in application on several experimental aircraft (the XAZ-1 and XV-11A of Mississippi State University, for instance, Reference 5). Although many investigations have been directed toward determining the thrust and overall performance characteristics of shrouded propellers, only little consideration has been given to determining the flow pattern about the shroud.

Shroud thrust calculations can be performed by the method of distributed singularities (References 1-4), which assumes a stagnation line at the trailing edge (satisfying the Kutta condition) but no stagnation line between the leading and trailing edges. In reality, viscous interaction of the propeller slipstream with the external flow alters this simple flow pattern so that, in addition to the stagnation line at the trailing edge, a stagnation line exists on the outer surface of the shroud, forward of the trailing edge. For instance, in the static condition the inviscid flow pattern shown in Figure 1 is altered by slipstream interaction, so that the actual flow pattern is that shown in Figure 2. Inviscid flow theory would have the two stagnation lines coinciding at the trailing edge. This forward movement of one stagnation line reduced the circulation about the shroud below that which would be calculated by the distributed singularities method. Thus, the shroud thrust will be less than the theoretical value, the reduction being a function of the distance between the outer surface stagnation line and the trailing edge, since this distance is zero if both stagnation lines coincide at the trailing edge as is assumed when viscous slipstream interaction is neglected.

Therefore, an investigation was undertaken to determine the flow pattern and pressure distribution about the shroud of a shrouded propeller in the static condition, in rearward motion, and in forward motion. The case of rearward motion was of special interest because of the recent application of shrouded propellers on VTOL aircraft.

TEST PROCEDURE

STATIC

For static testing, the shrouded propeller was mounted on a propeller test stand as shown in Figure 3. Testing was done in a large room in front of a door open to the outside in order to keep recirculation to a minimum. Power was supplied by a 10-horsepower electric motor. The rotational speed of the propeller was measured with a stroboscopic tachometer.

Both the propeller and the shroud were made of fiber glass. The propeller was of constant chord and untwisted. The shroud coordinates are given in Figure 4. The angle between the shroud chord and the axis of the system was 1 degree 10 minutes. The dimensions of the propeller and shroud were as follows:

propeller diameter	26.50 in.
propeller chord	2.00 in.
shroud mean diameter	30.15 in.
shroud chord	12.56 in.
shroud thickness	2.06 in.

The pressure measuring system is shown in Figure 3. Static pressure on the inside surface of the shroud was measured through 12 pressure taps in the shroud, flush with the surface. The static pressure on the outside surface of the shroud was measured through a 10-tube belt stretched over the surface. Pressure tap locations are shown in Figure 4. Total pressure behind the propeller was measured through a vertical 10-tube rake. The readings of all pressures were recorded simultaneously by a photomanometer.

The outside surface of the shroud was tufted in order to determine the location of the stagnation line. The tufts were placed 1 inch apart in lines parallel to the system axis. Adjacent lines were 2 inches apart and were displaced $\frac{1}{2}$ inch relative to each other along the chord. All tufts were 1 inch long except the rearmost ones, which were shortened so that none extended past the trailing edge of the shroud. The tufts were photographed by a remotely controlled camera mounted above the shroud, as shown in Figure 3.

In the static case, measurements were taken at four propeller rotational speeds (3500, 4000, 4500, 5000 rpm) at each of four propeller

pitch angles (5° , 10° , 15° , 20°). Measurements at a pitch angle of 25° were taken at 3500 and 4000 rpm. Four readings were taken at each setting in the interest of repeatability.

REARWARD MOTION

The entire propeller test stand used in the static testing was mounted on an automobile chassis, facing aft as shown in Figure 5. Electric power was supplied to the motor by a 10-kilowatt generator. The pressure measuring system and the shroud tuft system were the same as in the static testing.

Additional tufts on wires extending above the shroud (Figure 6) were added for both the rearward and forward motion testing. The tufts on the wires were 1 inch long and were $3/4$ inch apart. Three tuft wires were used, one 3 inches ahead of the shroud leading edge, one at the half-chord location, and the third 4 inches aft of the trailing edge. All the wires intersected the system axis and were in vertical planes perpendicular to the axis. The center wire was vertical, while the others were inclined at about 10° angles on either side to eliminate interference among the wires. The wire tufts were photographed by a camera mounted to one side of the shroud.

Testing was done only on still days to eliminate the effects of crosswinds. Measurements were taken at three propeller rotational speeds (4000, 4500, 5000 rpm) at each of three propeller pitch angles (5° , 10° , 15°) at each of five speeds (5, 10, 15, 20, 30 mph). Measurements at a pitch angle of 20° were taken at 4000 rpm at all five speeds. Again, four readings were taken at each setting.

FORWARD MOTION

Again, the entire propeller test stand was mounted on the automobile chassis, but facing forward as shown in Figure 7. The pressure measuring system and the tuft system were the same as in the rearward motion testing. Measurements were taken at two propeller rotational speeds (4000, 5000 rpm) at each of three propeller pitch angles (5° , 10° , 15°) at each of five speeds (5, 10, 15, 20, 30 mph). Measurements at a pitch angle of 20° were taken at 4000 rpm at all five speeds. Again, four readings were taken at each setting.

TEST RESULTS

STATIC

The shroud pressure distributions are shown in Figures 8a-8d. The pressure distributions at all propeller pitch angles and rotational speeds are similar in shape but differ in relative magnitudes. The static thrust division is shown as a function of the total static thrust coefficient in Figure 9. The points for all rotational speeds except the lowest, 3500 rpm, are well correlated on a single curve which levels off just above 0.5. Since this shroud does exhibit a reasonably high thrust, it was considered to be a good choice on which to evaluate the thrust reduction and flow pattern as influenced by the movement of the stagnation line.

Typical shroud tuft pictures are shown in Figure 10. The leading edge (0.0-chord position) of the shroud is at the top in these pictures. The left number is the pitch angle, and the one on the right is the propeller rotational speed in rpm. The positions of the tufts indicate that there definitely is a stagnation line forward of the trailing edge. The location of this stagnation line is shown by the white line drawn on the photographs. Since fluctuations in the flow made the stagnation lines somewhat irregular in some cases, the locations used in data correlation were averages over all tufts on the four pictures taken in each case.

Figure 11 shows the stagnation line location as a function of the shroud thrust coefficient. It can be seen that an increase in shroud thrust corresponds to a movement of the stagnation line back toward the trailing edge. Thus, in the static case the thrust decreases as the distance between this stagnation line and the trailing edge increases. At 5° pitch angle, the stagnation line is located fairly far forward, around the three-quarter-chord position. As the shroud circulation increases, either because of pitch angle increase or rotational speed increase, the stagnation line moves toward the trailing edge, rapidly at first and then more slowly, approaching a chord fraction between 0.90 and 0.92. Although there is some irregularity due to the flow fluctuations, the curves are of the same general shape for all rotational speeds.

REARWARD MOTION

In rearward motion, essentially three types of shroud pressure distribution (Figures 12a-12r) were observed, as sketched in Figure 13. Type A, occurring at the higher circulations and lower speeds, is the same type of pressure distribution observed in the static case. Type B, occurring at intermediate circulations and speeds, is characterized by

the occurrence of positive values of the pressure coefficient on the inner shroud surface and one intersection in the curve. Type C, at lower circulations and higher speeds, exhibits two intersections, with lower pressure on the outer surface over most of the shroud. The transition from Type A to Type B is much more sudden than that from B to C. In some cases, two types of pressure distribution were observed at the same pitch angle, rotational speed, and vehicle linear speed (Figures 12c, e, f, g, i, m, and n, on which the heavier line indicates the more probable pressure distribution in each case). Thus, the occurrence of a particular type of pressure distribution seems to be a question of stability.

The tufts on the surface of the shroud and on the wires above, in front of, and behind the shroud are shown in Figure 14. The surface tuft pictures were taken first, with the wires removed; then the wire tuft pictures were taken. This was necessary since the center wire was held in place by two wires running to the sides over the shroud surface (Figures 6, 14). These side wires caused interference with the tufts on the shroud surface, as can be seen in several of the photographs in Figure 14. Consequently, the surface tufts that appear in the wire tuft pictures are not of interest and should be disregarded.

In these pictures, the direction of motion of the vehicle is indicated by an arrow. The normal "leading edge" (0.0-chord position) of the shroud is at the top of the surface tuft pictures and on the right in the wire tuft pictures. In rearward motion, this actually was the trailing edge, of course. The pitch angle is given by the number on the left in each picture, the vehicle linear speed in mph by the center number, and the propeller rotational speed in rpm by the number on the right.

The smooth flow indicated by the tufts on the shroud surface and on the wires in the pictures marked "No Prop" (taken with the propeller still) is clear evidence as to the lack of interference effects from the propeller test stand and other associated apparatus on the vehicle. Again, the positions of the surface tufts clearly indicate the presence of a stagnation line between the leading and trailing edges. The location of this stagnation line is shown by the white line drawn on the photographs. Of particular interest is the considerable region of flow above the shroud in the direction of vehicle motion, which is evident from the wire tufts in some of the pictures. The existence of such a large region of flow opposite in direction to the prevailing free-stream flow is somewhat surprising and is a clear indication of the complicated flow pattern caused by viscous slipstream interaction.

The flow patterns about the shroud, as indicated by the wire tufts, are drawn in Figures 15a-15c. At all speeds, the shroud is surrounded by a ring vortex which encloses another ring vortex on the outer surface of the shroud. For the sake of brevity, the 0.0-chord position will be referred to as the leading edge, and the 1.0-chord position as the trailing edge in both rearward and forward motion, even though in the rearward case these terms are misnomers. The transition of flow patterns proceeds as follows:

(1) (Figure 15a). At low speed, the enclosed vortex on the outer surface is located near the trailing edge and is very small. This condition results in a stagnation line located at high chord position. The flow turns sharply around the leading edge of the shroud, which causes a low pressure peak near the leading edge and results in a pressure distribution of Type A, similar to that of the static condition.

(2) (Figure 15a). As speed increases, the enclosed vortex grows, and the stagnation line moves toward lower chord positions. The pressure distribution remains of Type A, but the low pressure peak decreases, since the turn about the leading edge is more gradual.

(3) (Figure 15b). When the stagnation line nears the leading edge, the enclosed vortex has become quite large. The turn around the leading edge is very gradual, so that the low pressure peak has disappeared. The increase in pressure across the propeller now results in positive pressure coefficients on the inner surface near the trailing edge, since the pressure upstream of the propeller has increased. This results in a pressure distribution of Type B.

(4) (Figure 15b). Further increase in speed causes the enclosed vortex to be inclined rearward, with a small stagnation line movement toward larger chord positions. The increased velocity on the outer surface causes the pressure on the outer surface to decrease. However, the lowest pressures still occur near the leading edge on the inner surface, so that the pressure distribution is still of Type B.

(5) (Figure 15c). Still further speed increase causes the inclination of the enclosed vortex to increase, so that it becomes pressed down on the outer surface of the shroud. This increased velocity on the outer surface of the shroud results in lower pressures on the outer surface than on the inner. The stagnation line reverses directions again and moves toward the leading edge as the vortex is pressed down on the surface.

The flow pattern and pressure distribution type at each pitch angle, rotational speed, and vehicle linear speed are given in the table on page 83. Not all of these types of flow patterns were observed at each pitch angle. The transition, however, is the same, regardless of where it starts or ends. As shroud circulation increases, through an increase either in pitch angle or in rotational speed, the pressure distribution types move toward the Type A end of the sequence.

In Figure 16, the shroud thrust coefficient is plotted against the advance ratio, with the pressure distribution type given for each point. The points are well correlated by one curve for each pitch angle. Although several points fall off the curves, most of these points represent pressure distributions of types not consistent with those of neighboring points on the curves. This results from the above-mentioned temporary occurrence of

pressure distributions of a type not the most stable at the particular values of pitch angle, propeller rotational speed, and vehicle linear speed. The shape of the lines at high advance ratio is questionable because of the scarcity of points in that region.

It is again evident that a movement of the stagnation line away from the trailing edge results in a loss in thrust. The stagnation line location is plotted in Figure 17 as a function of advance ratio. As mentioned above, the trend is for the stagnation line to move toward the leading edge as J increases. Upon reaching the vicinity of the leading edge, the motion of the stagnation line is reversed, and it moves toward higher chord positions as J increases. Still further increase in J causes another reversal and movement toward the leading edge.

The correlation between stagnation line location and thrust loss is made even stronger by the fact that for 5° and 10° pitch angles the thrust coefficient passes through a minimum and then increases with advance ratio at the higher advance ratios. Figure 17 shows that for these pitch angles the stagnation line moves forward from the trailing edge as advance ratio increases, but then reverses its motion and moves back toward the trailing edge at the higher advance ratios. This reversal of motion and subsequent rearward movement at the higher advance ratios cause the thrust coefficient to pass through a minimum and then to increase as the stagnation line moves back toward the trailing edge. At higher pitch angles the reversal of motion of the stagnation line is slight or nonexistent for the range of advance ratios considered, so that no minimum occurs in the thrust coefficient curves. Figure 18 shows a correlation of shroud thrust coefficient with stagnation line location. Again, it is possible to draw one line for each pitch angle. However, in this case, errors in measurement of stagnation line location compound errors in measurement of thrust to produce more scatter.

FORWARD MOTION

Shroud pressure distributions for forward motion are shown in Figures 19a-19j. In contrast to the case of rearward motion, the shroud pressure distributions for forward motion do not exhibit any distinctive types which can be classified. As a consequence, the occurrence of two different pressure distributions at the same pitch angle, propeller rotational speed, and vehicle linear speed was never observed in forward motion.

Figure 20 shows the tufts on the surface of the shroud and on the wires above, in front of, and behind the shroud. Again, the surface tuft pictures were taken first, with the wires removed to eliminate interference from the side wires crossing over the shroud surface. Also, the surface tufts appearing in the wire tuft pictures were subject to interference from these side wires and should again be disregarded. An

arrow is used to indicate the direction of vehicle motion. As before, the number on the left is the pitch angle; the one in the center is the vehicle linear speed in mph; and the right-hand number is the propeller rotational speed in rpm.

In forward motion, the wire tufts are never seen aligned opposite to the direction of vehicle motion, as they were just above the shroud in rearward motion. Thus, the flow pattern about the shroud in forward motion is much more simple, with no ring vortices involved. Flow patterns are drawn in Figure 21. Even at low speeds, the stagnation line is located forward of the quarter-chord point, which yields a flow pattern as shown in Figure 21a. Large increases in speed cause the stagnation line to move to the leading edge, with a flow pattern as in Figure 21b. As speed is further increased, leading edge separation and reattachment occur on the outer surface. The speed at which separation occurs is lower at the lower circulations.

Figure 22 is a plot of shroud thrust coefficient against advance ratio. Again, the points are correlated by one curve for each pitch angle, although there is some scatter. The stagnation line location is plotted in Figure 23 as a function of advance ratio. It should be noted that here the initial forward movement of the stagnation line is the same for all propeller rotational speeds, while in the case of rearward motion this initial forward movement decreases as rotational speed increases. The stagnation line moves rapidly forward toward the leading edge with the initial increase in advance ratio. It then continues to approach the leading edge, but more slowly. After the stagnation line reaches the leading edge, leading edge separation occurs with further increase in advance ratio. Thus, the low points at high advance ratio and low circulation do not represent the location of the above-mentioned stagnation line, which is still at the leading edge, but rather the location of the reattachment after the leading edge separation bubble.

No meaningful correlation can be drawn between thrust loss and the distance between the stagnation line and the trailing edge in forward motion, since the initial forward movement of the stagnation line is so rapid that, for any forward speed above 5 mph, the stagnation line is located within a narrow region near the leading edge.

CONCLUSIONS

Viscous interaction of the propeller slipstream with the external flow does indeed cause a stagnation line to be located on the outer surface of the shroud of a shrouded propeller, as well as at the trailing edge. The forward movement of this stagnation line causes a reduction in circulation about the shroud and, consequently, in shroud thrust. Furthermore, the existence of this stagnation line on the outer surface of the shroud means that the actual thrust will be less than that calculated by the distributed singularities method.

In the static condition, this stagnation line is located aft of the three-quarter-chord position. Increases in propeller pitch angle and/or rotational speed cause the stagnation line to move rearward to the vicinity of the 0.9-chord position.

In rearward motion, the stagnation line moves forward from a chord fraction of about 0.9 in the static condition to the vicinity of the leading edge as the advance ratio increases. This forward movement of the stagnation line results in a significant decrease in shroud thrust, and it is possible to correlate this thrust loss with stagnation line location. This correlation is sustained by the fact that at the lower pitch angles the stagnation line reverses itself after nearing the leading edge and then moves back toward the trailing edge at the higher advance ratios. This reverse and subsequent rearward movement results in a minimum in the thrust coefficient versus advance ratio curve, followed by an increase in the thrust coefficient. No such minimum was observed at the higher pitch angles, where no reversal of stagnation line motion occurred.

In forward motion, the stagnation line moves forward very rapidly from the 0.9-chord position to the immediate vicinity of the leading edge. No reversal of stagnation line motion was observed. The arrival of the stagnation line at the leading edge is followed by leading edge separation. The suddenness of the forward movement of the stagnation line precludes a correlation with thrust loss in forward motion, although the shroud thrust does decrease as the stagnation line moves forward.

The flow pattern in rearward motion consists of two coaxial ring vortices, one located on the outer surface of the shroud, and the other surrounding both the first vortex and the shroud. This complicated flow pattern results in essentially three types of pressure distribution. Although these types are not completely distinct from each other, the particular type existing under a given set of conditions is a question of stability. In some cases, two types were observed at the same pitch angle, propeller rotational speed, and vehicle linear speed. In forward motion and in the static condition, the flow pattern is much simpler with no vortices. The occurrence of two different pressure distributions at the same pitch angle, rotational speed, and vehicle linear speed was

never observed in forward motion. Leading edge separation was observed at low circulation and high speed.

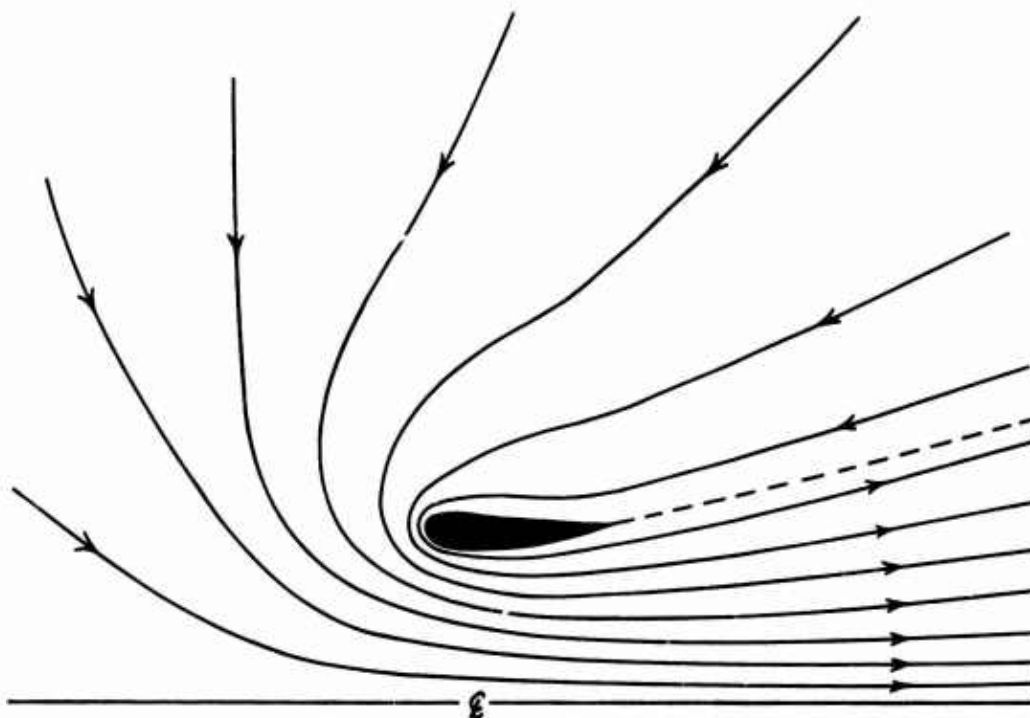


Figure 1. Inviscid Flow Pattern - Static Condition.

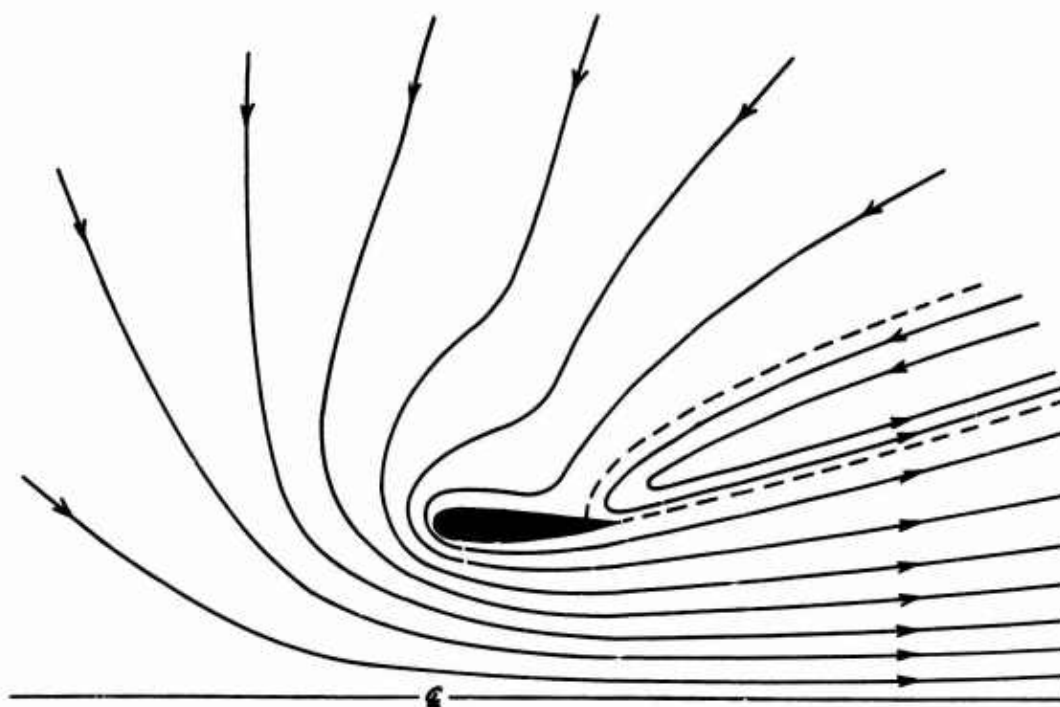


Figure 2. Actual Flow Pattern - Static Condition.

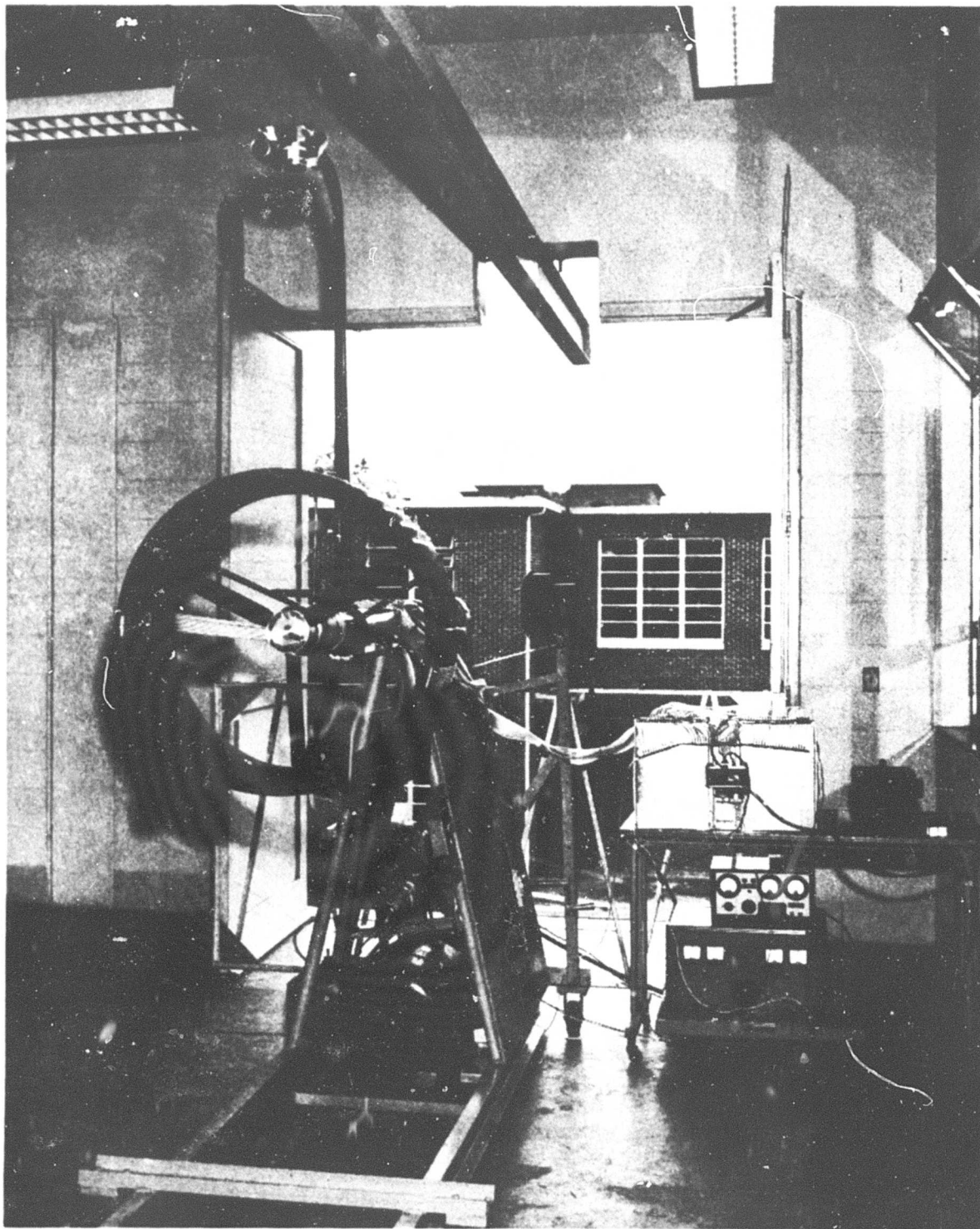
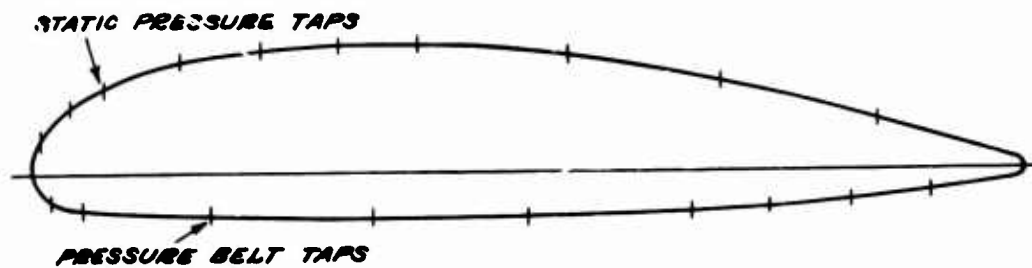


Figure 3. Static Test Apparatus.



INNER SURFACE		OUTER SURFACE	
$\frac{x}{c}$	$\frac{y}{c}$	$\frac{x}{c}$	$\frac{y}{c}$
0	0	0	0
0.015	0.0358	0.016	-0.0245
0.045	0.0605	0.050	-0.0312
0.081	0.0784	0.181	-0.0378
0.159	0.1009	0.340	-0.0414
0.236	0.1142	0.502	-0.0406
0.314	0.1198	0.663	-0.0350
0.392	0.1226	0.741	-0.0312
0.549	0.1094	0.825	-0.0245
0.700	0.0822	0.906	-0.0171
0.859	0.0434		
0.999	0.0076		

Figure 4. Shroud Coordinates.

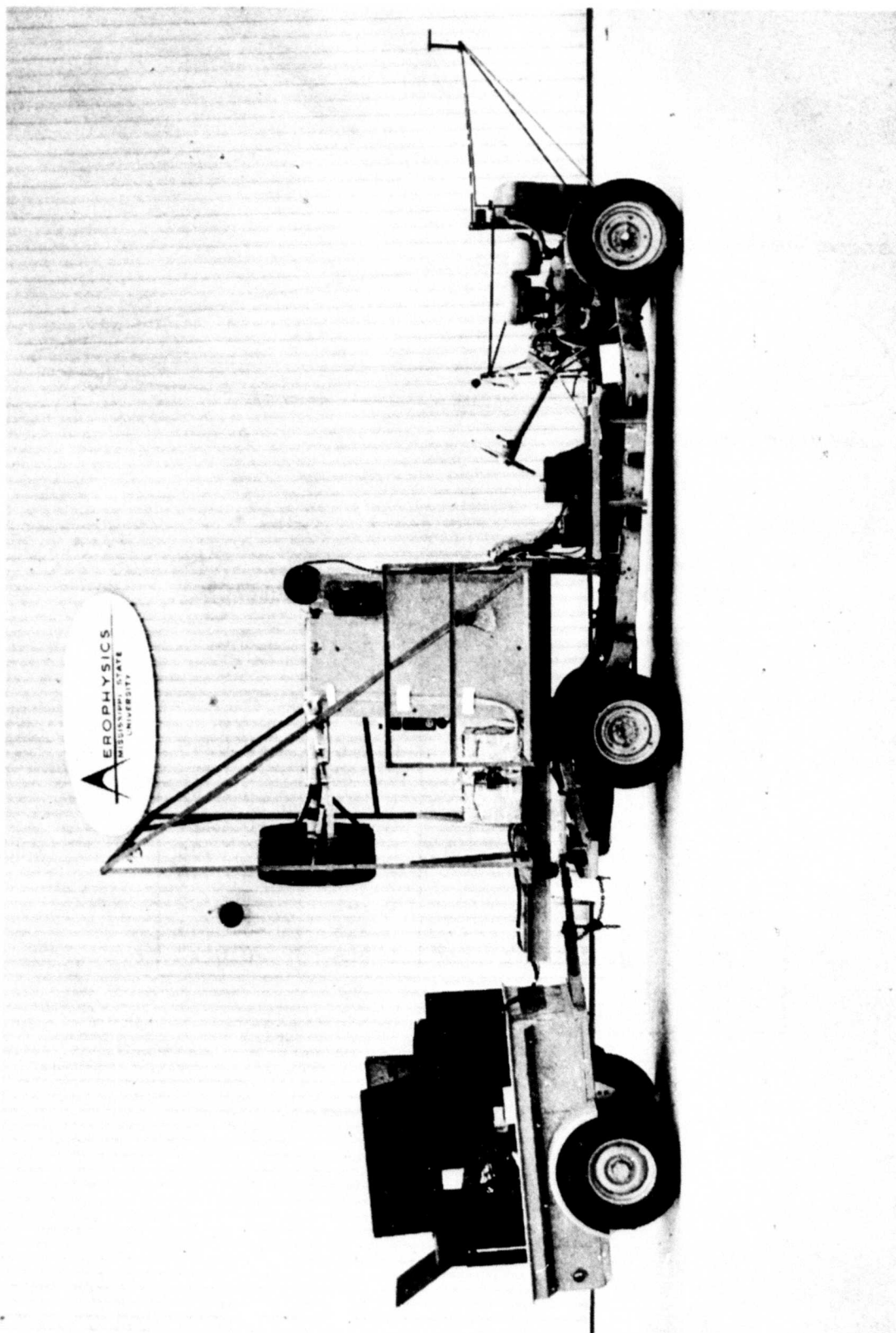


Figure 5. Rearward Motion Test Apparatus.

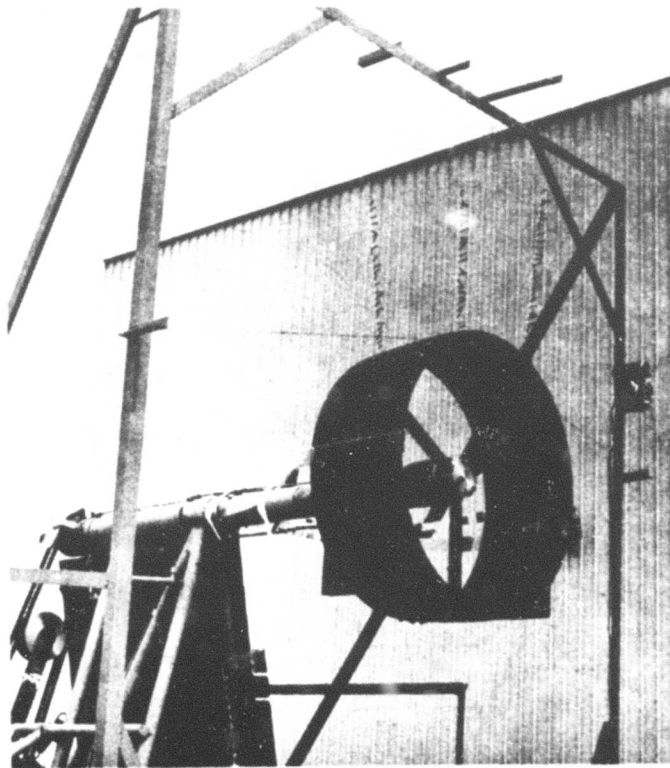


Figure 6. Wire Tuft Assembly Used in Both Rearward and Forward Tests.

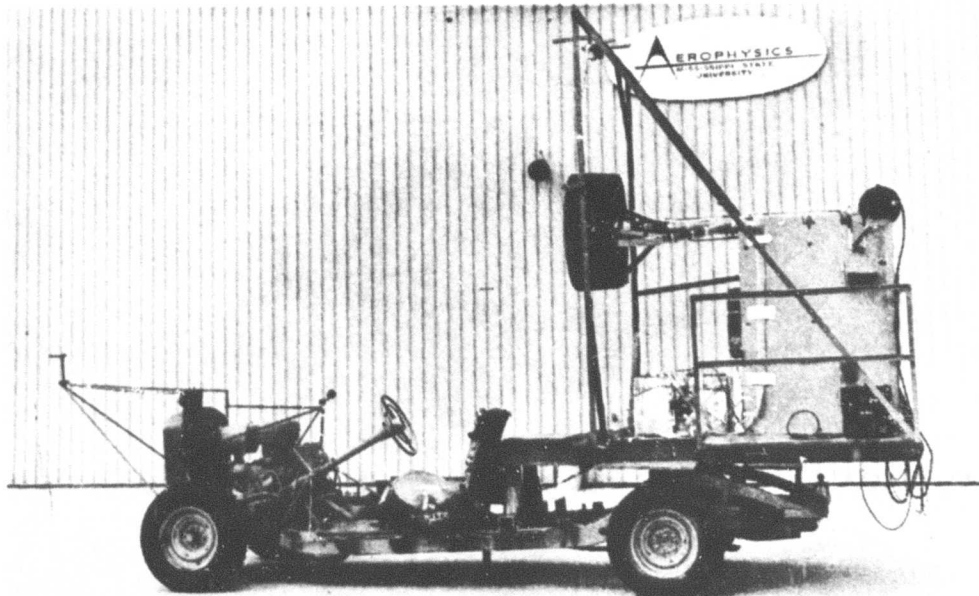








Figure 7. Forward Motion Test Apparatus.

Figure 8 (a-d). Shroud Pressure Distributions - Static Condition.

Legend:

	5° pitch angle
	10° pitch angle
	15° pitch angle
	20° pitch angle
	25° pitch angle
	curves which correspond to inside surface of shroud

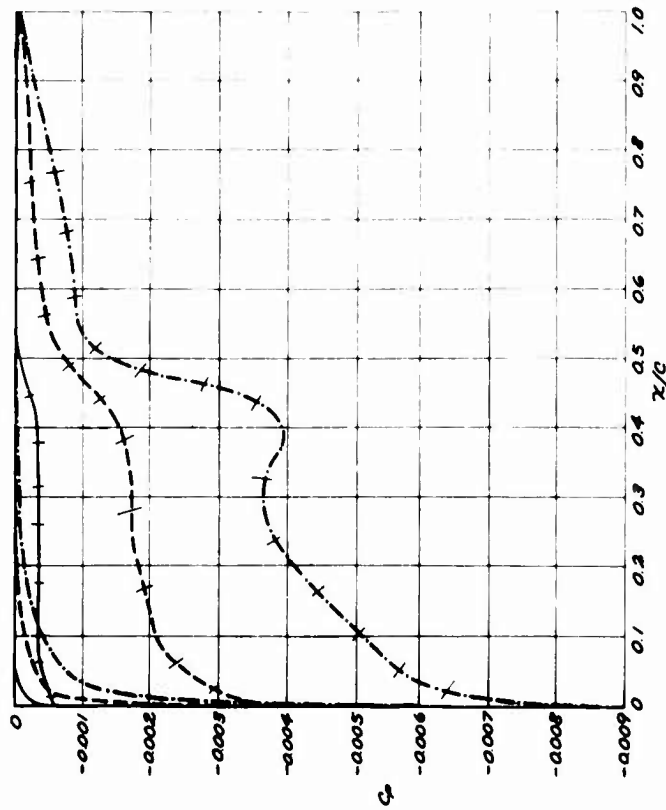
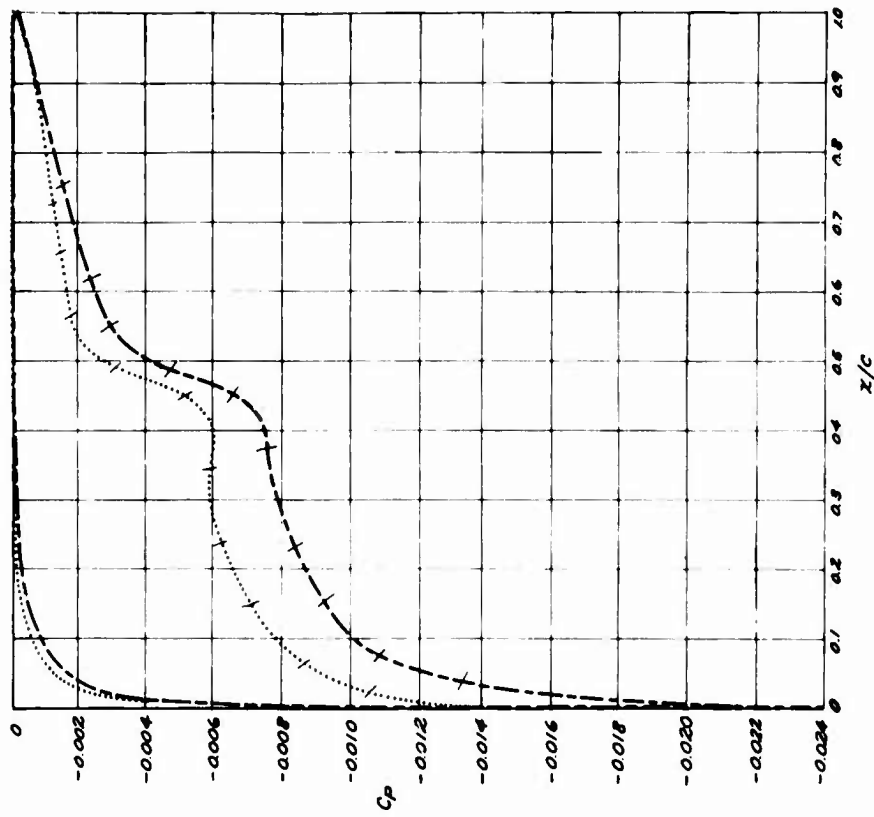


Figure 8-a. Shroud Pressure Distribution - Static Condition, 3500 RPM.

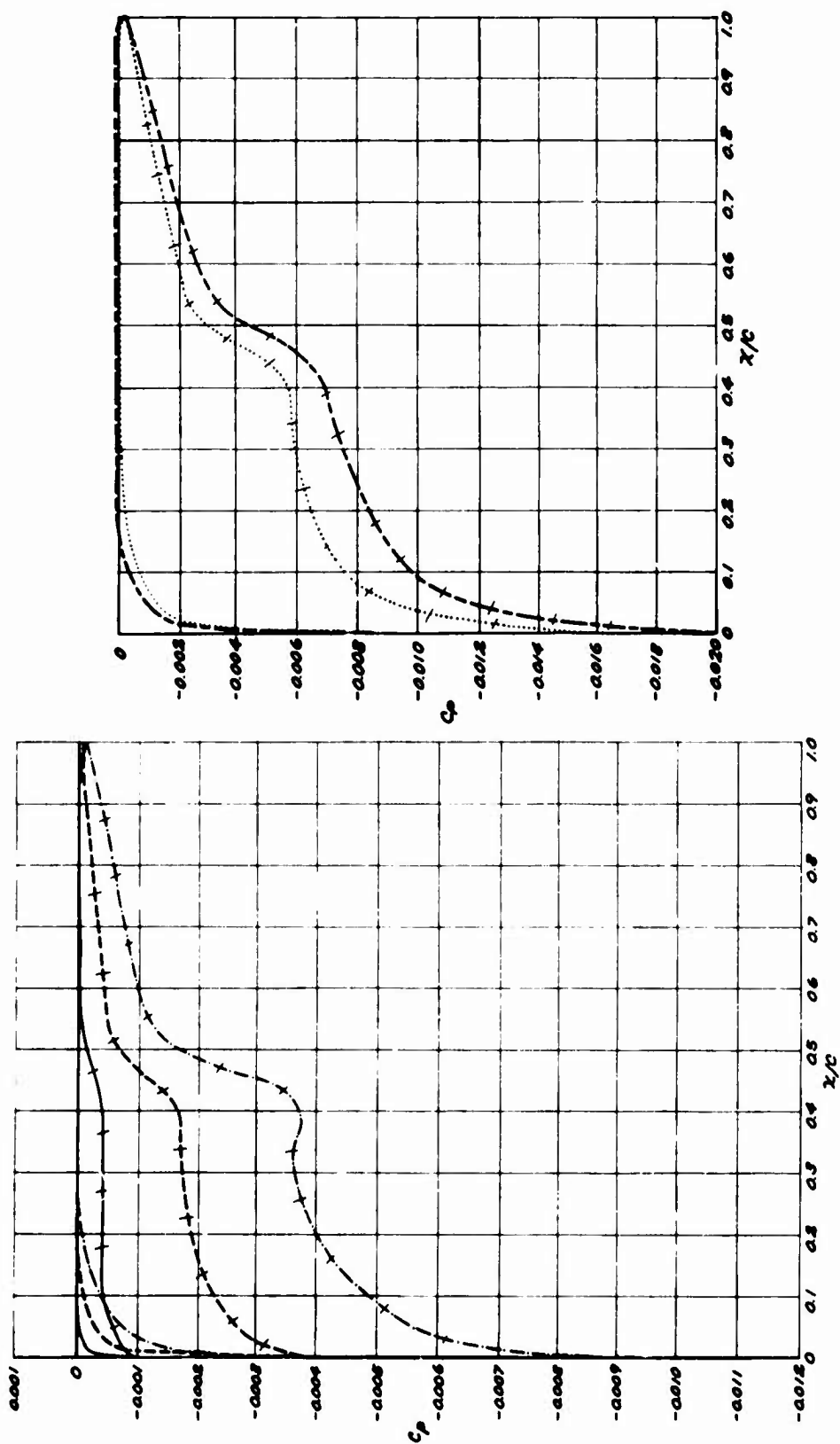


Figure 8-b. Shroud Pressure Distribution - Static Condition, 4000 RPM.

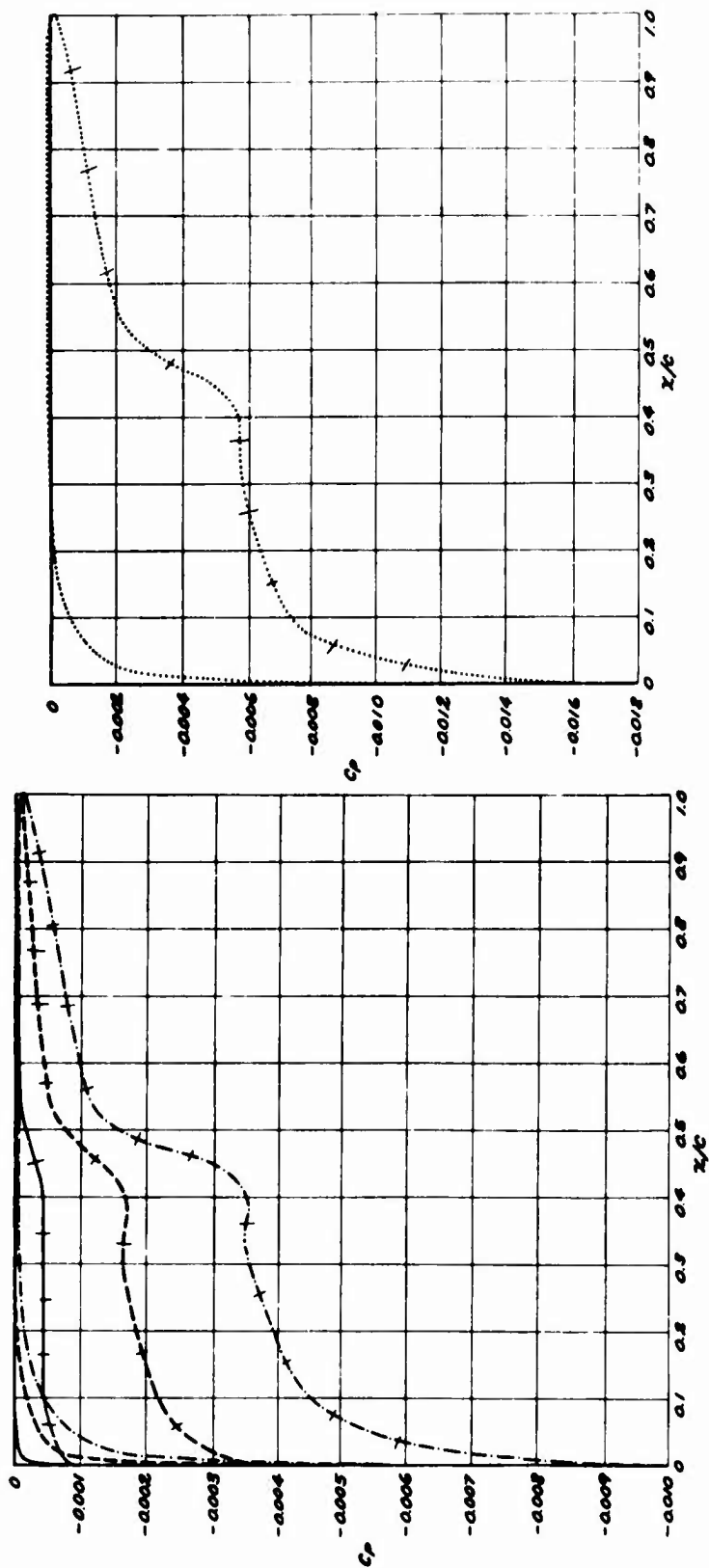


Figure 8-c. Shroud Pressure Distribution - Static Condition, 4500 RPM.

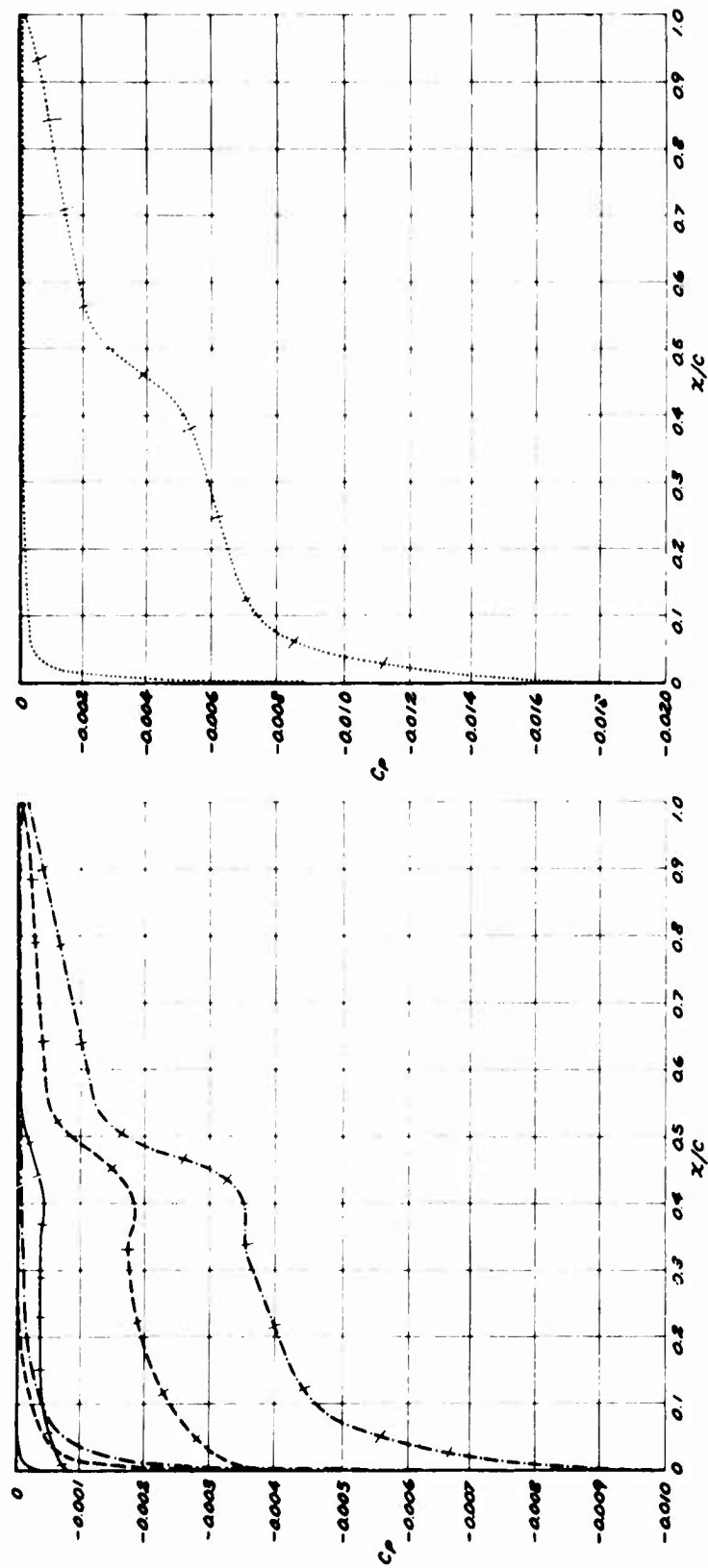


Figure 8-d. Shroud Pressure Distribution - Static Condition, 5000 RPM.

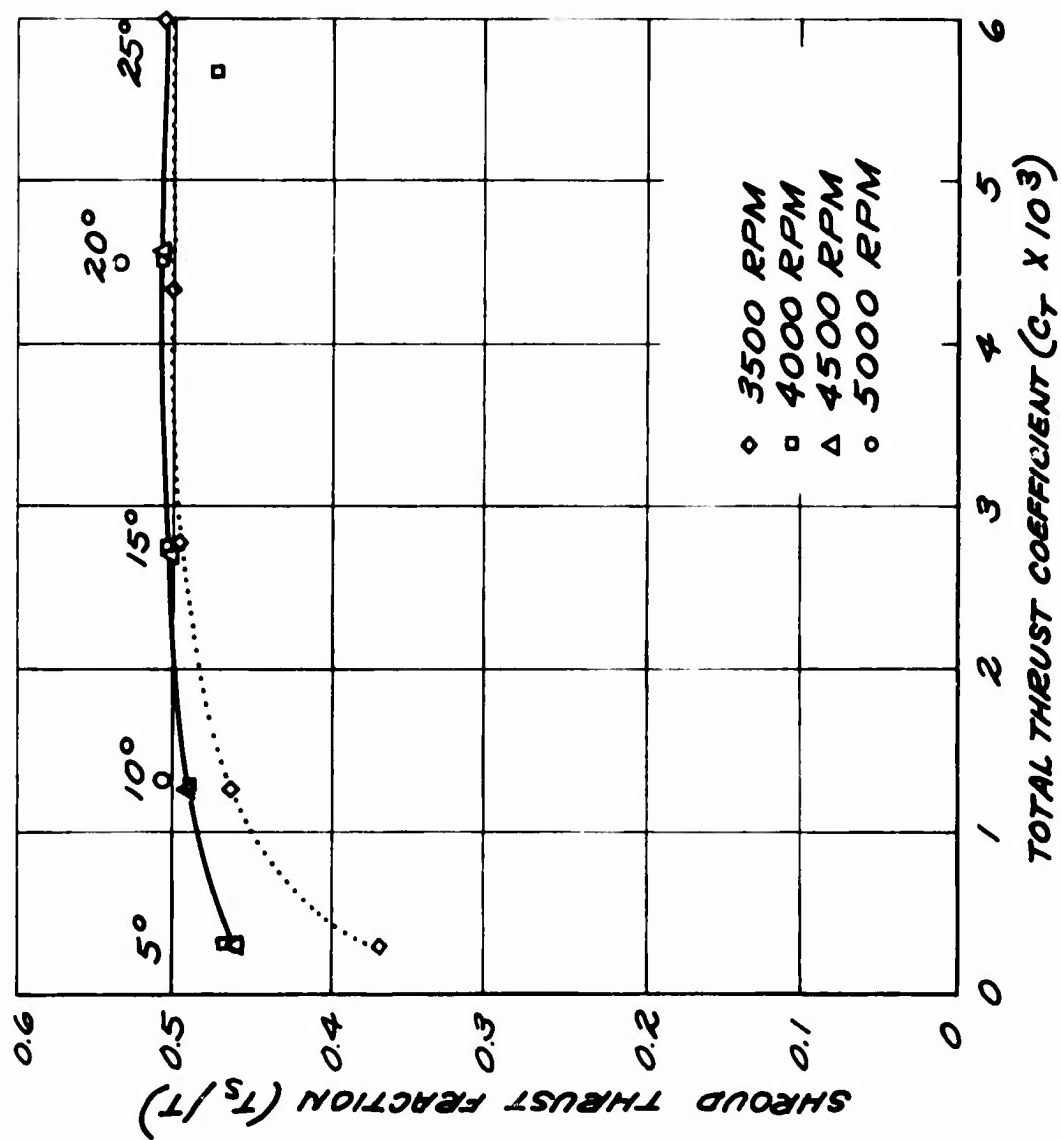


Figure 9. Static Thrust Division.

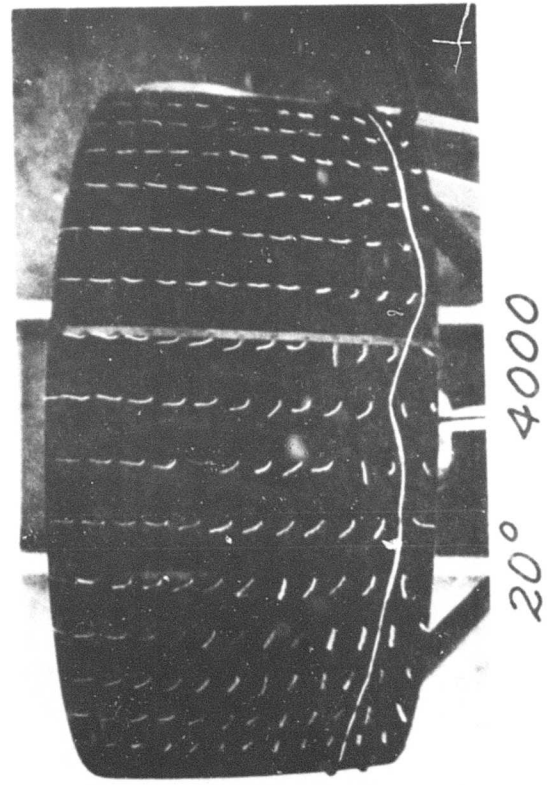
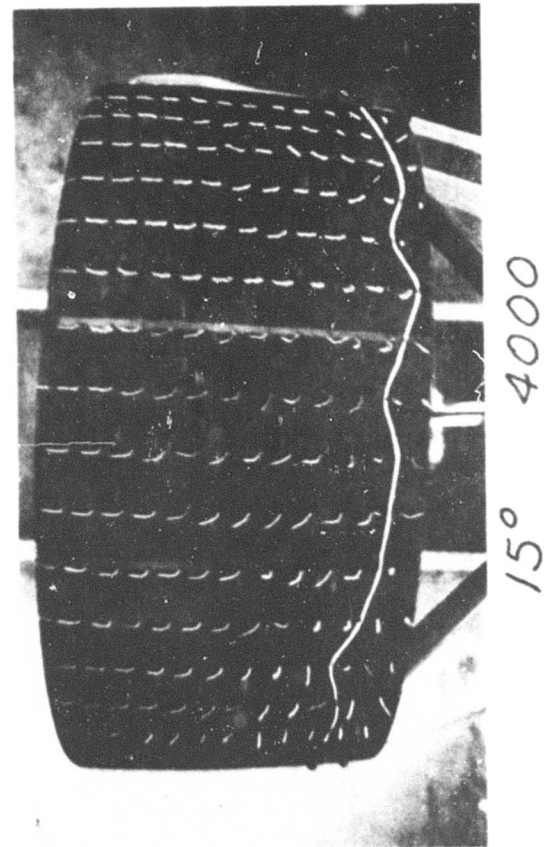
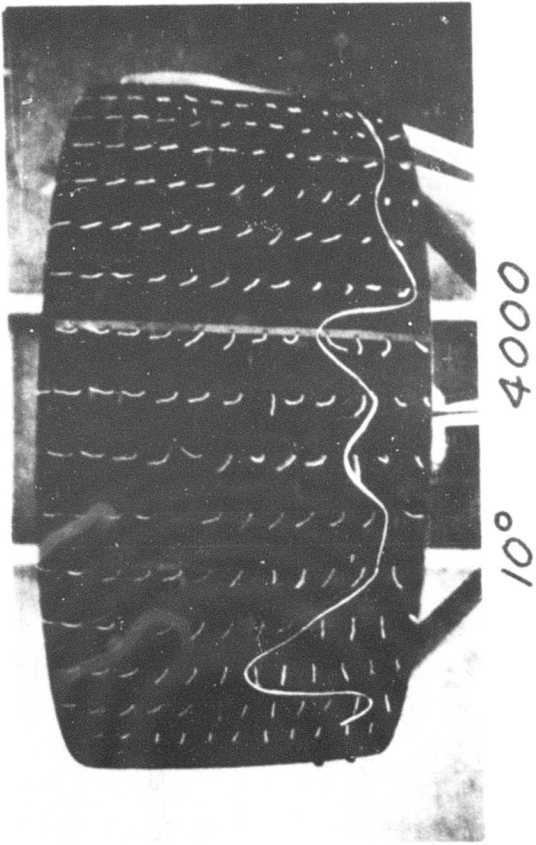
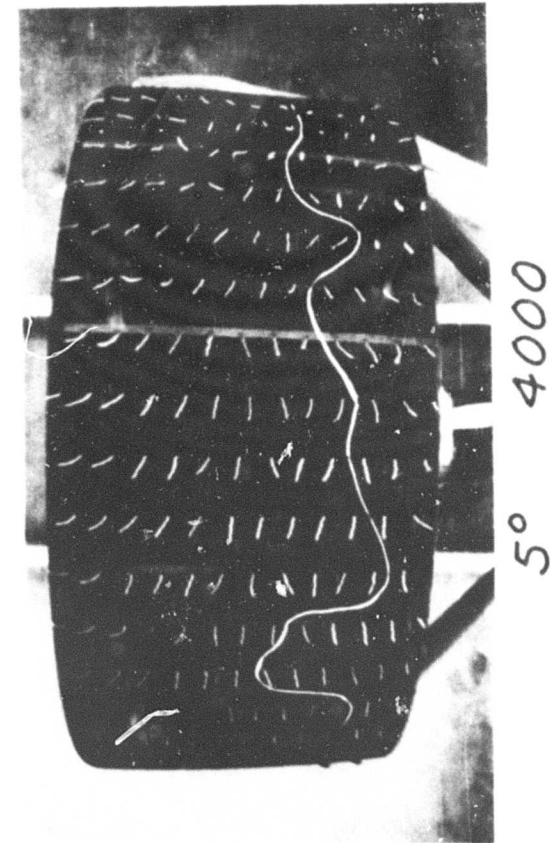
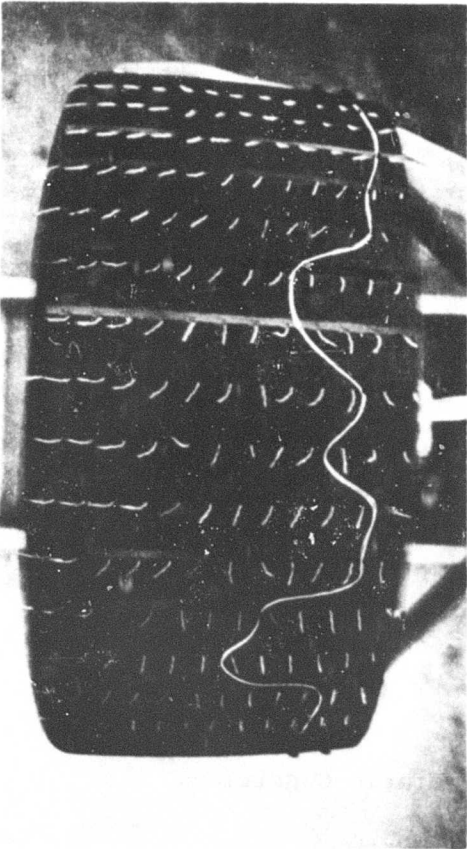
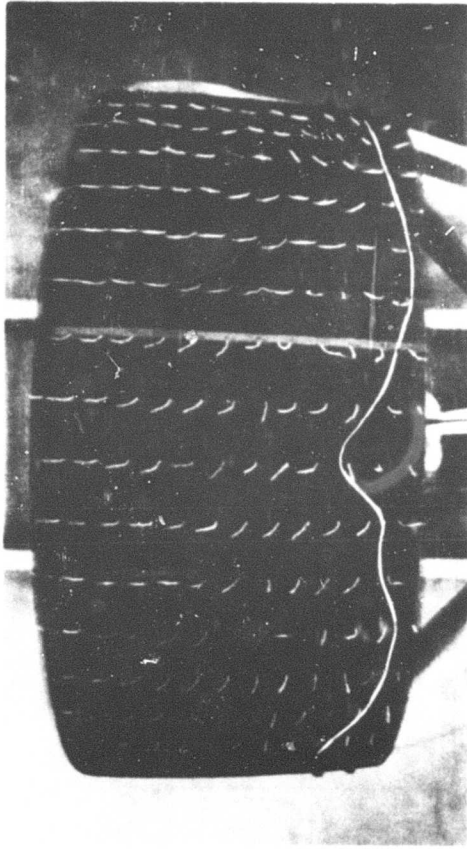


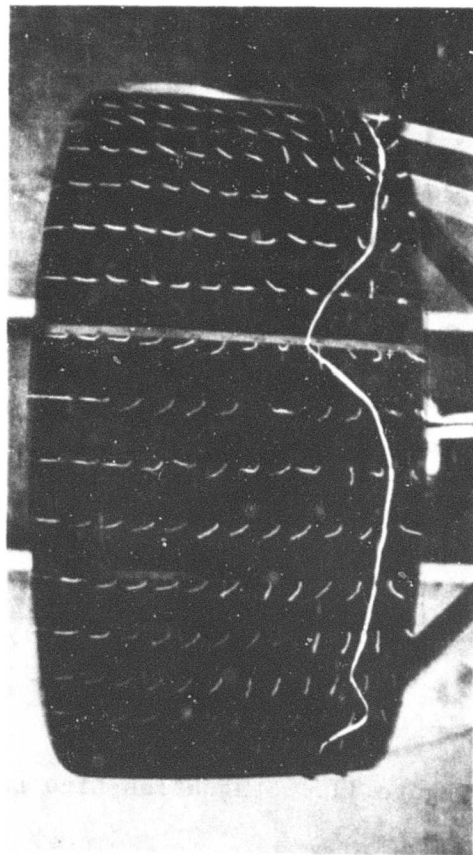
Figure 10. Tuft Patterns - Static Condition.



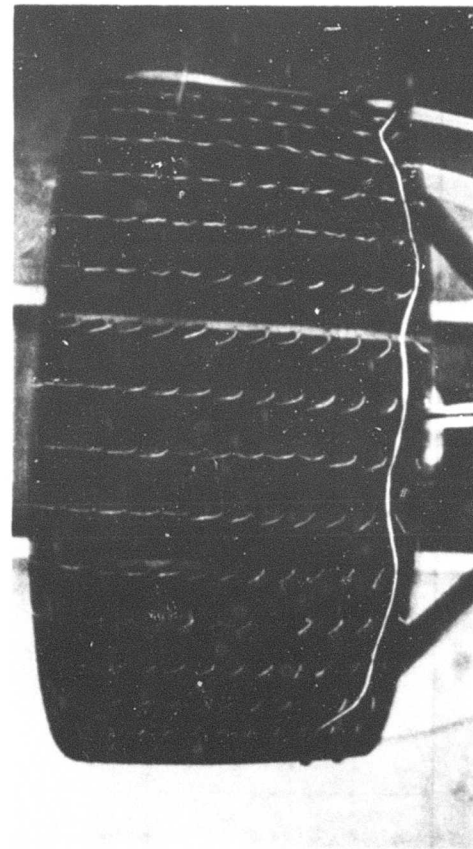
5° 5000



10° 5000



15° 5000



20° 5000

Figure 10 (Cont.). Tuft Patterns - Static Condition.

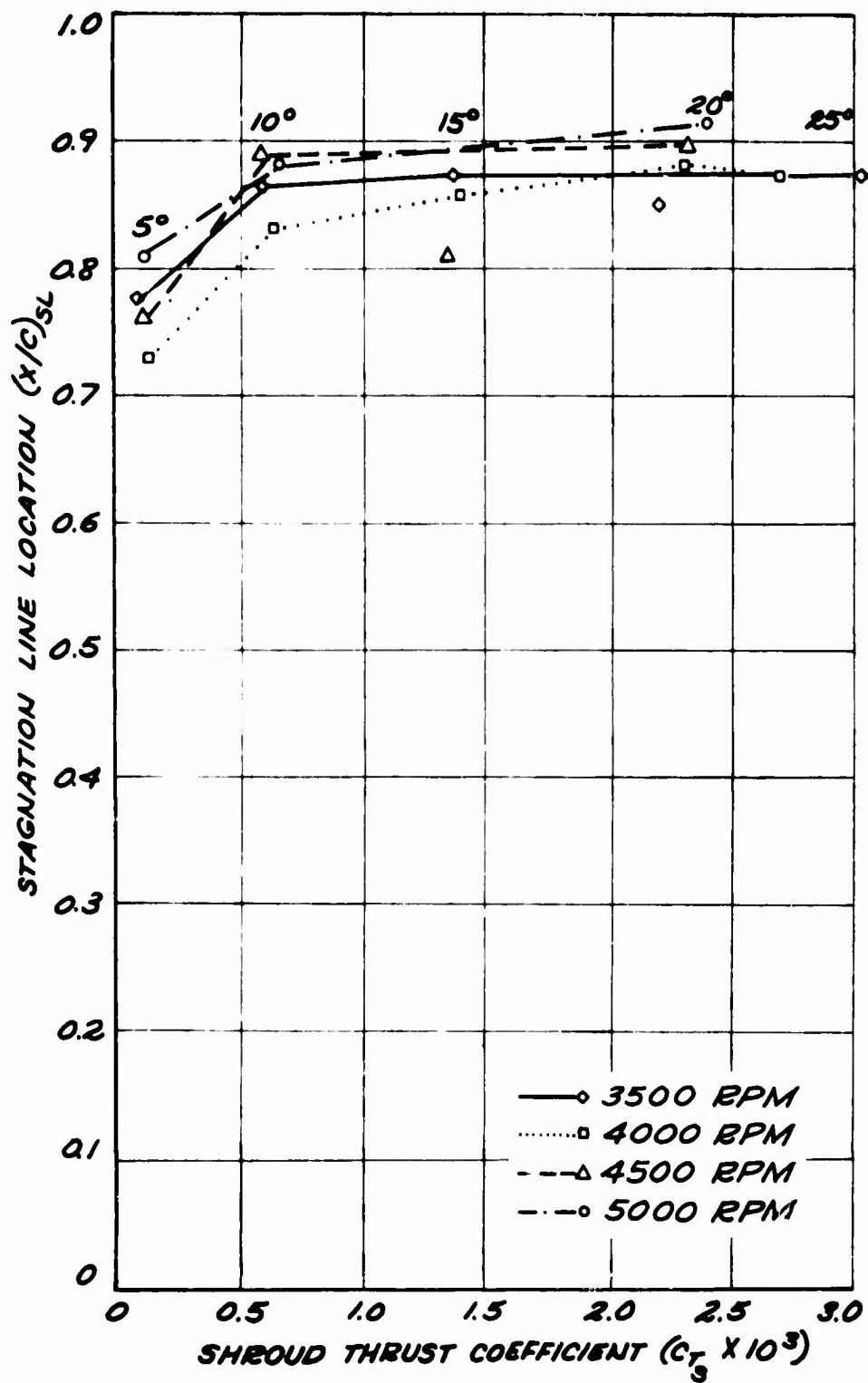







Figure 11. Stagnation Line Location - Static Condition.

Figure 12 (a-r). Shroud Pressure Distributions - Rearward Motion.

Legend:  5° pitch angle
  10° pitch angle
  15° pitch angle
  20° pitch angle
  curves which correspond to
 inside surface of shroud

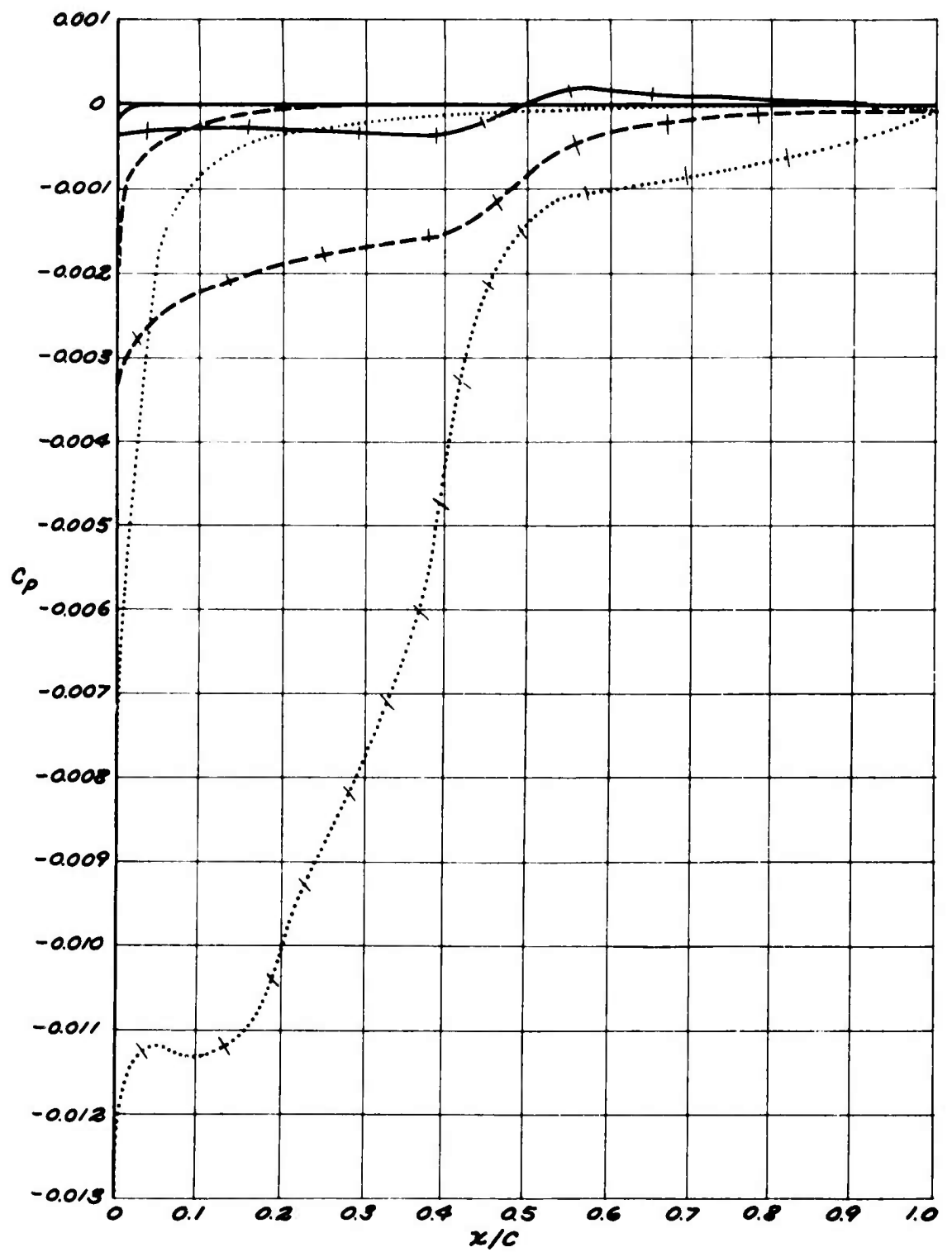


Figure 12-a. Shroud Pressure Distribution - Rearward Motion, 4000 RPM, 5 MPH.

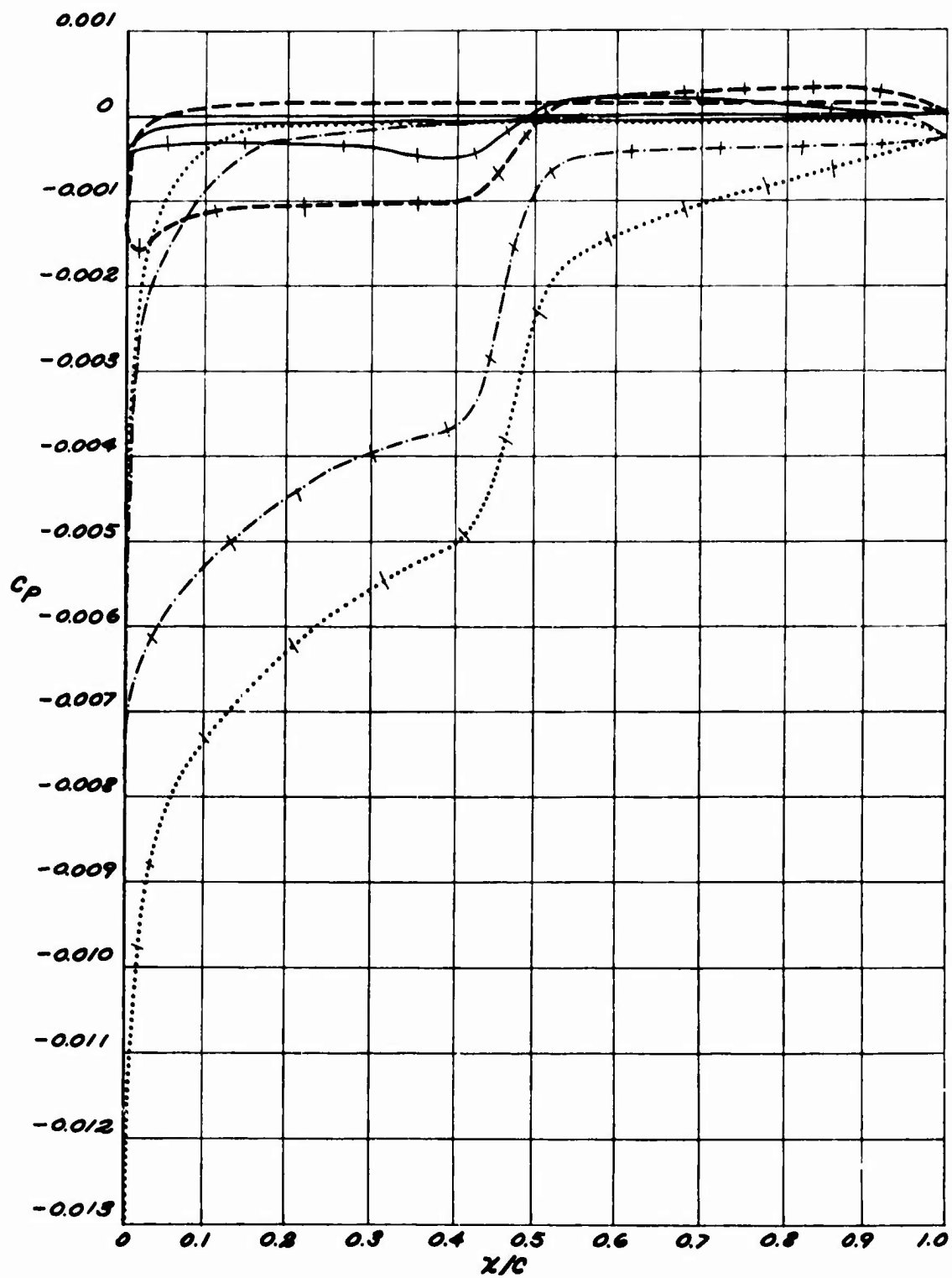


Figure 12-b. Shroud Pressure Distribution - Rearward Motion,
4000 RPM, 10 MPH.

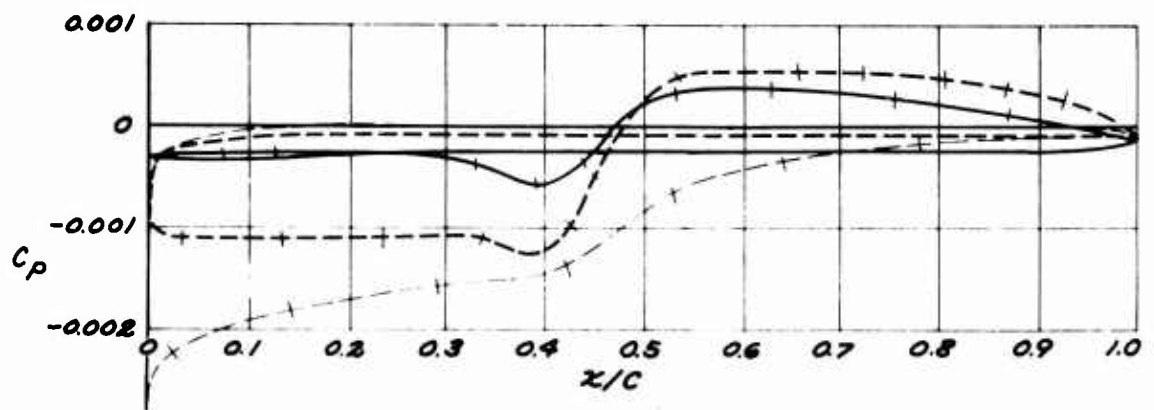


Figure 12-c. Shroud Pressure Distribution - Rearward Motion, 4000 RPM, 15 MPH.

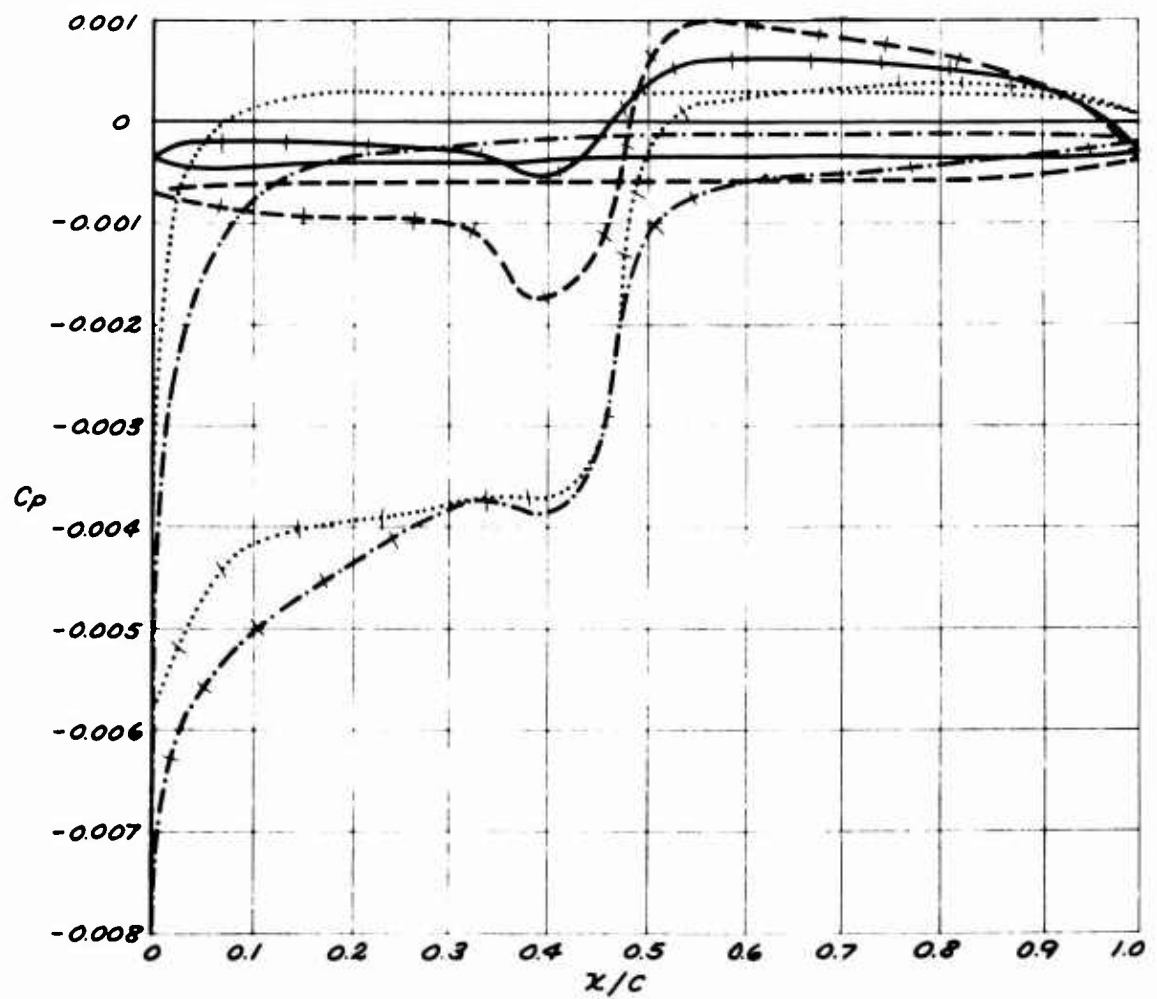


Figure 12-d. Shroud Pressure Distribution - Rearward Motion, 4000 RPM, 20 MPH.

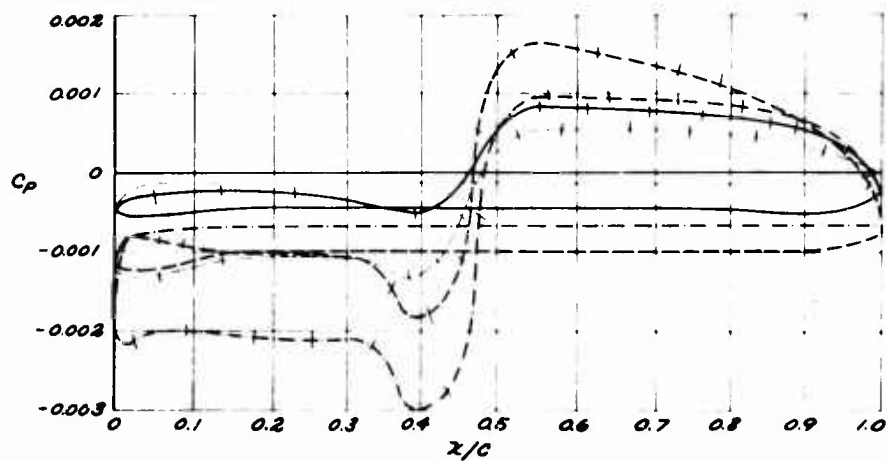


Figure 12-e. Shroud Pressure Distribution - Rearward Motion, 4000 RPM, 25 MPH.

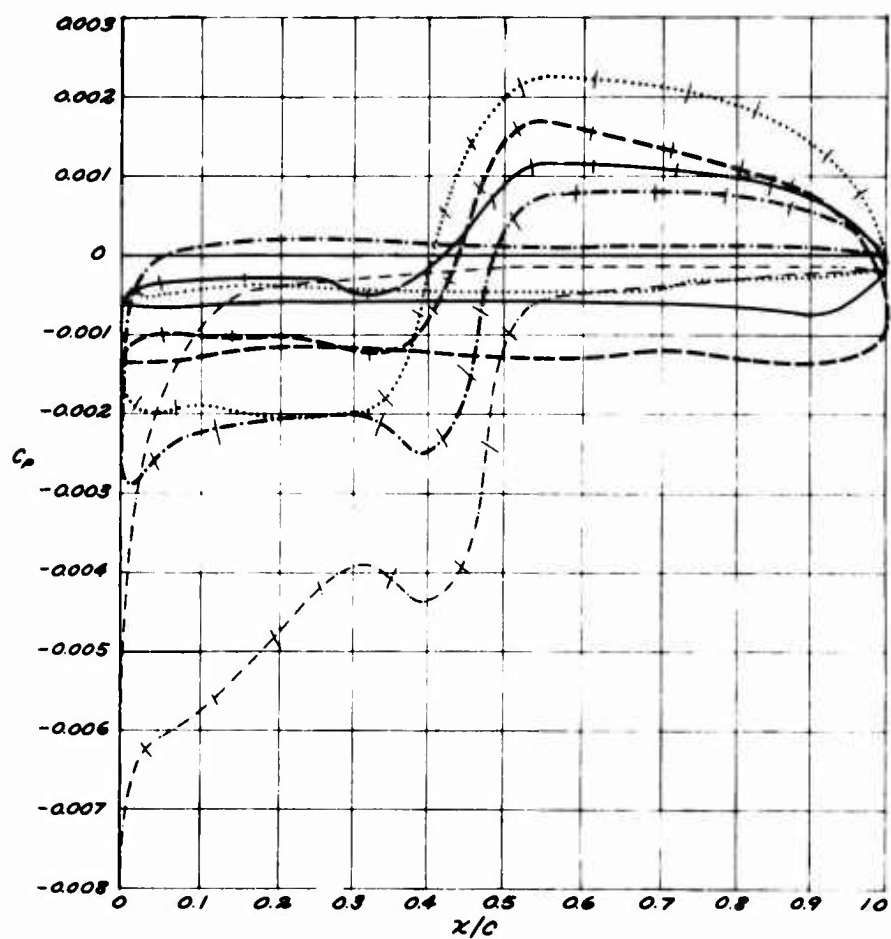


Figure 12-f. Shroud Pressure Distribution - Rearward Motion, 4000 RPM, 30 MPH.

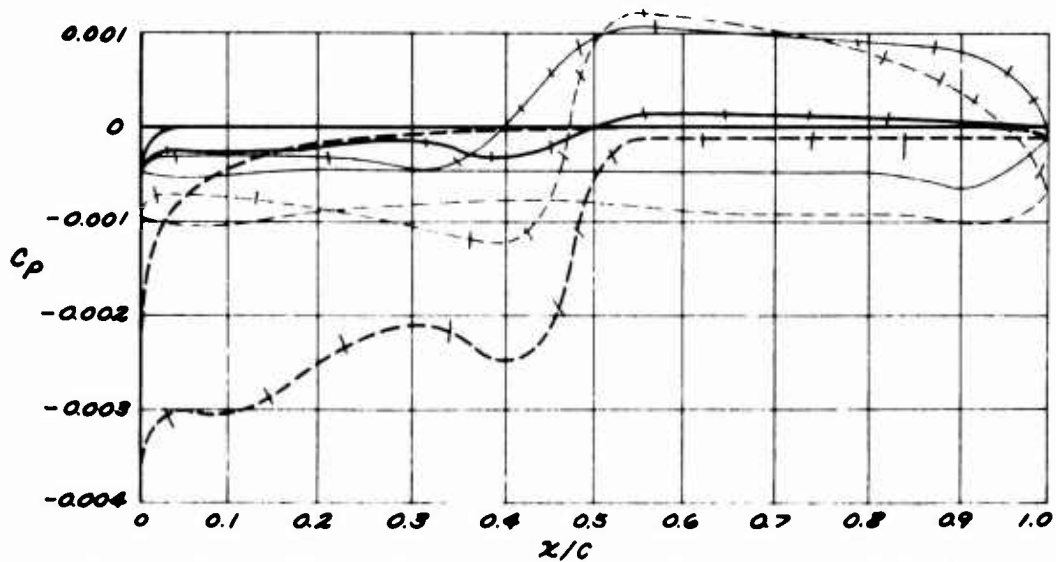


Figure 12-g. Shroud Pressure Distribution - Rearward Motion, 4500 RPM, 5 MPH.

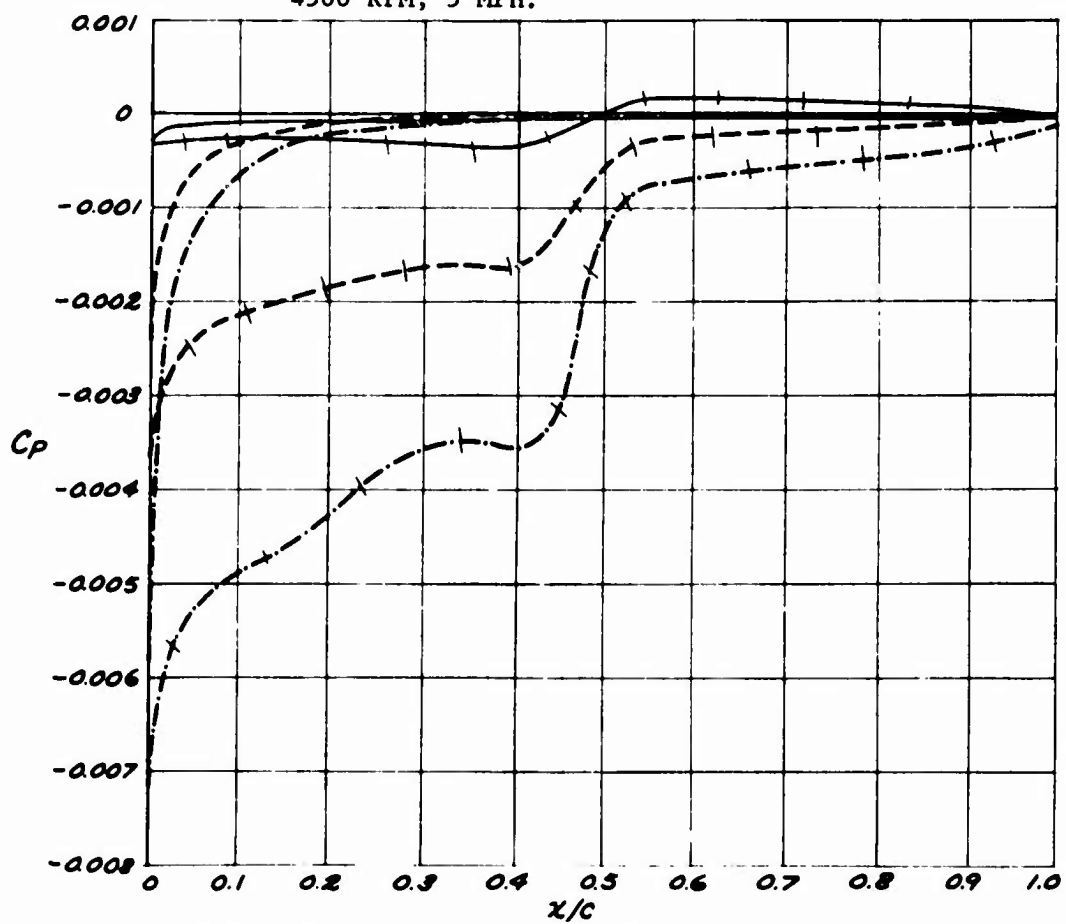


Figure 12-h. Shroud Pressure Distribution - Rearward Motion, 4500 RPM, 10 MPH.

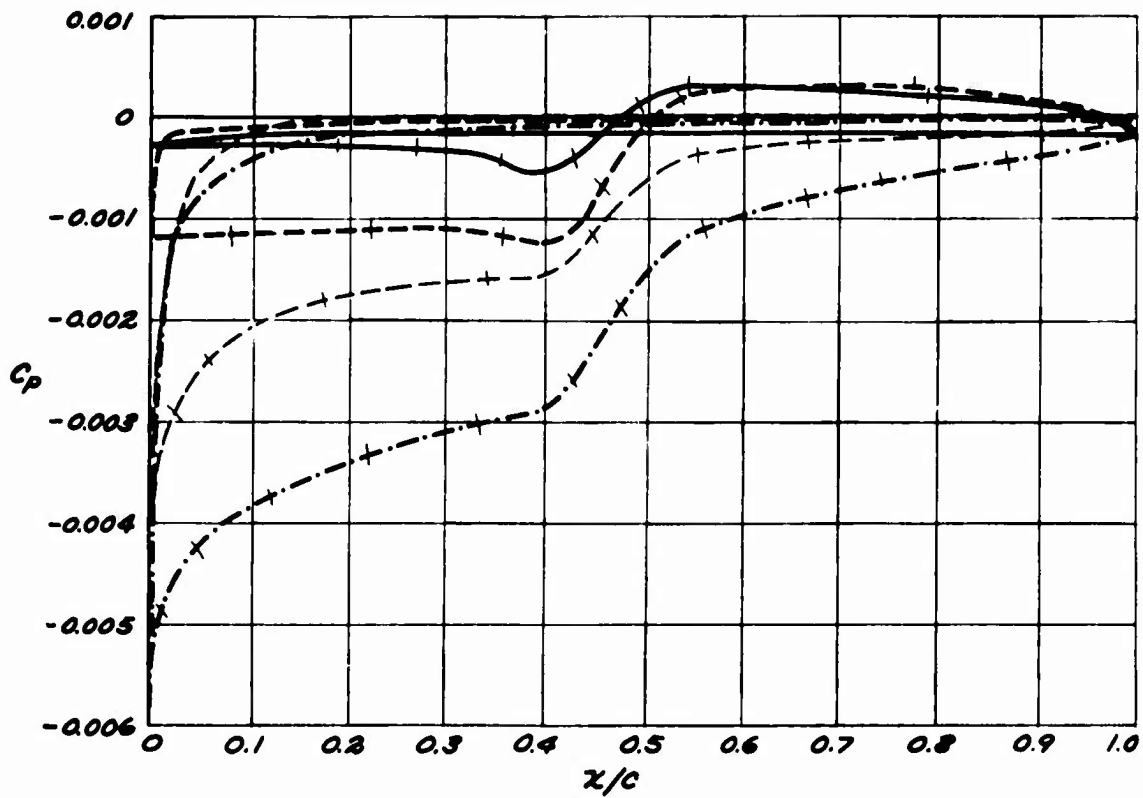


Figure 12-i. Shroud Pressure Distribution - Rearward Motion, 4500 RPM, 15 MPH.

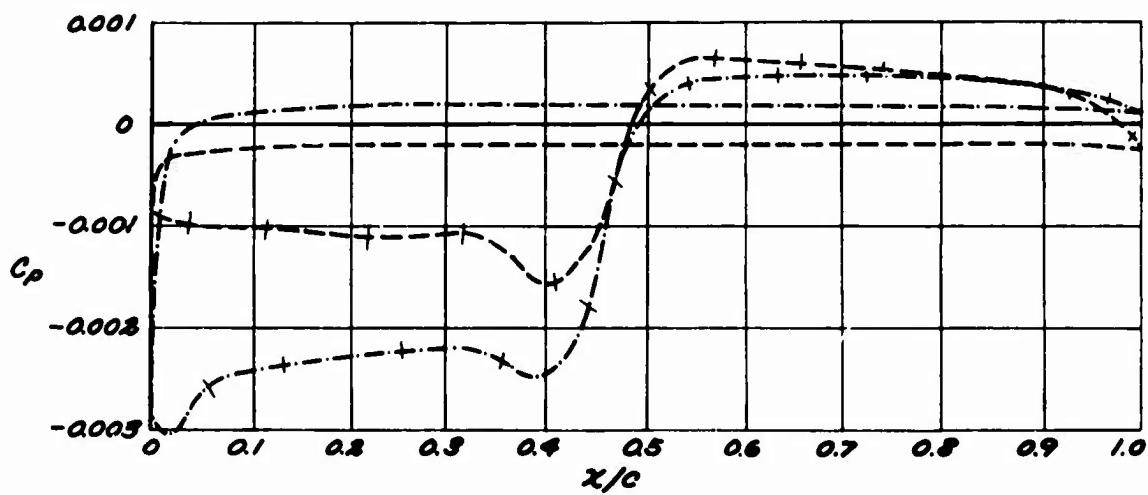


Figure 12-j. Shroud Pressure Distribution - Rearward Motion, 4500 RPM, 20 MPH.

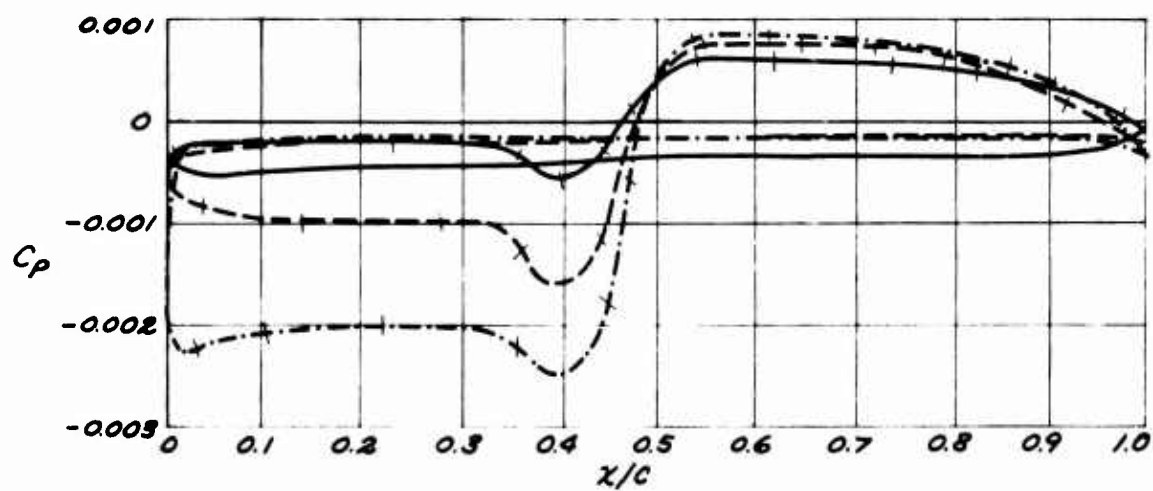


Figure 12-k. Shroud Pressure Distribution - Rearward Motion, 4500 RPM, 25 MPH.

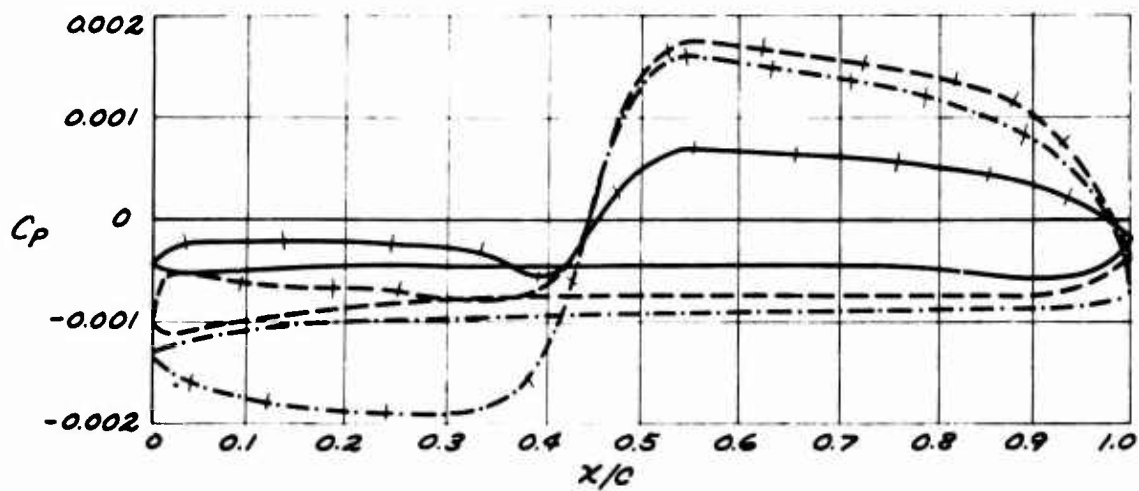


Figure 12-l. Shroud Pressure Distribution - Rearward Motion, 4500 RPM, 30 MPH.

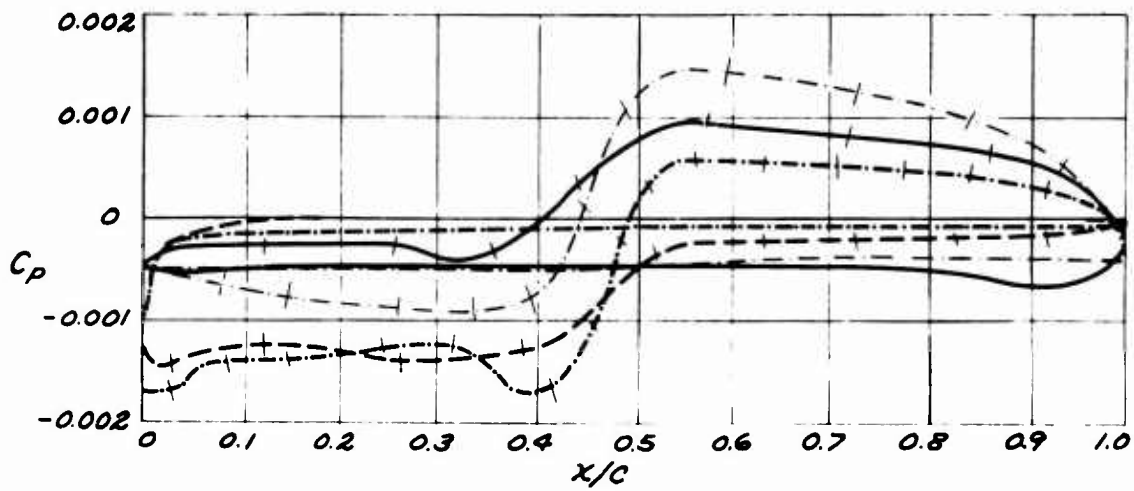


Figure 12-m. Shroud Pressure Distribution - Rearward Motion, 5000 RPM, 5 MPH.

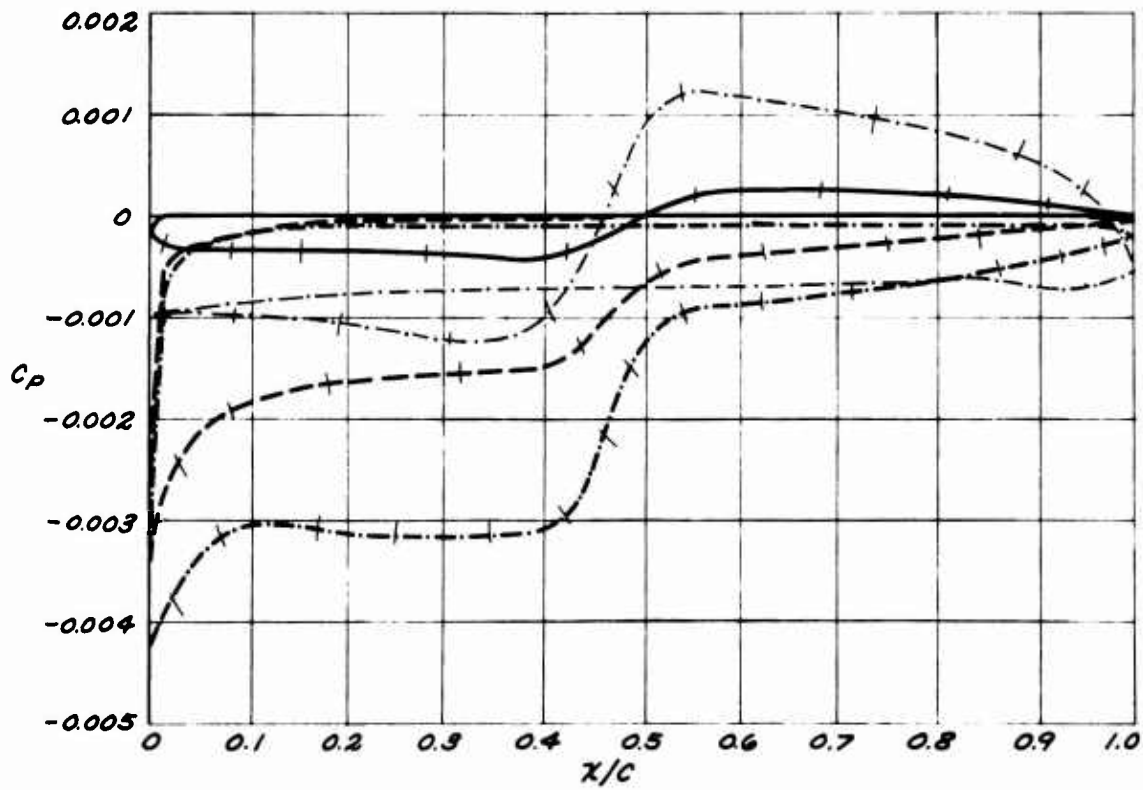


Figure 12-n. Shroud Pressure Distribution - Rearward Motion, 5000 RPM, 10 MPH.

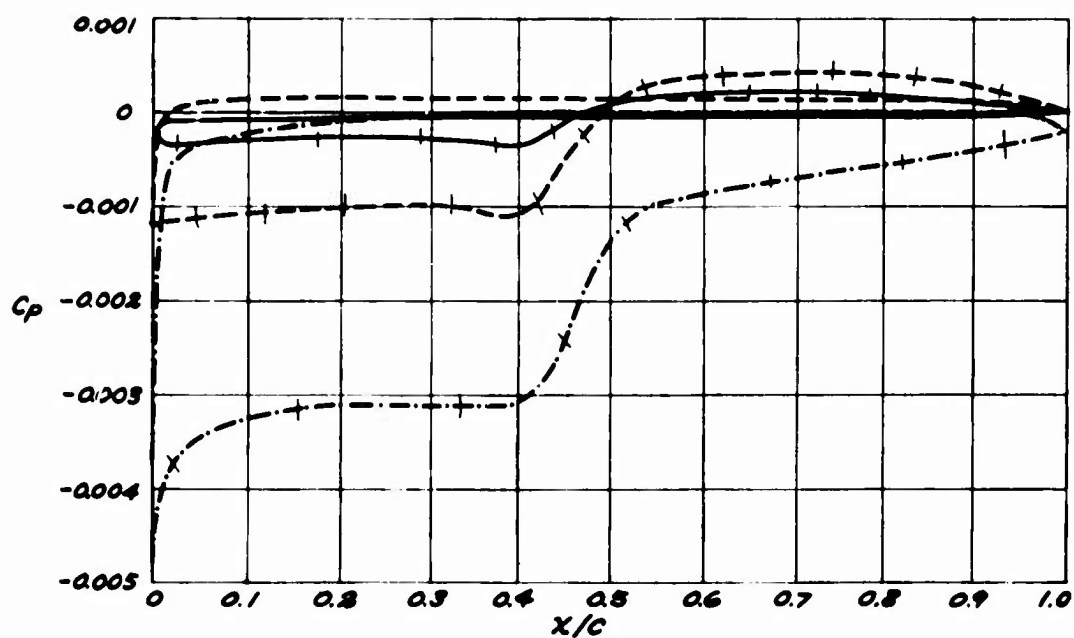


Figure 12-o. Shroud Pressure Distribution - Rearward Motion, 5000 RPM, 15 MPH.

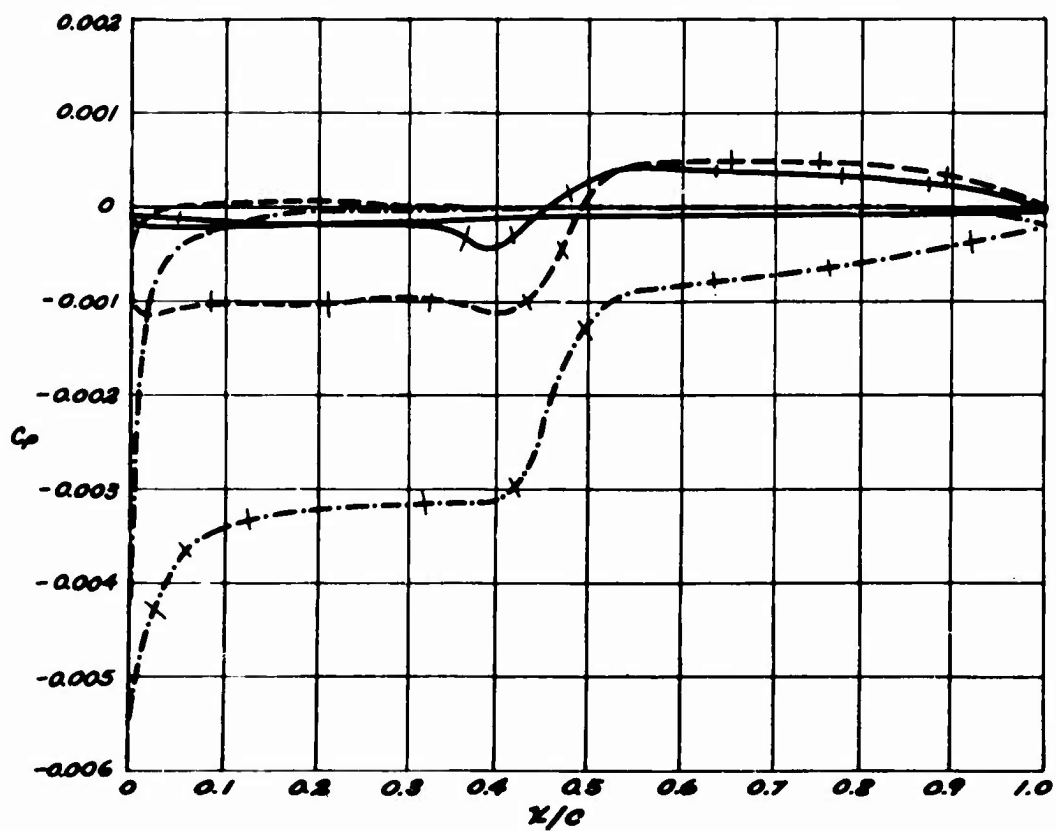


Figure 12-p. Shroud Pressure Distribution - Rearward Motion, 5000 RPM, 20 MPH.

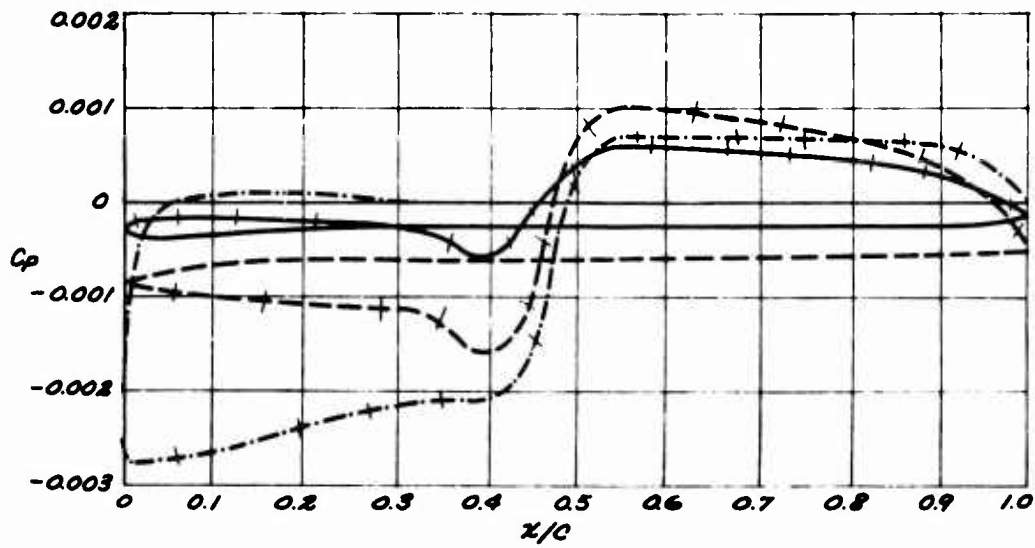


Figure 12-q. Shroud Pressure Distribution - Rearward Motion, 5000 RPM, 25 MPH.

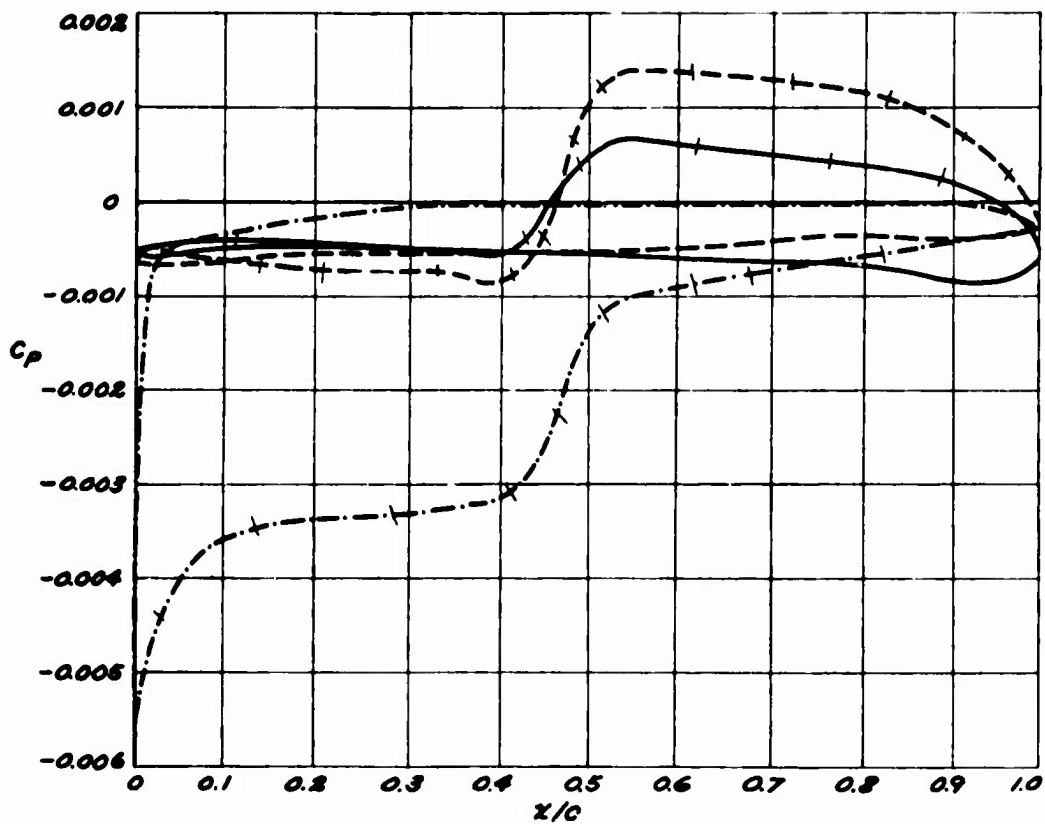


Figure 12-r. Shroud Pressure Distribution - Rearward Motion, 5000 RPM, 30 MPH.

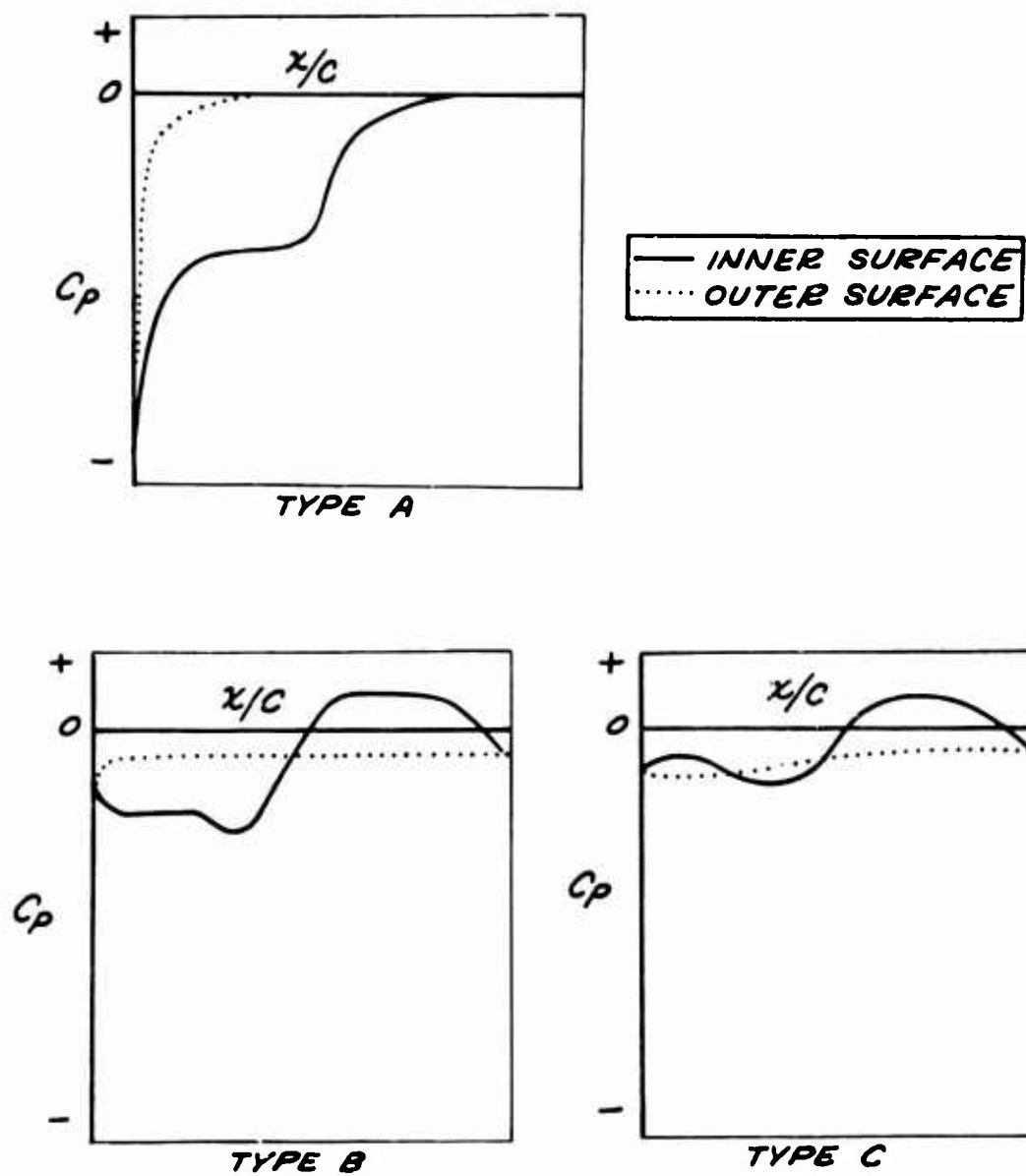


Figure 13. Pressure Distribution Types - Rearward Motion.

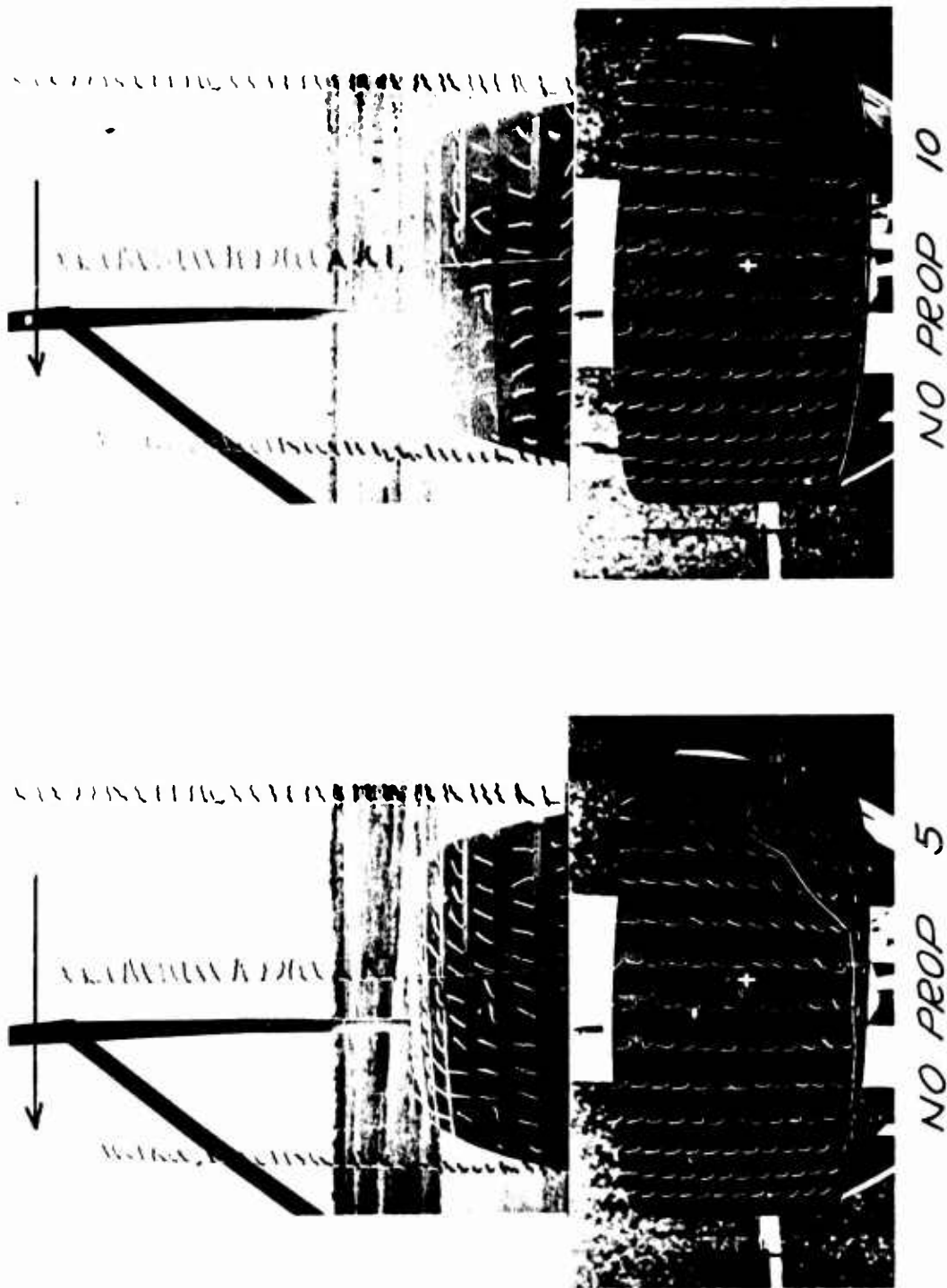


Figure 14. Tuft Patterns - Rearward Motion.

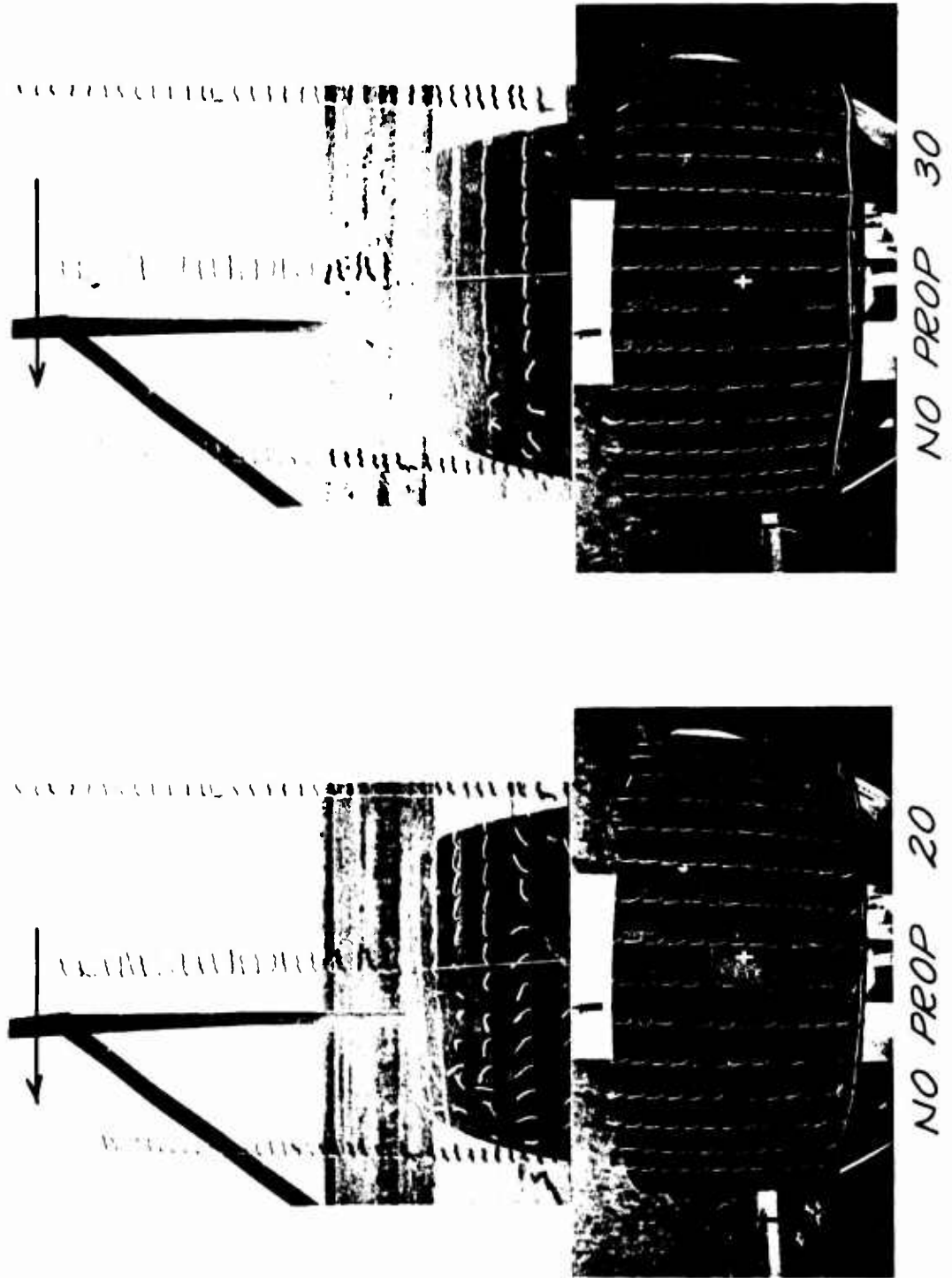


Figure 14 (Cont.). Tuft Patterns - Rearward Motion.

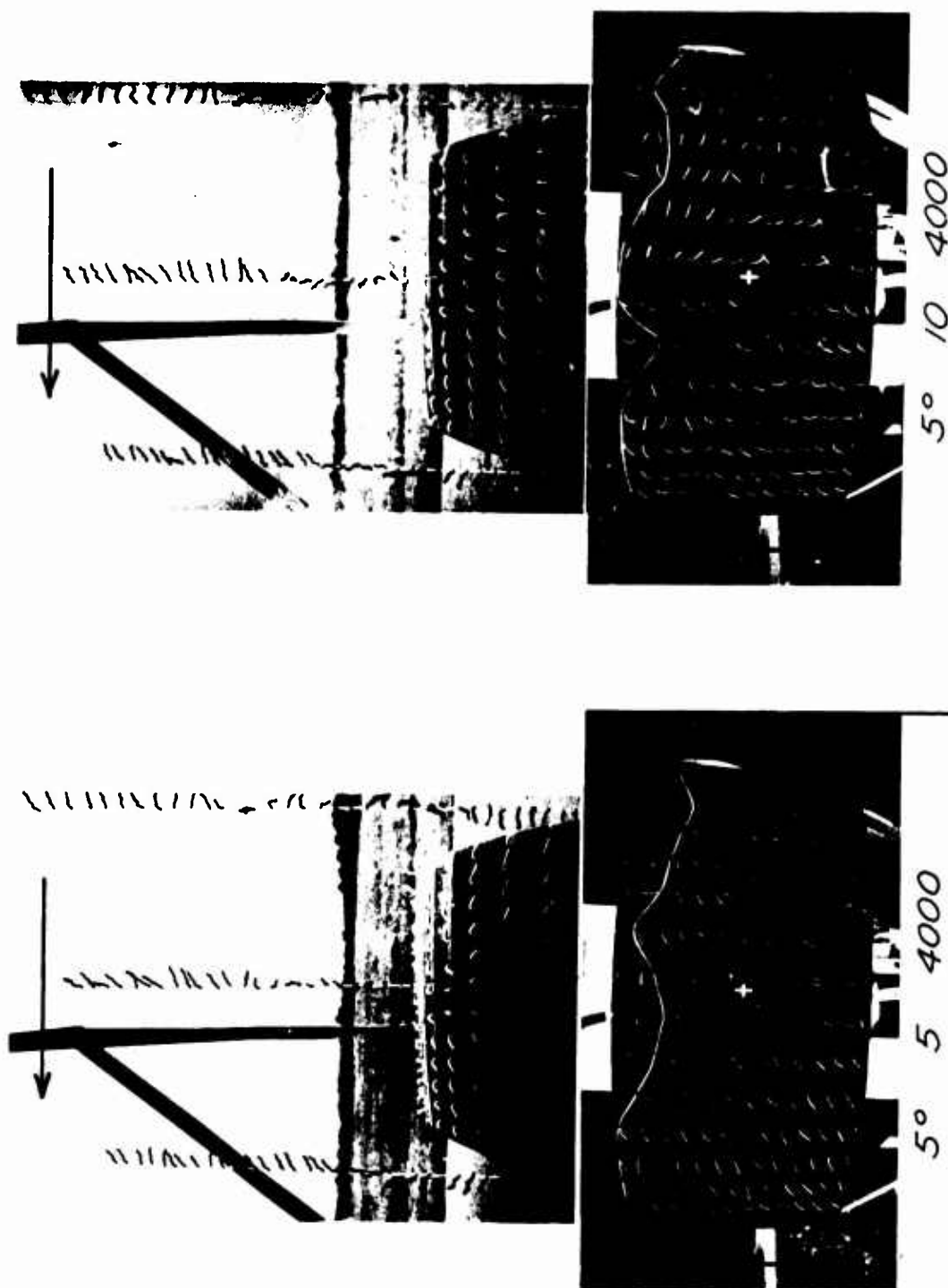


Figure 14 (Cont.). Tuft Patterns - Rearward Motion.

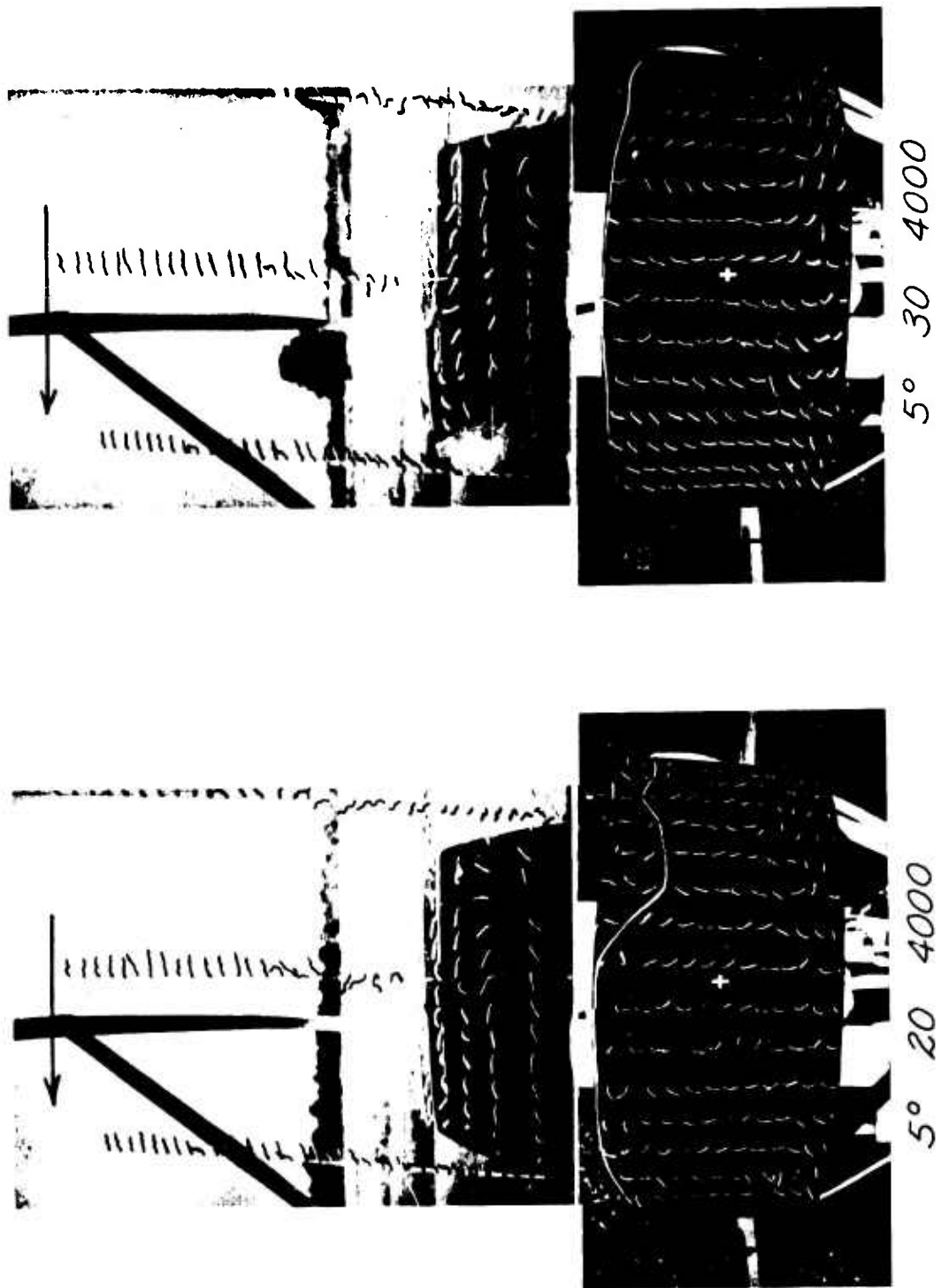


Figure 14 (Cont.). Tuft Patterns - Rearward Motion.

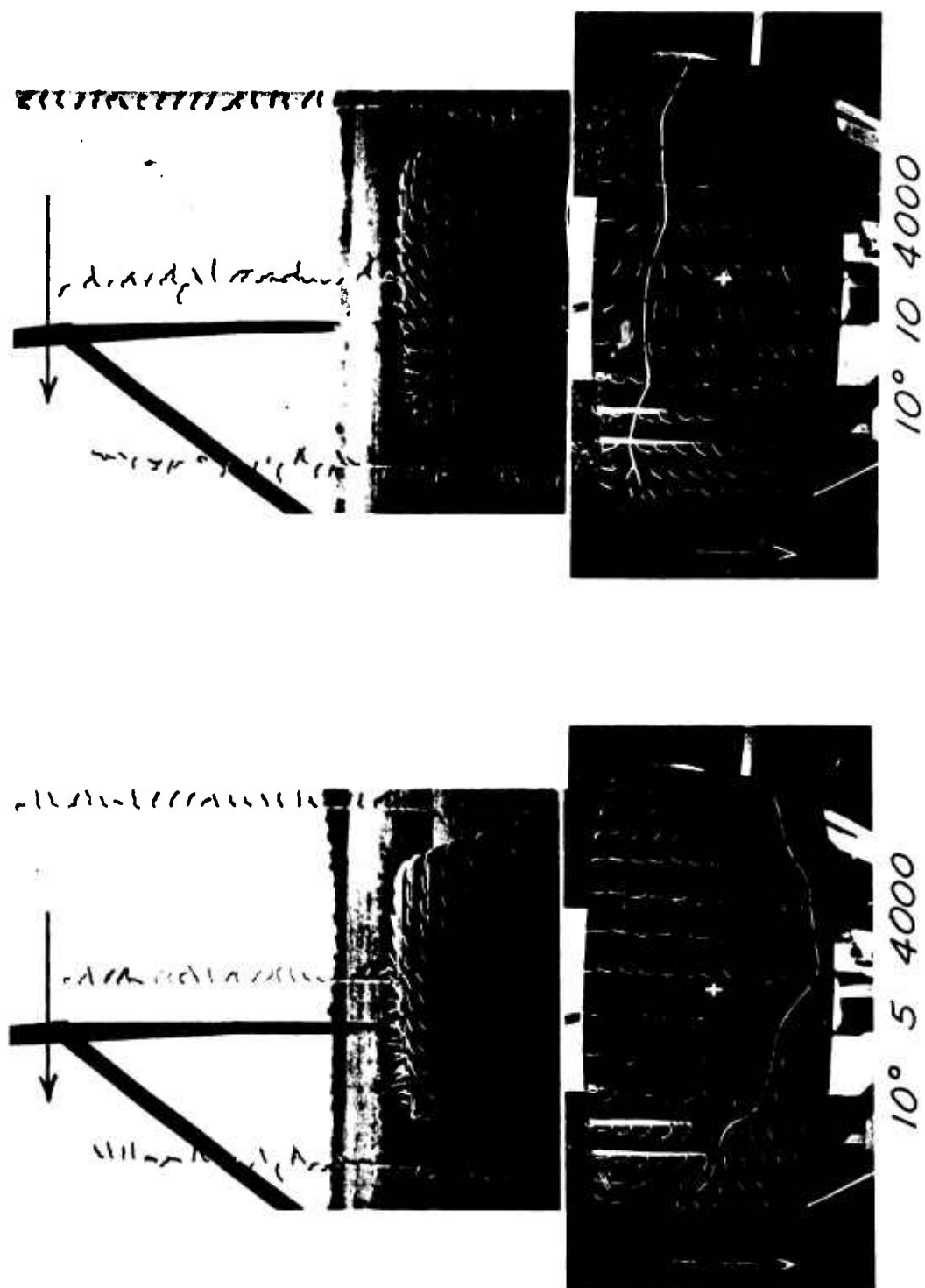


Figure 14 (Cont.). Tuft Patterns - Rearward Motion.

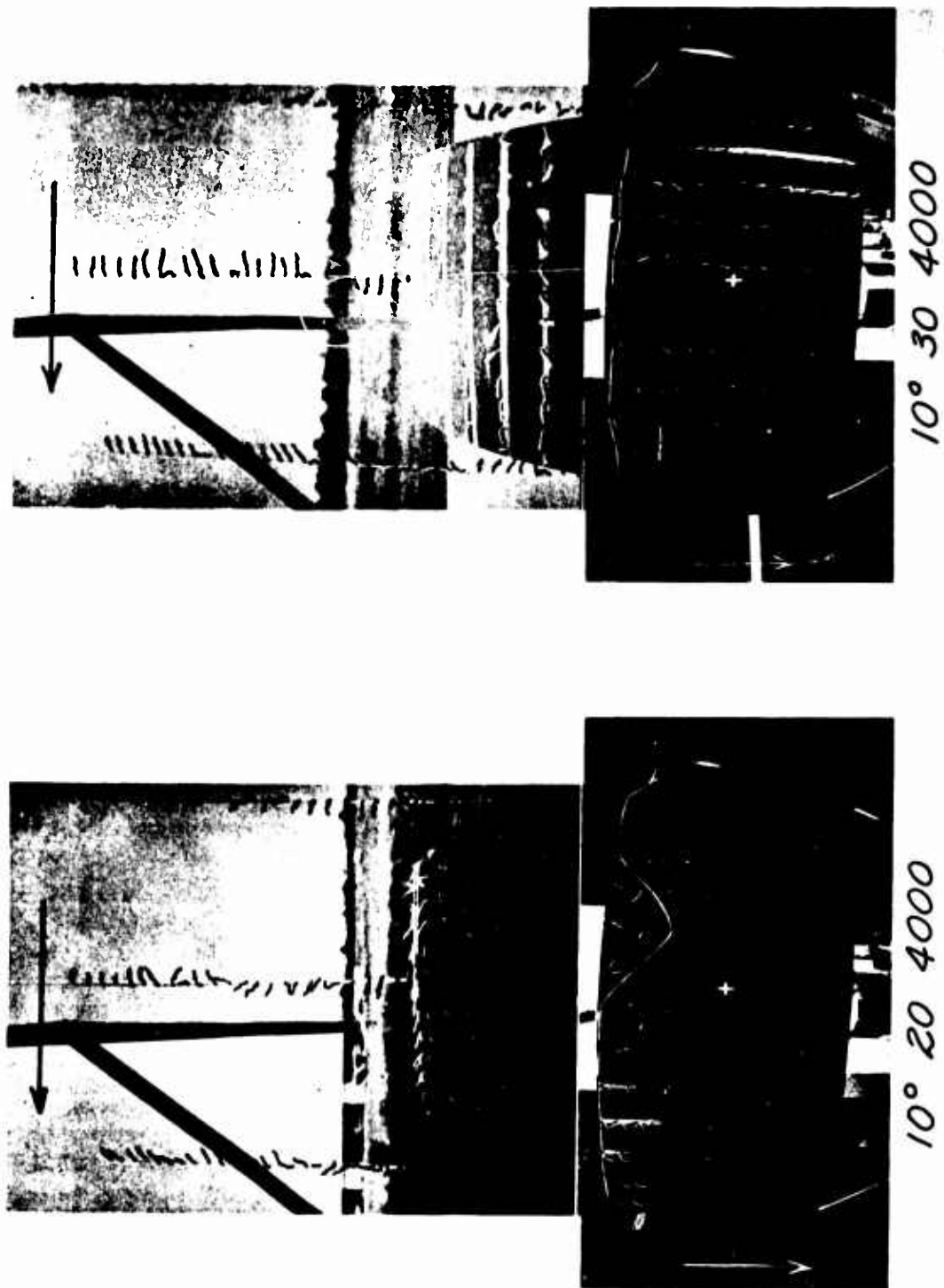
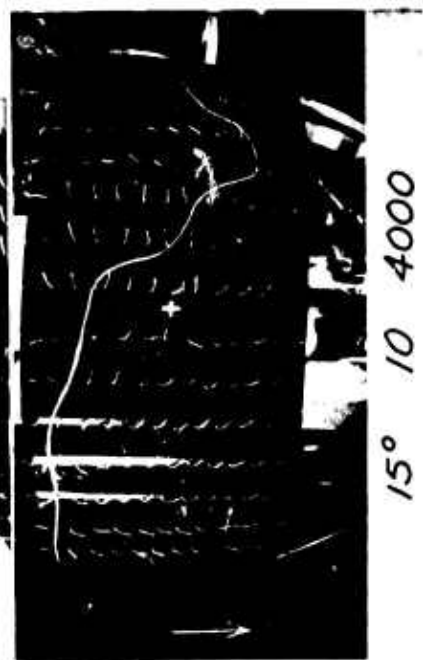
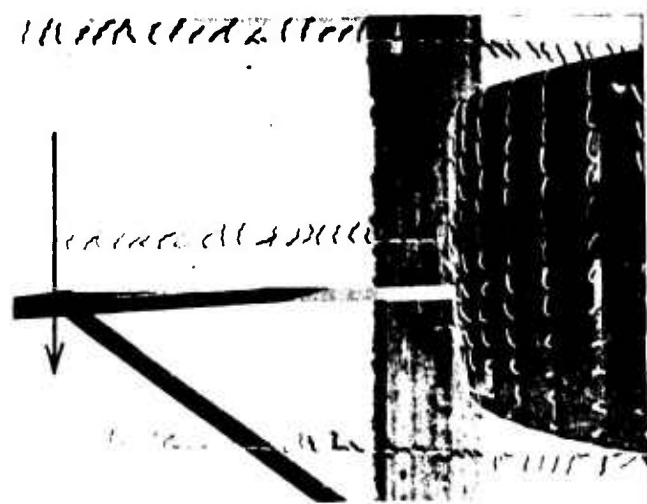
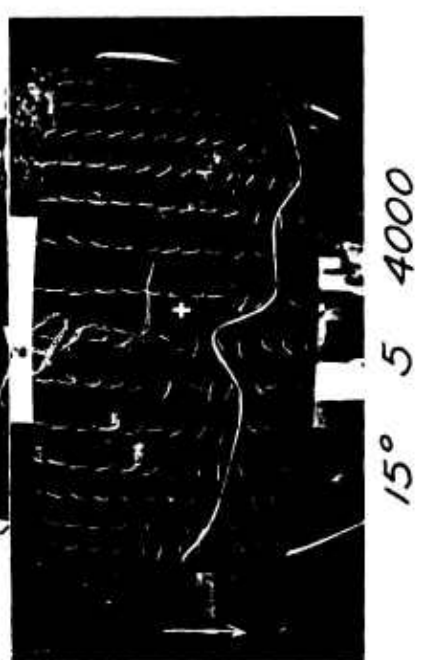
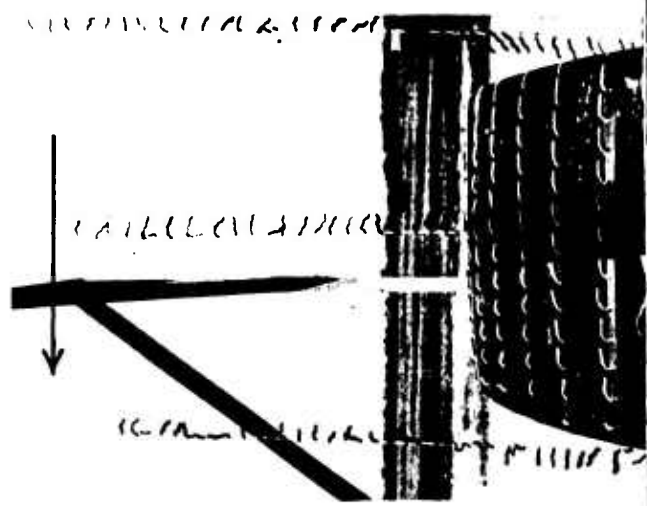


Figure 14 (Cont.). Tuft Patterns - Rearward Motion.



15° 10 4000



15° 5 4000

Figure 14 (Cont.). Tuft Patterns - Rearward Motion.

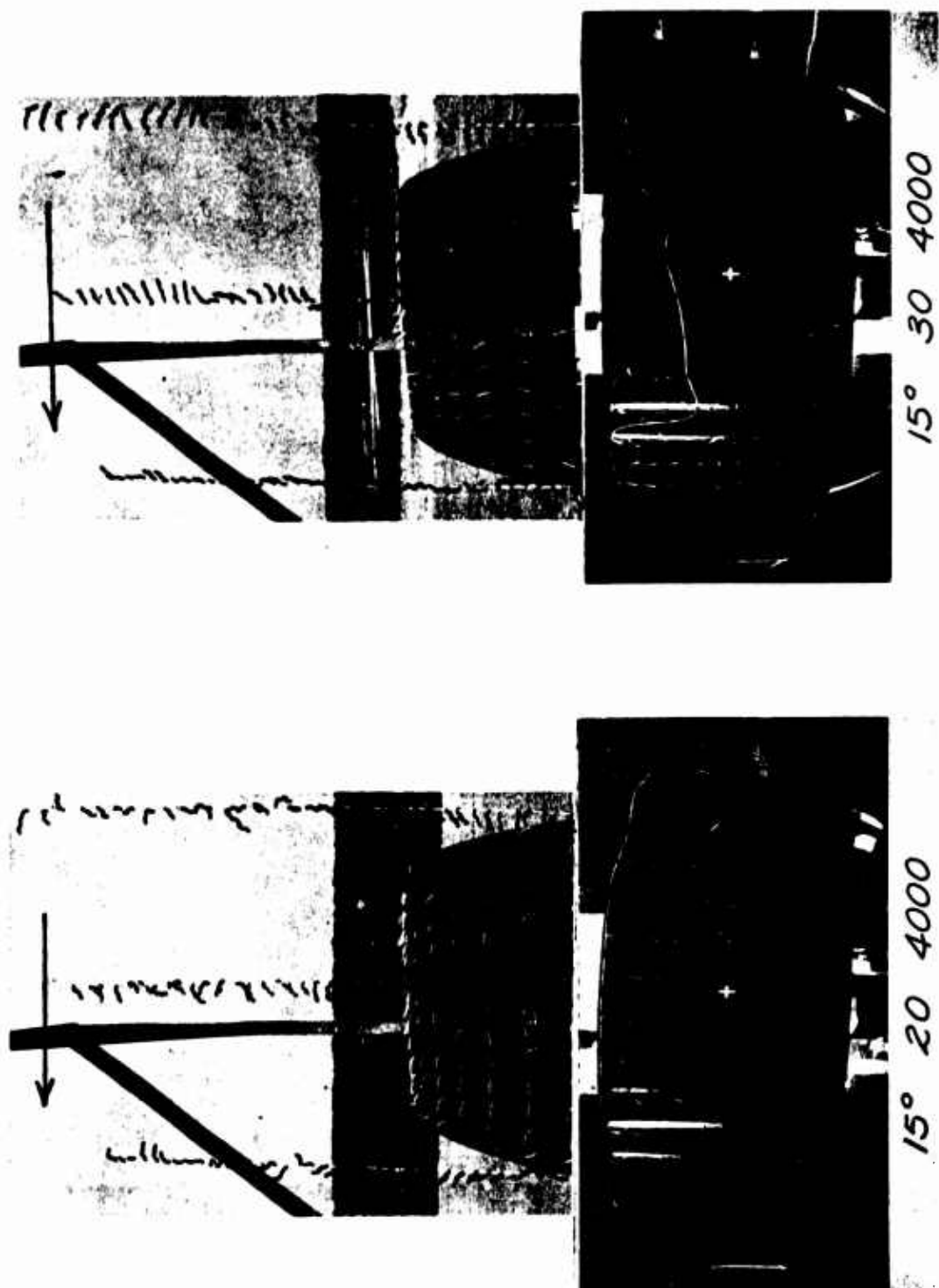


Figure 14 (Cont.). Tuft Patterns - Rearward Motion.

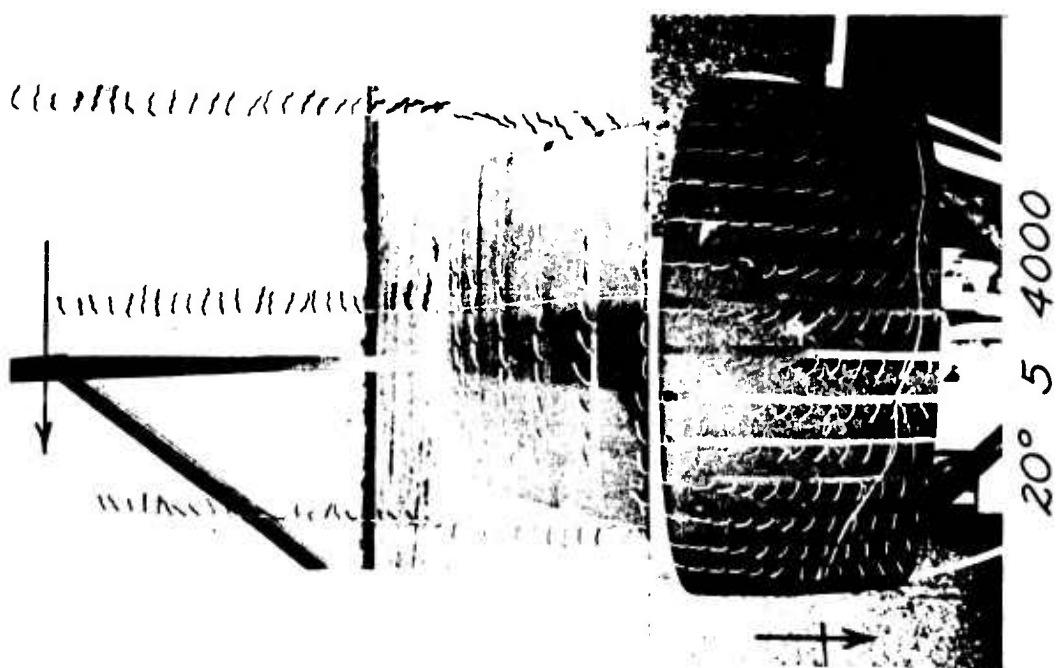
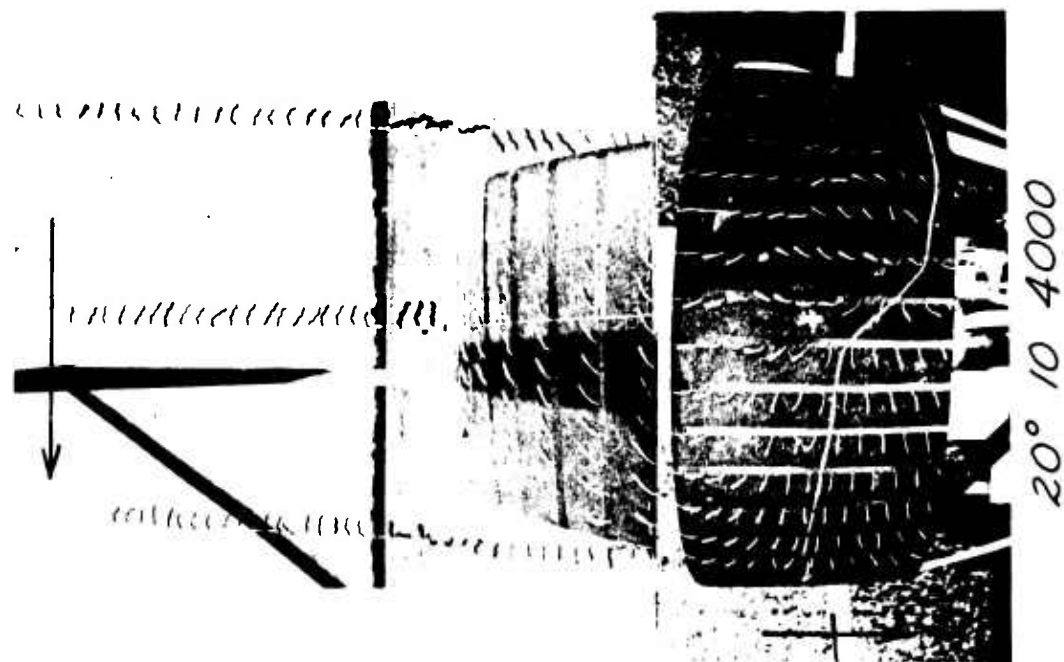


Figure 14 (Cont.). Tuft Patterns - Rearward Motion.

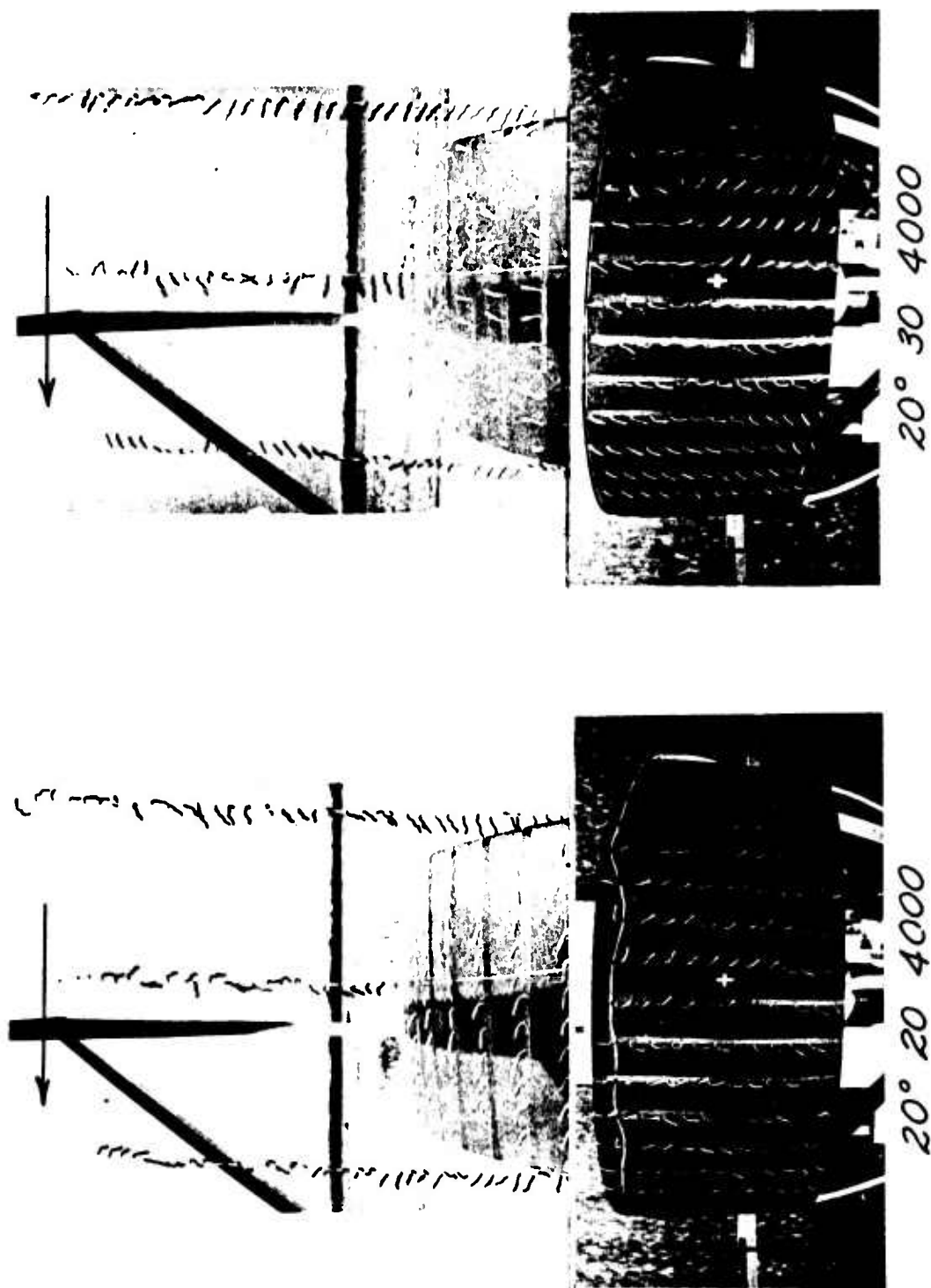


Figure 14 (Cont.). Tuft Patterns - Rearward Motion.



5° 10 5000



5° 5 5000

Figure 14 (Cont.). Tuft Patterns - Rearward Motion.

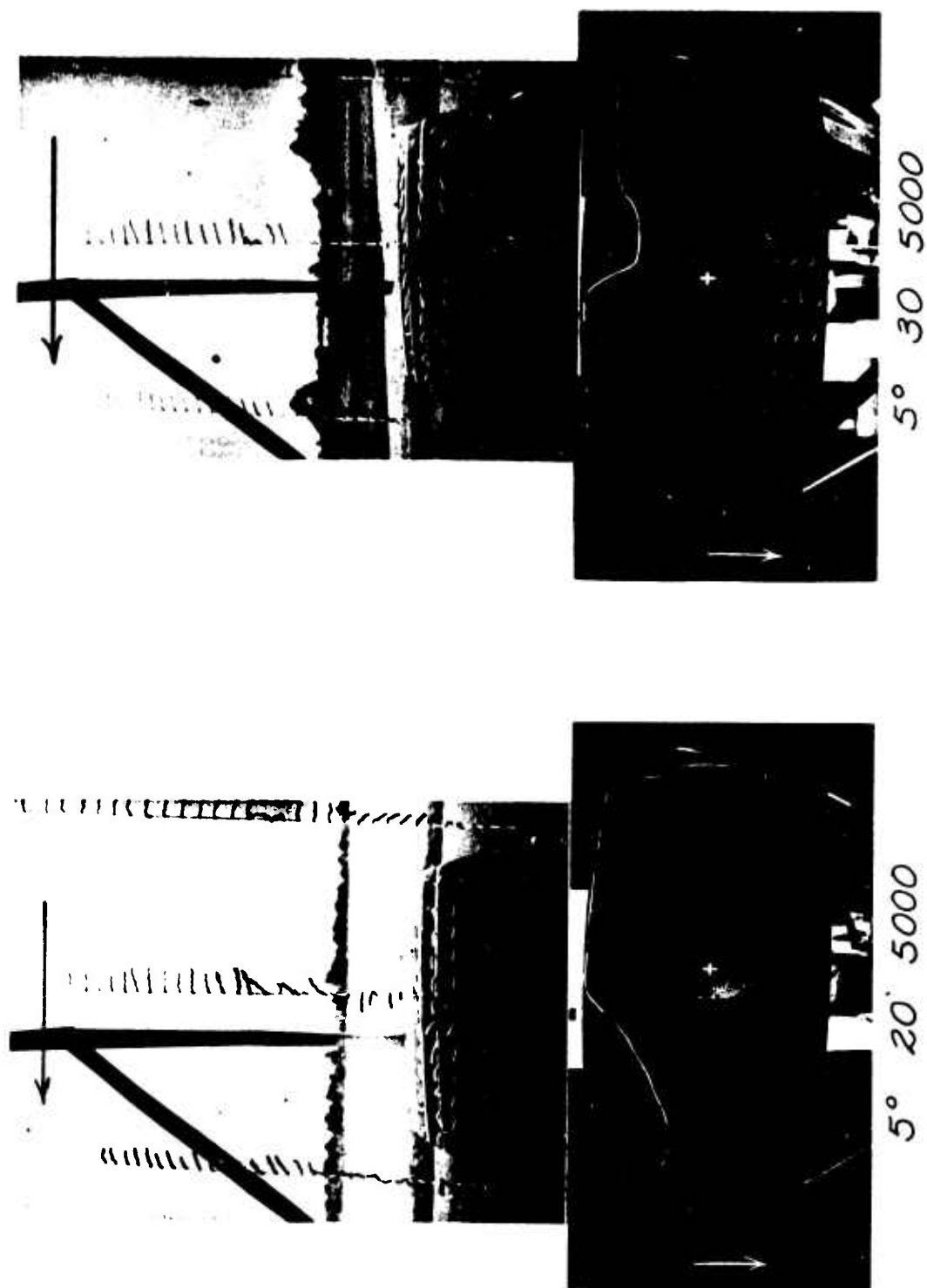


Figure 14 (Cont.). Tuft Patterns - Rearward Motion.

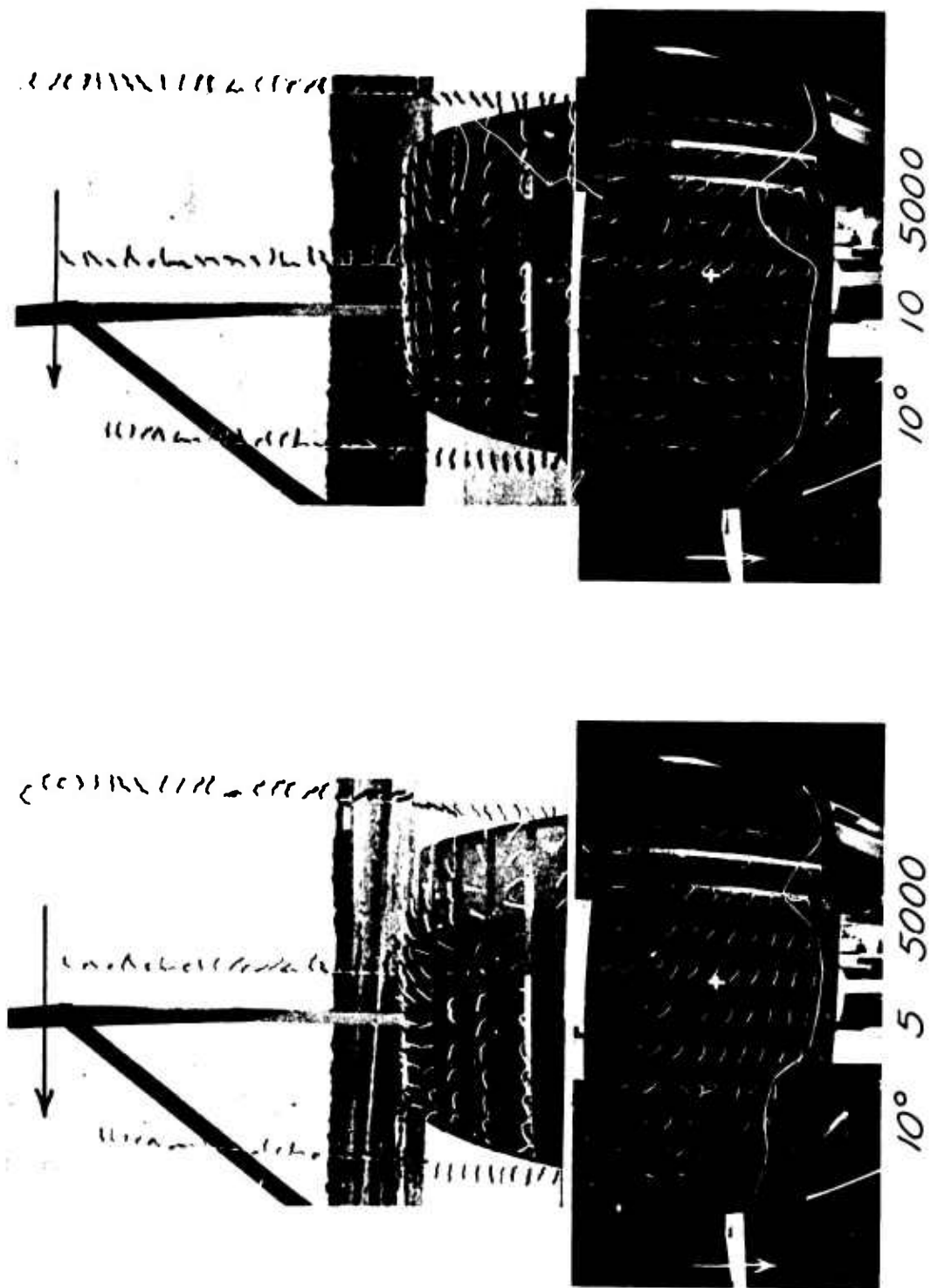
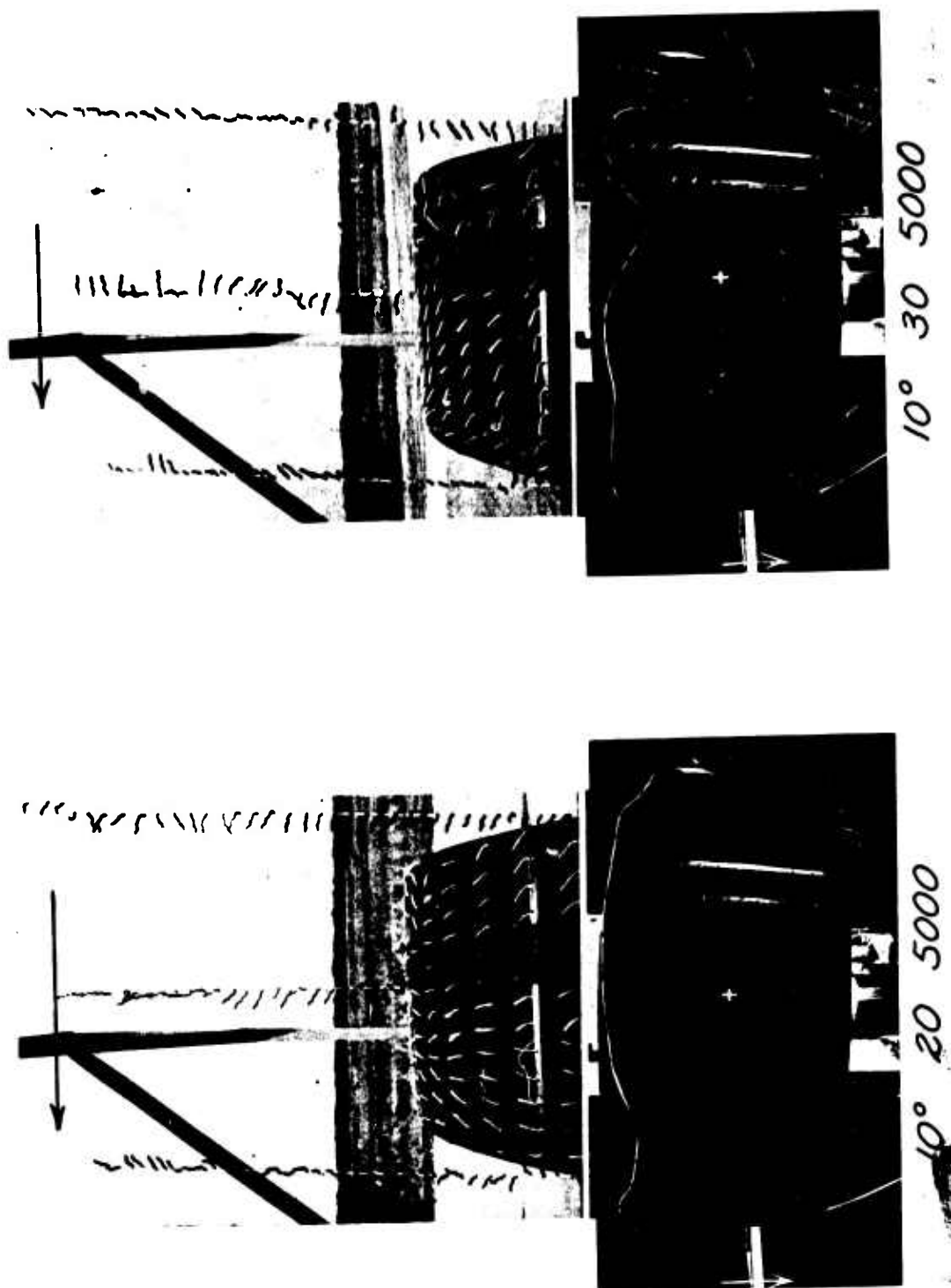


Figure 14 (Cont.). Tuft Patterns - Rearward Motion.



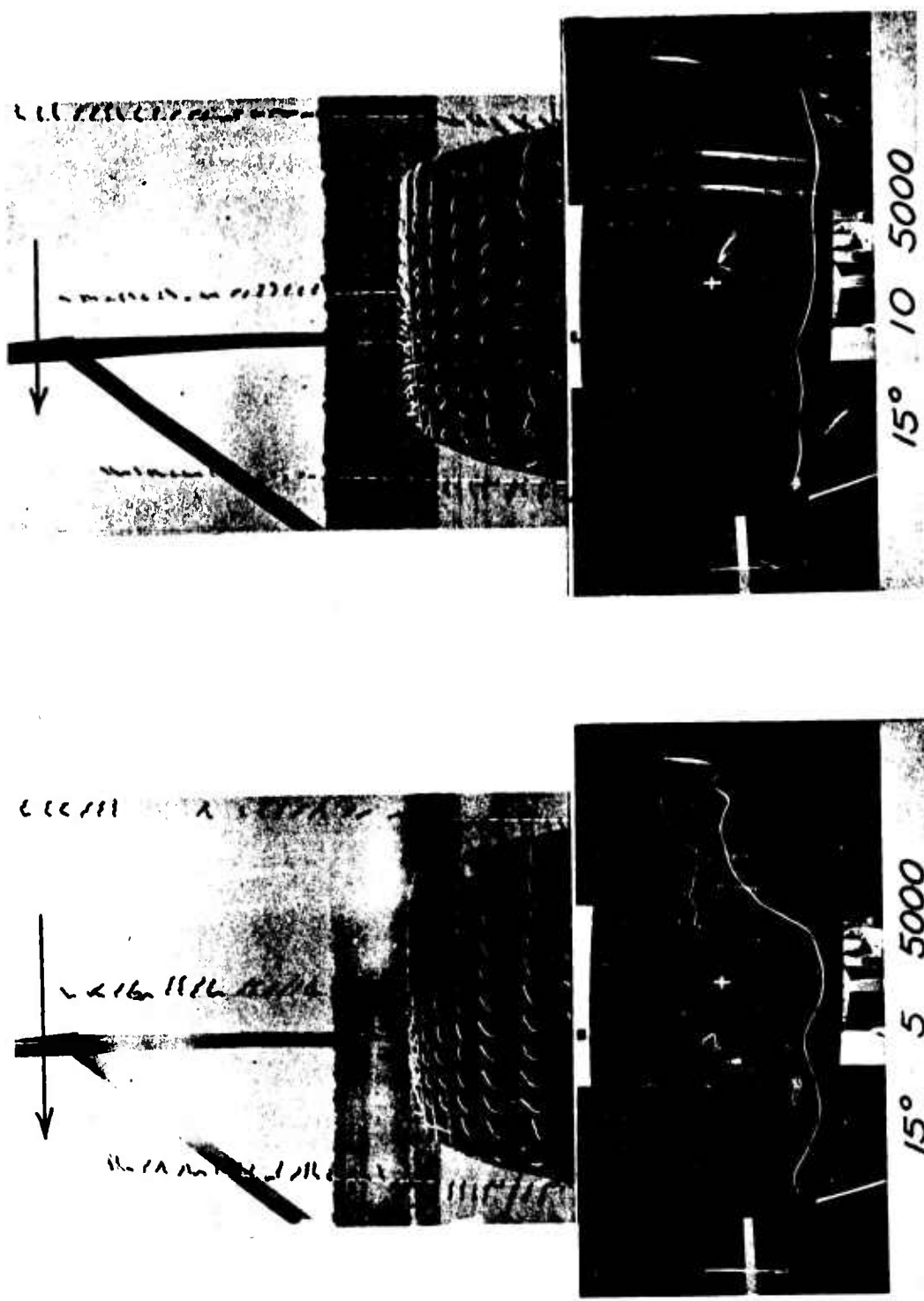


Figure 14 (Cont.). Tuft Patterns - Rearward Motion.

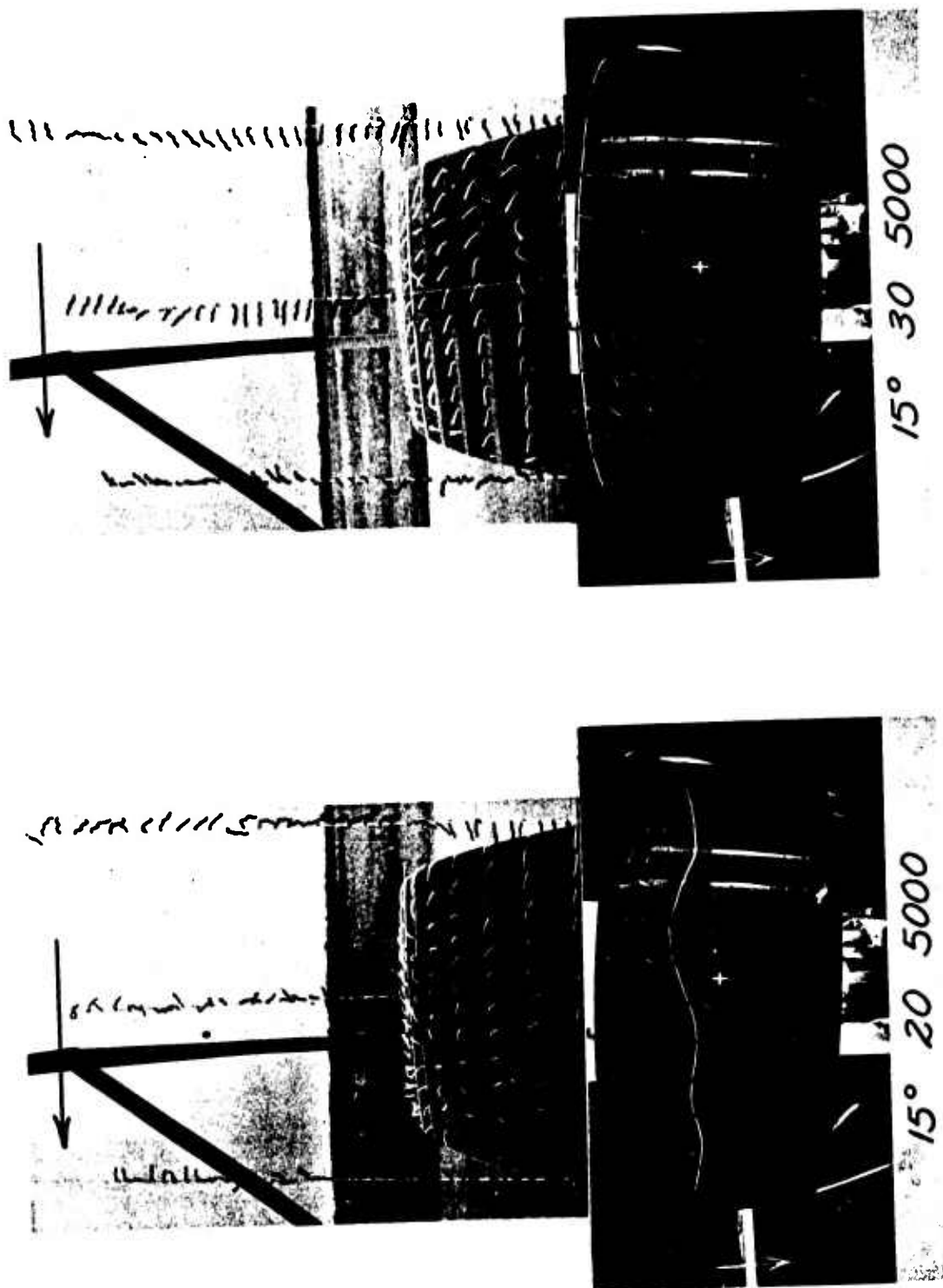


Figure 14 (Cont.). Tuft Patterns - Rearward Motion.

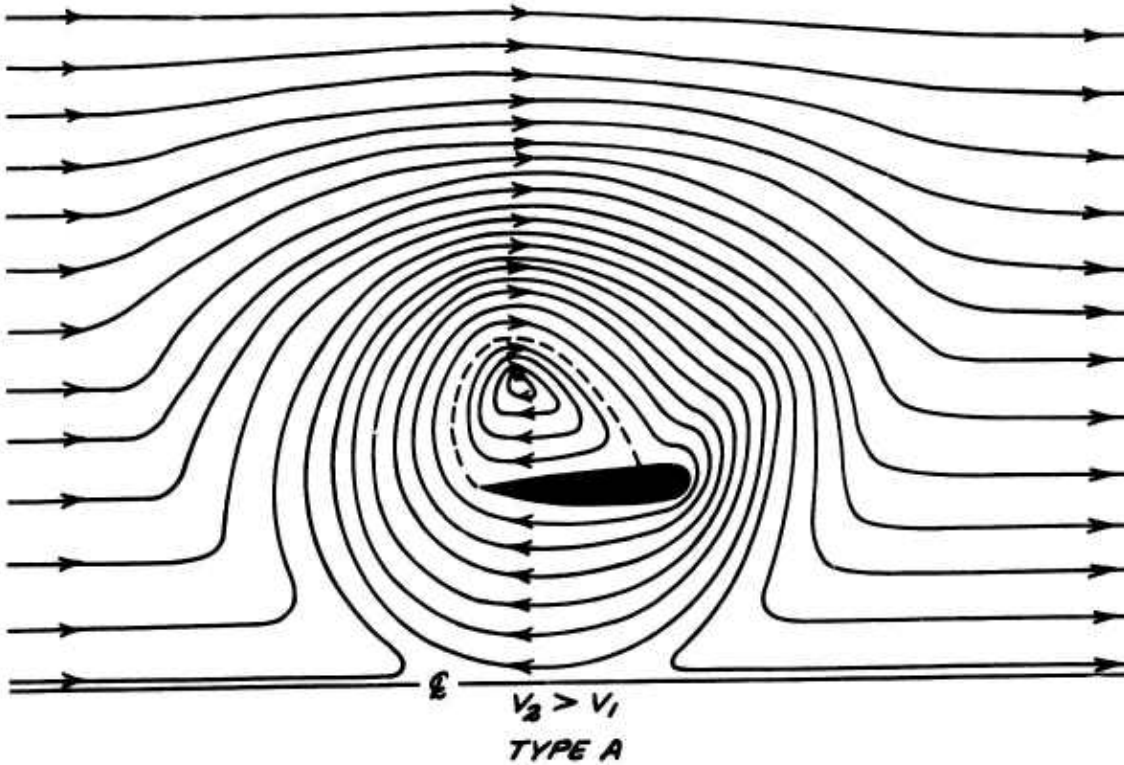
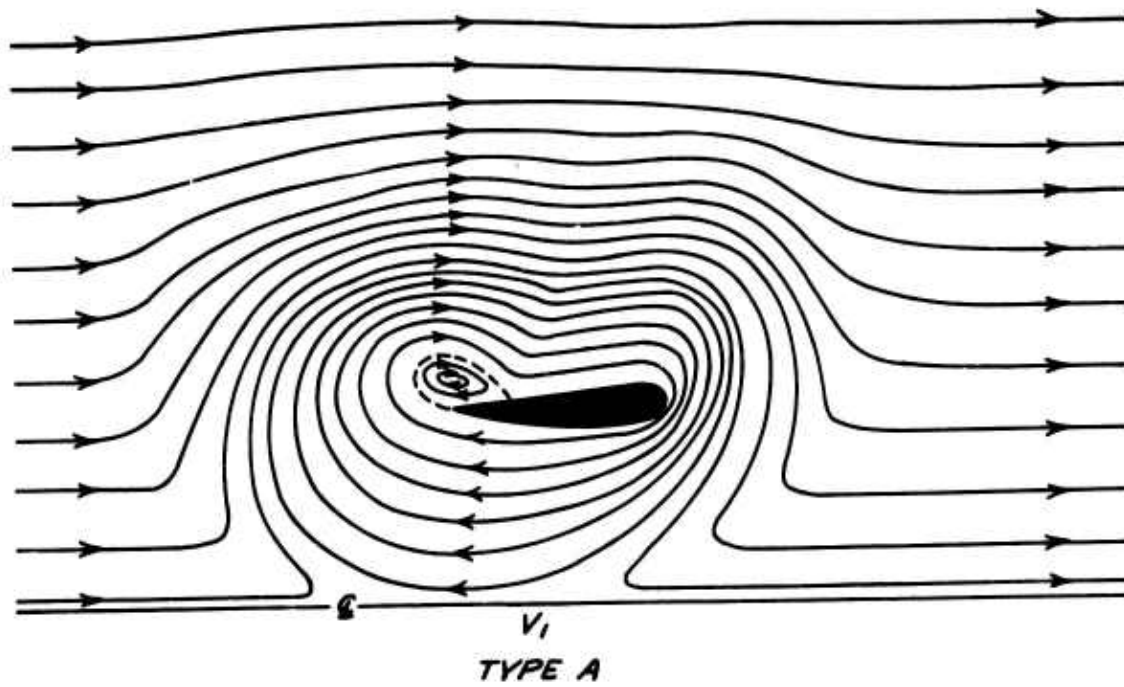


Figure 15-a. Flow Patterns - Rearward Motion.

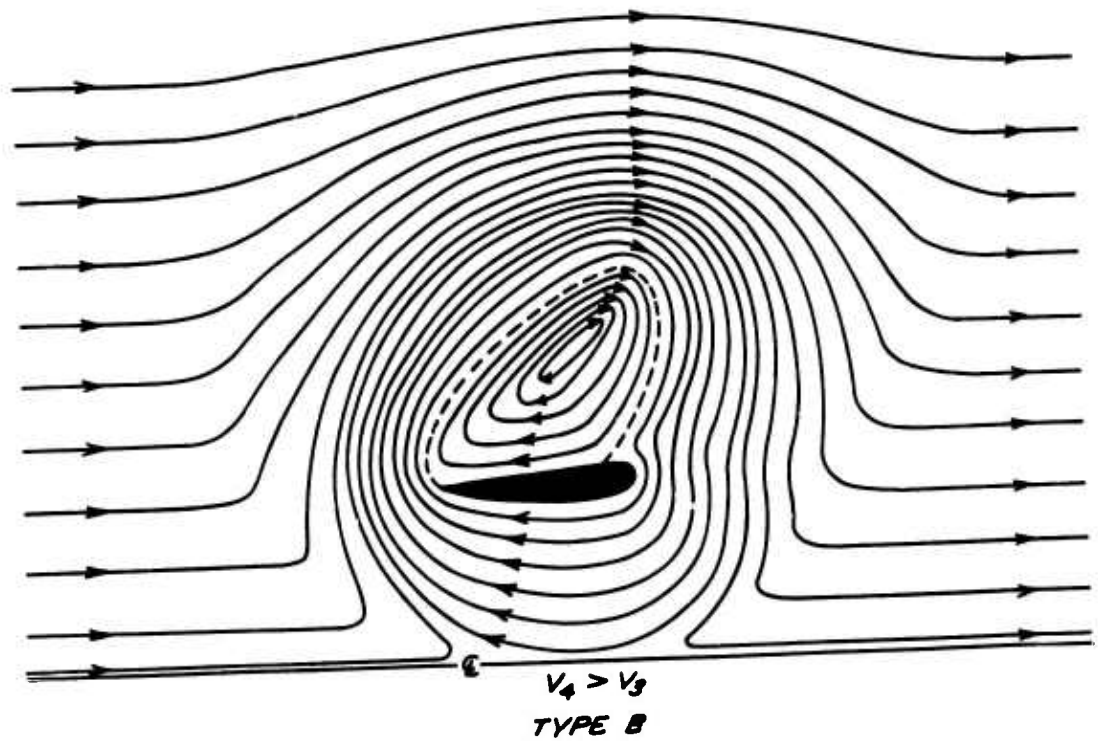
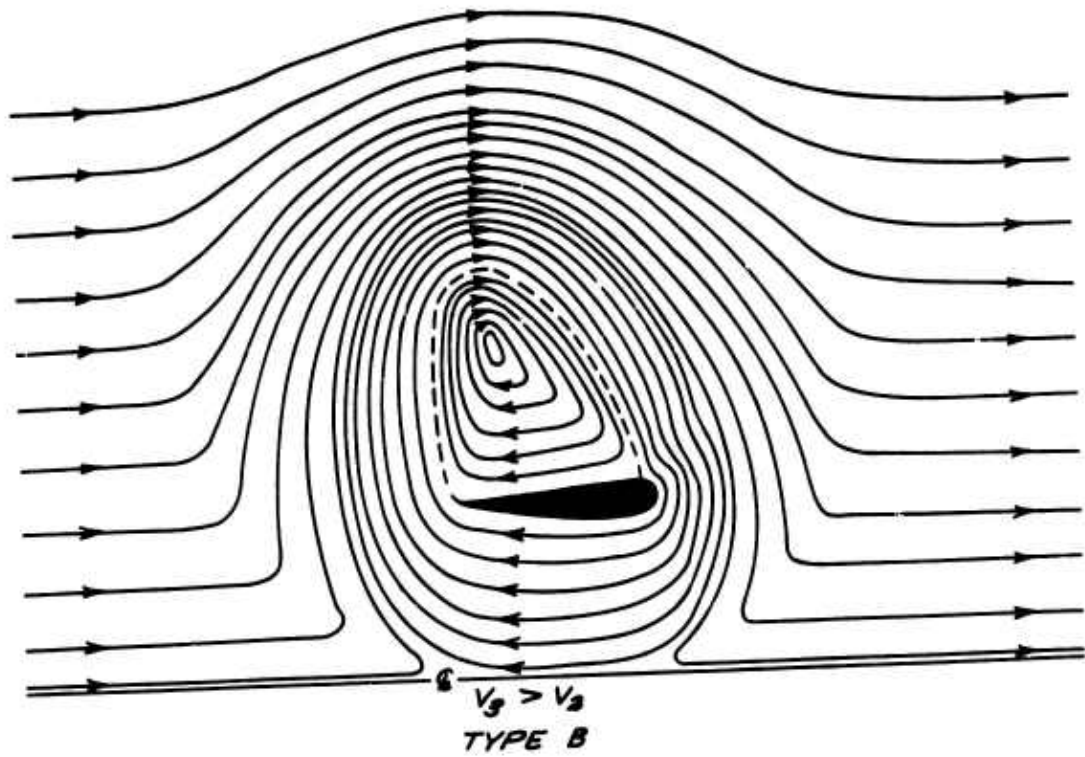


Figure 15-b. Flow Patterns - Rearward Motion.

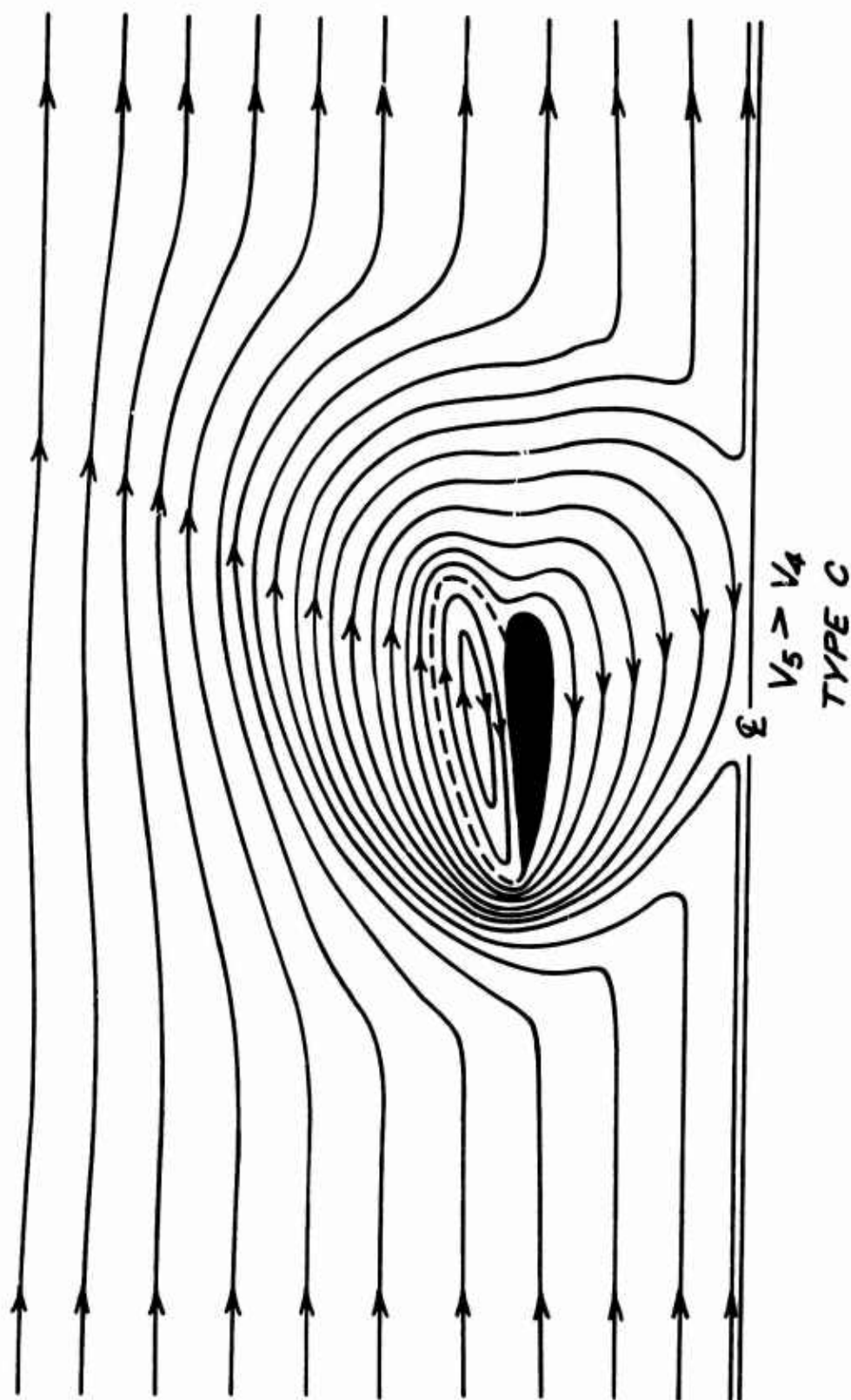


Figure 15-c. Flow Patterns - Rearward Motion.

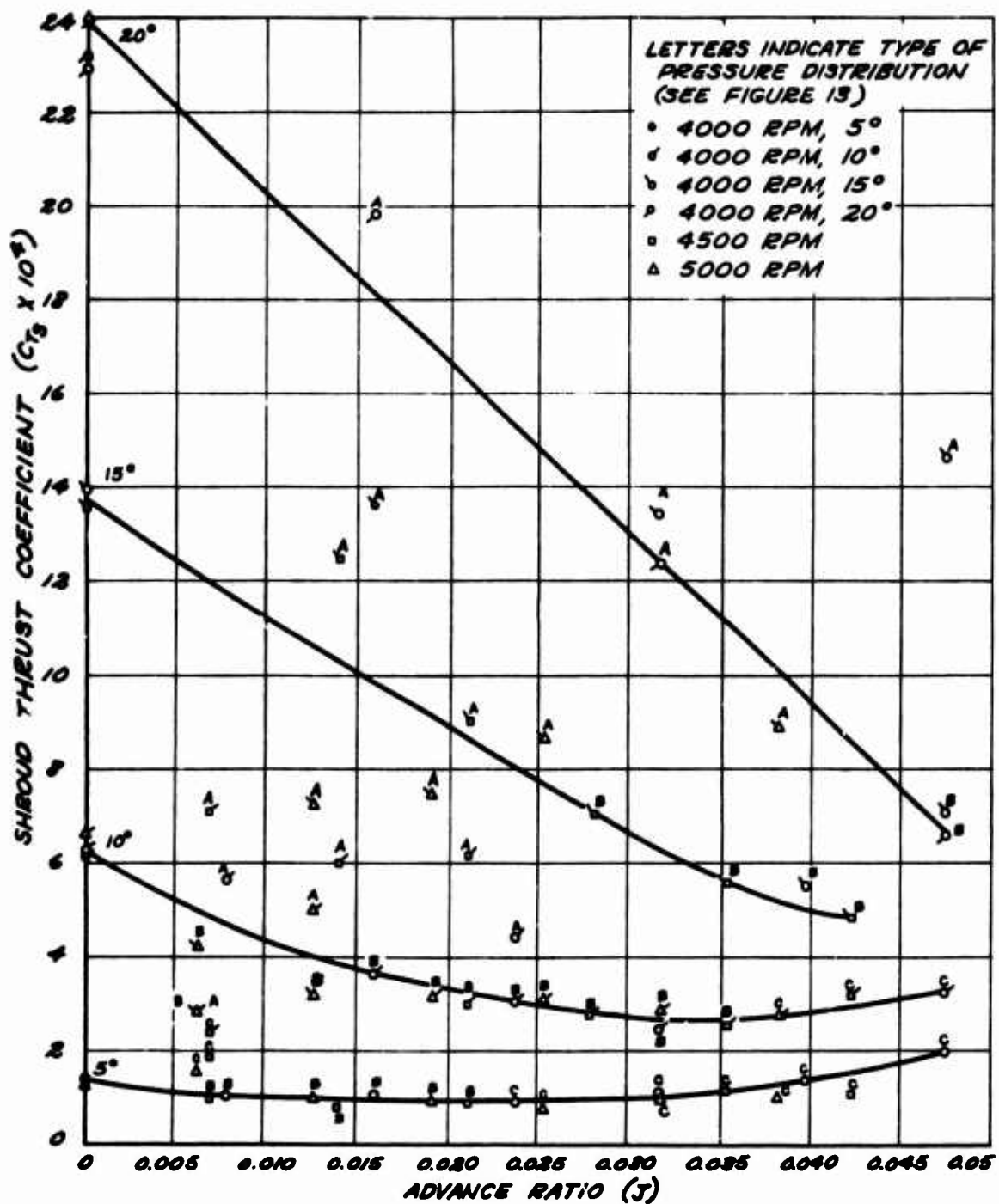


Figure 16. Shroud Thrust - Rearward Motion.

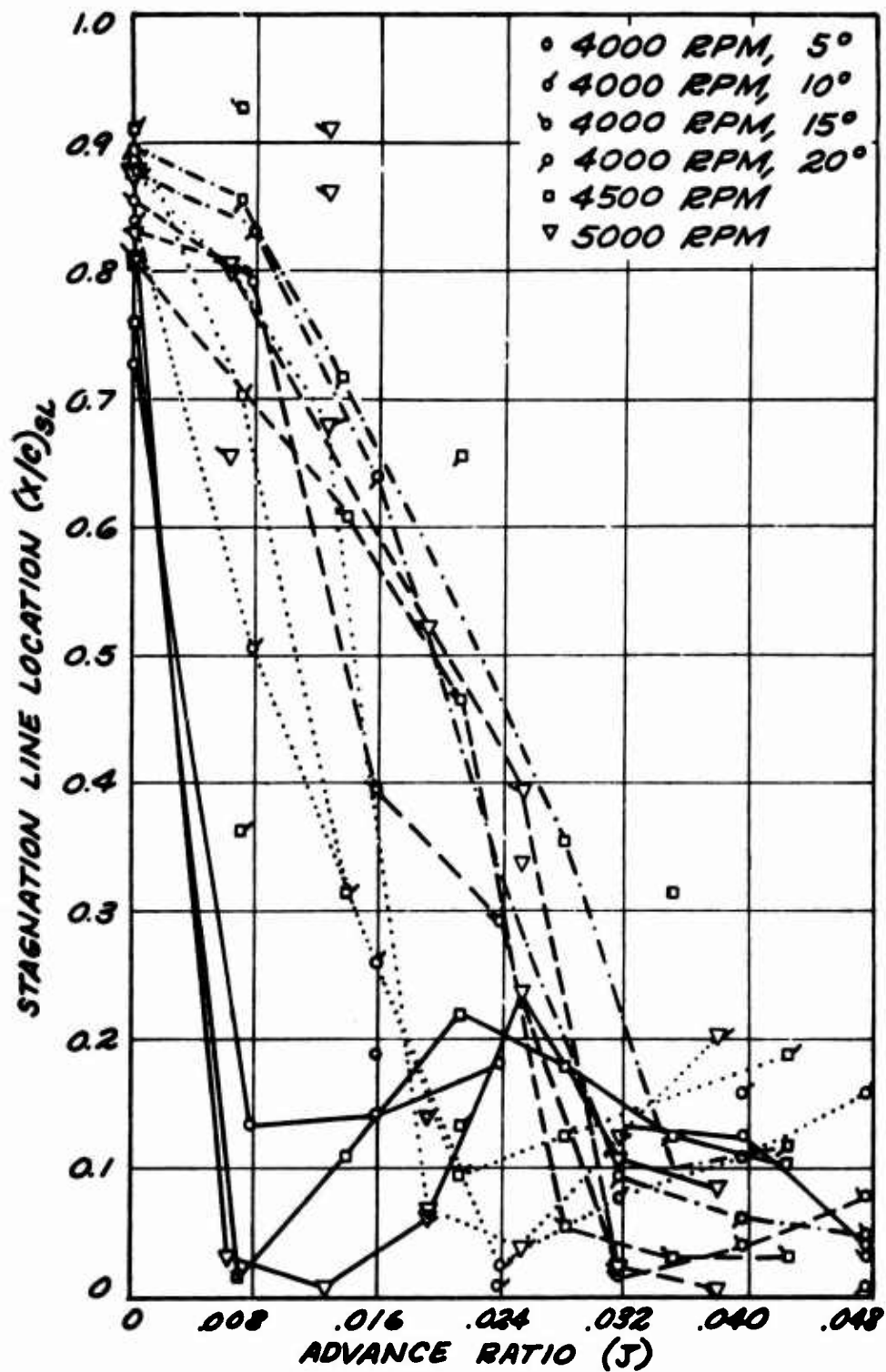


Figure 17. Stagnation Line Location - Rearward Motion.

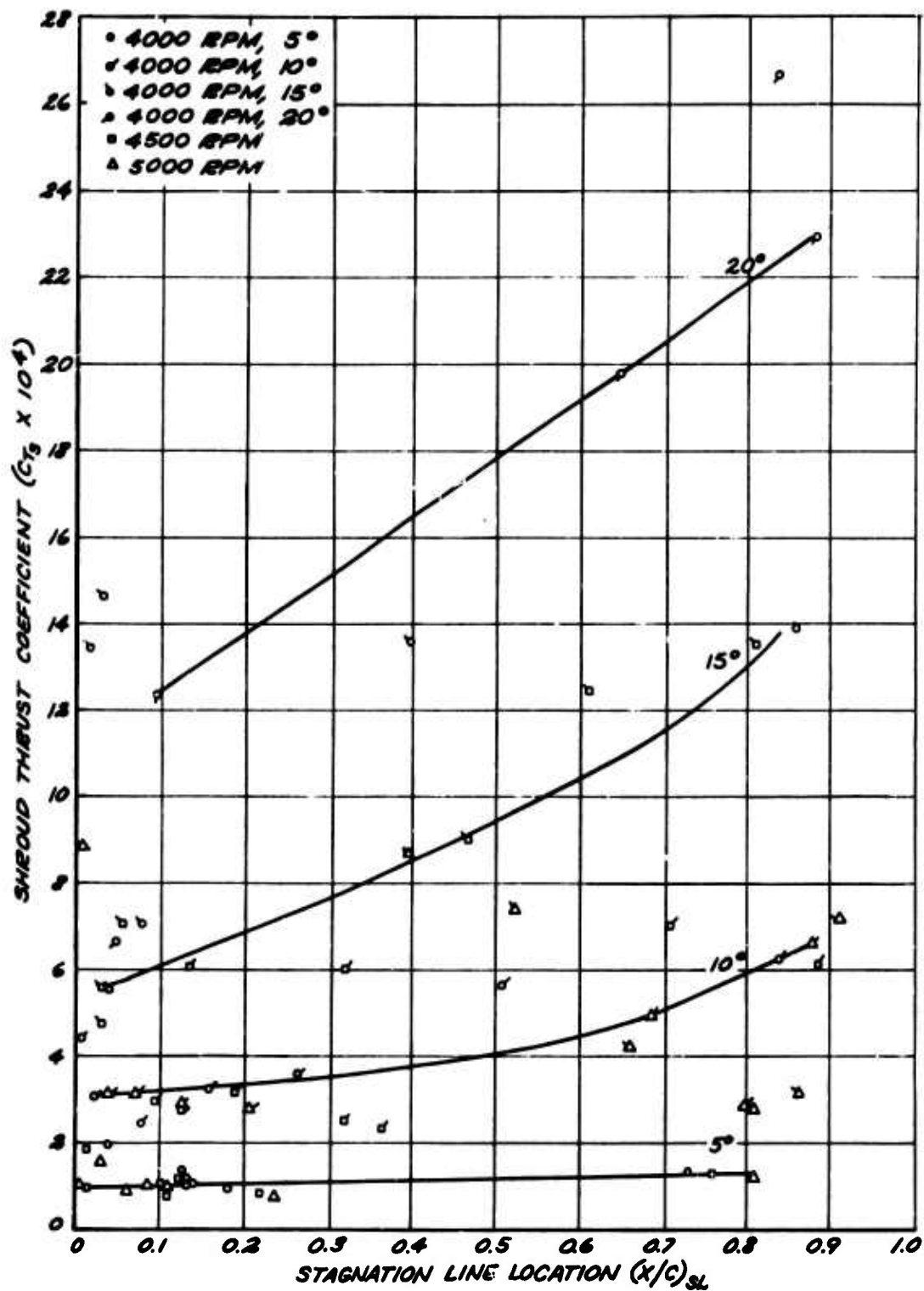


Figure 18. Relation of Shroud Thrust to Stagnation Line Location.

Figure 19 (a-j). Shroud Pressure Distributions - Forward Motion.

Legend: ————— 5° pitch angle
— — — — — 10° pitch angle
— · — — — 15° pitch angle
· · · · · 20° pitch angle
— + — + — curves which correspond to
inside surface of shroud

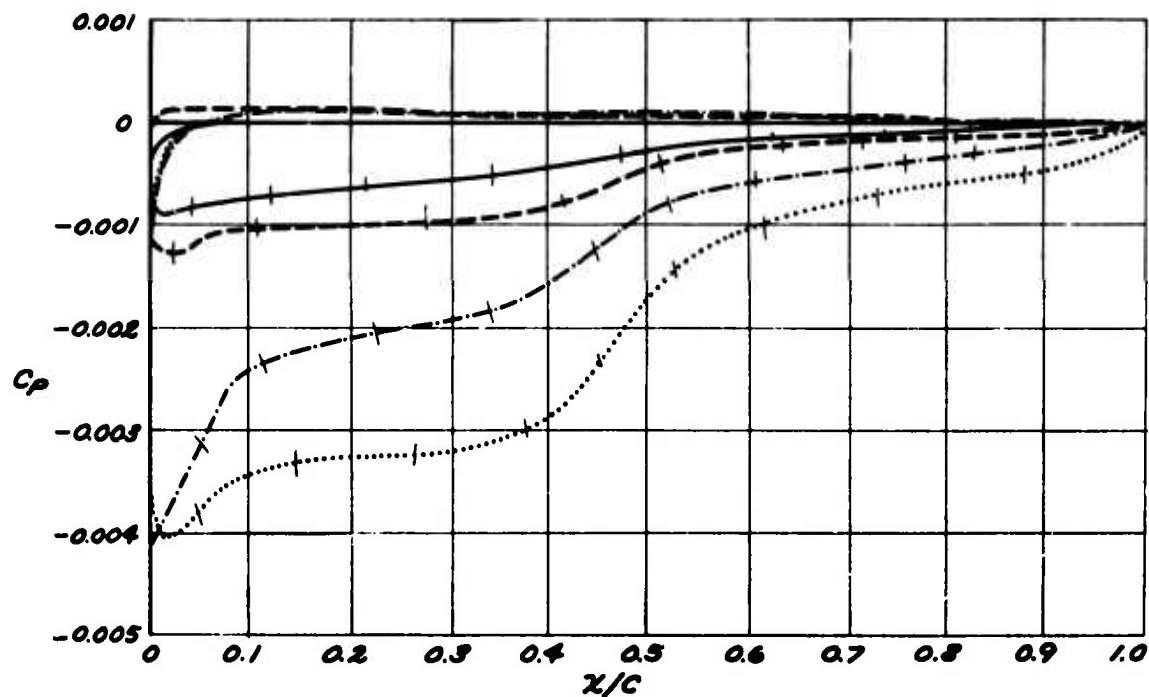


Figure 19-a. Shroud Pressure Distribution - Forward Motion, 4000 RPM, 5 MPH.

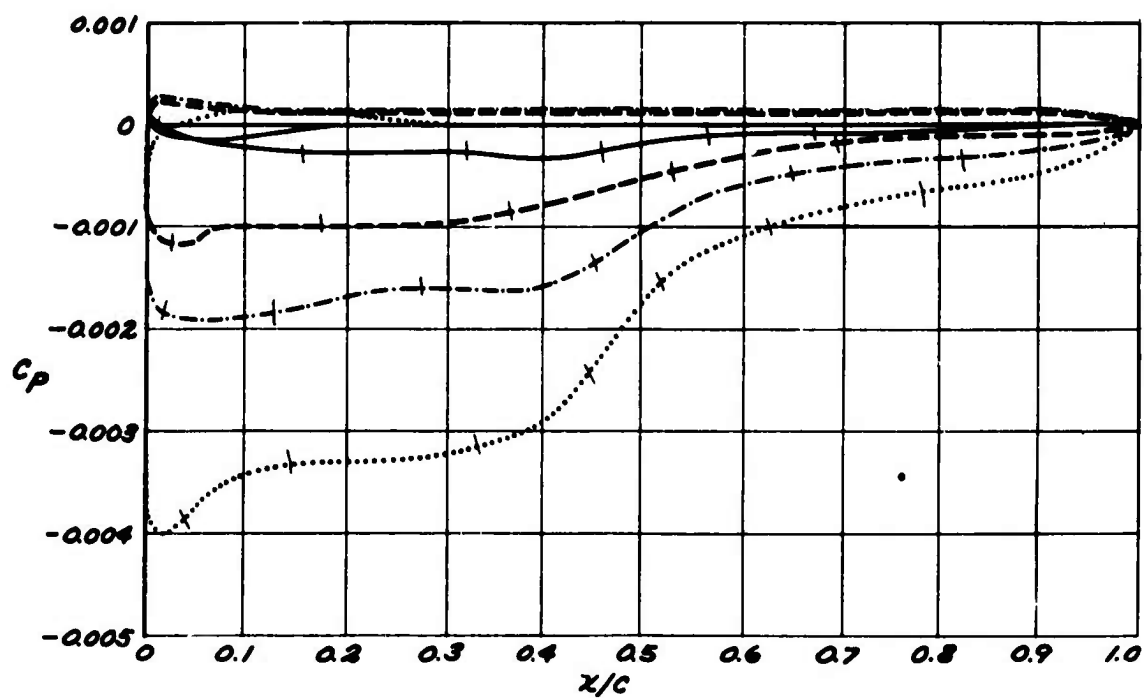


Figure 19-b. Shroud Pressure Distribution - Forward Motion, 4000 RPM, 10 MPH.

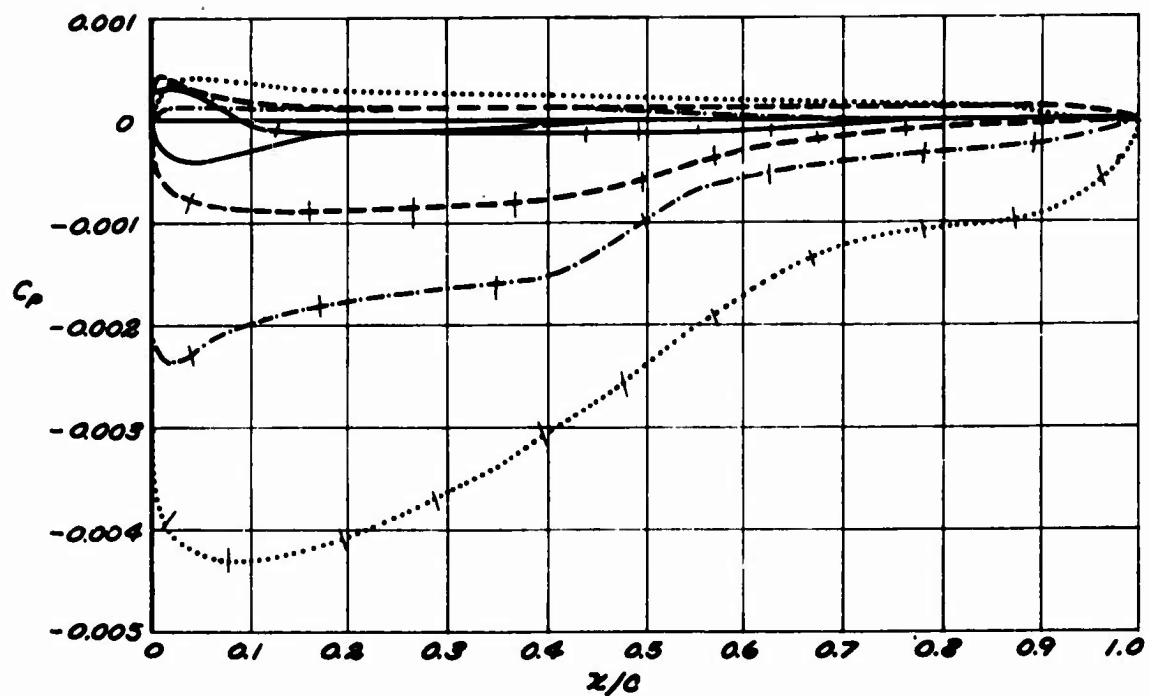


Figure 19-c. Shroud Pressure Distribution - Forward Motion, 4000 RPM, 15 MPH.

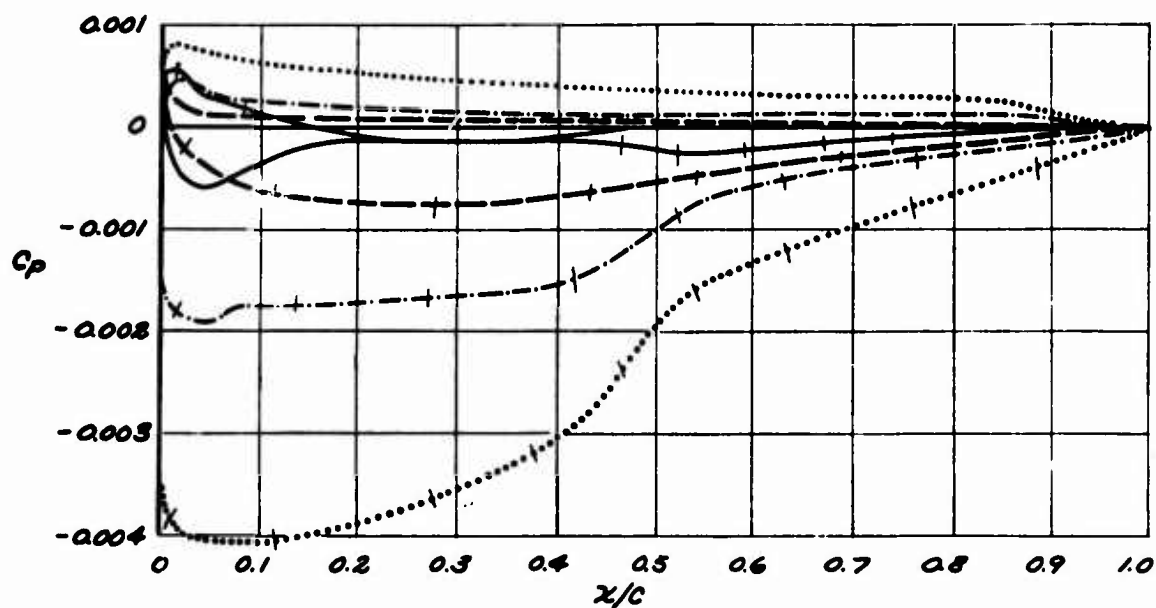


Figure 19-d. Shroud Pressure Distribution - Forward Motion, 4000 RPM, 20 MPH.

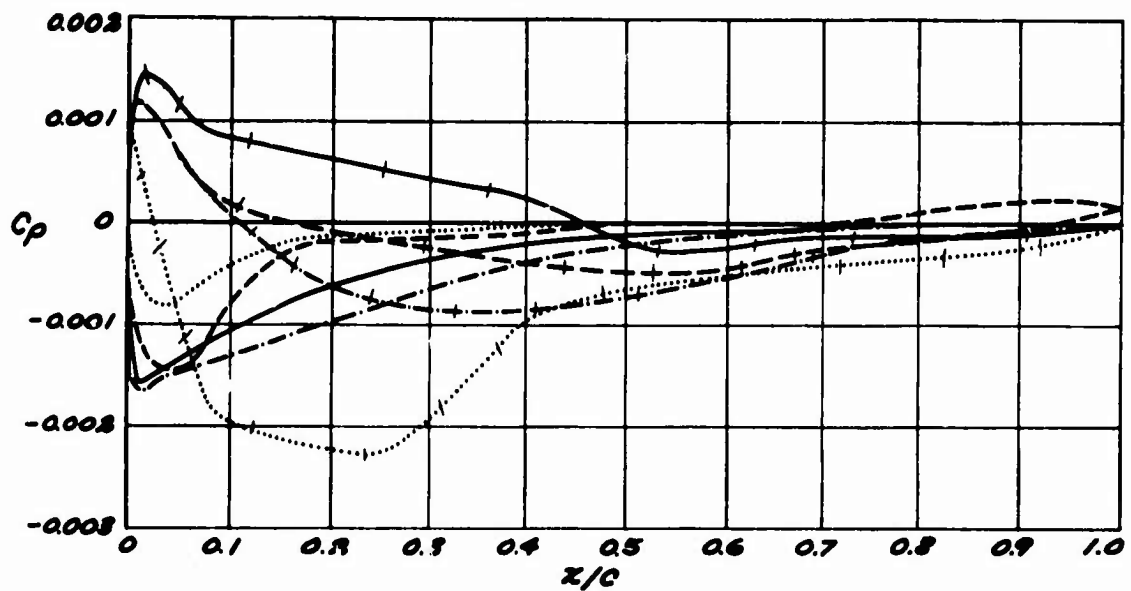


Figure 19-e. Shroud Pressure Distribution - Forward Motion, 4000 RPM, 30 MPH.

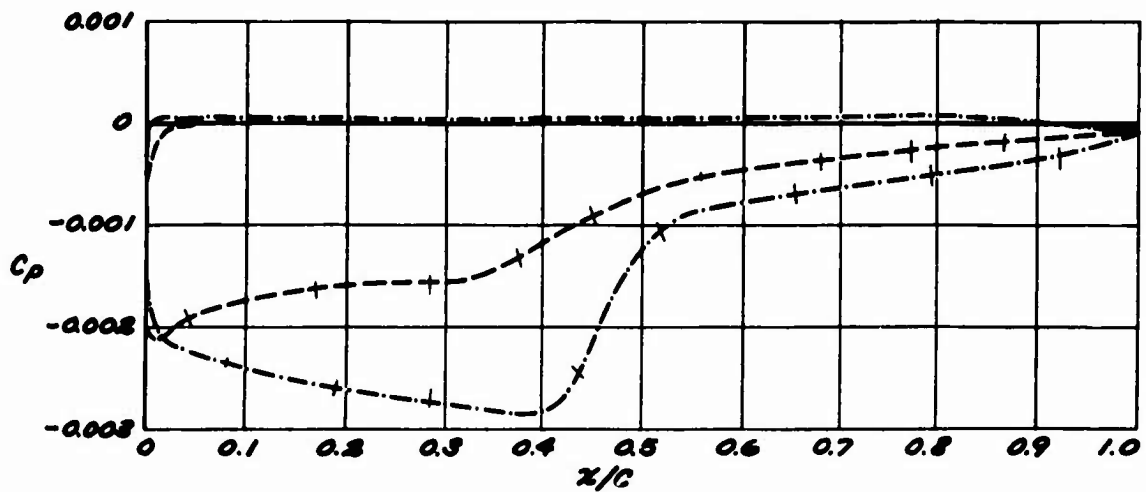


Figure 19-f. Shroud Pressure Distribution - Forward Motion, 5000 RPM, 5 MPH.

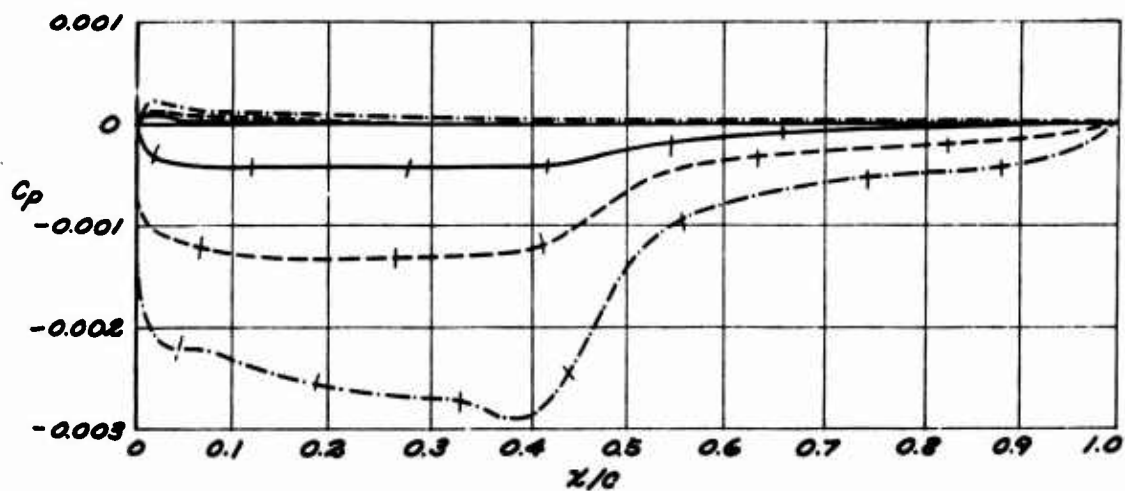


Figure 19-g. Shroud Pressure Distribution - Forward Motion,
5000 RPM, 10 MPH.

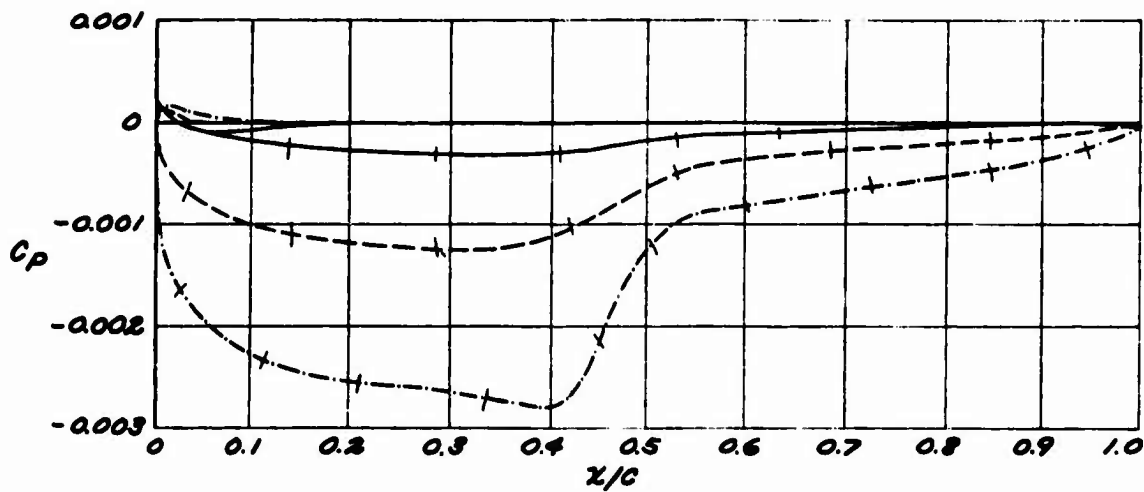


Figure 19-h. Shroud Pressure Distribution - Forward Motion,
5000 RPM, 15 MPH.

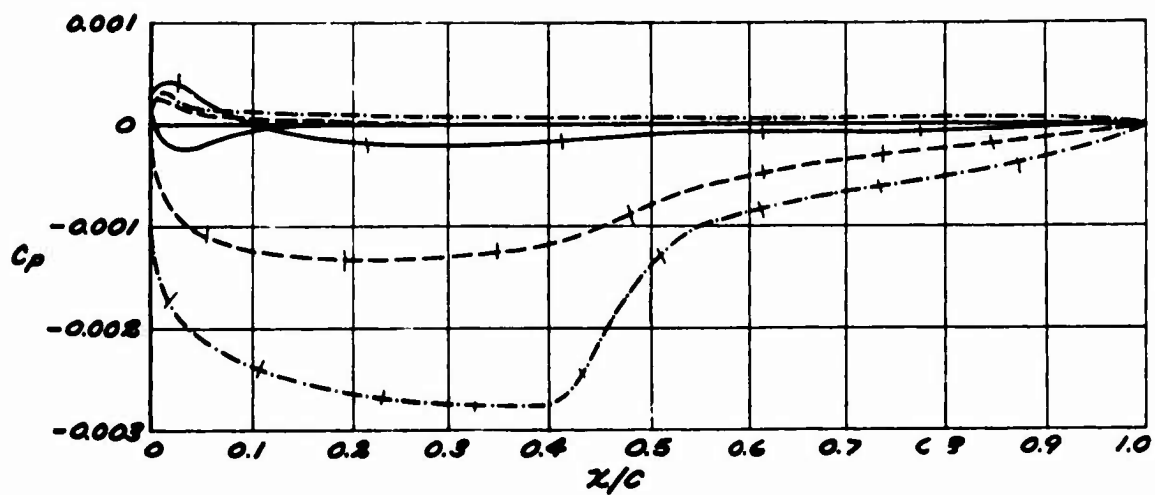


Figure 19-i. Shroud Pressure Distribution - Forward Motion, 5000 RPM, 20 MPH.

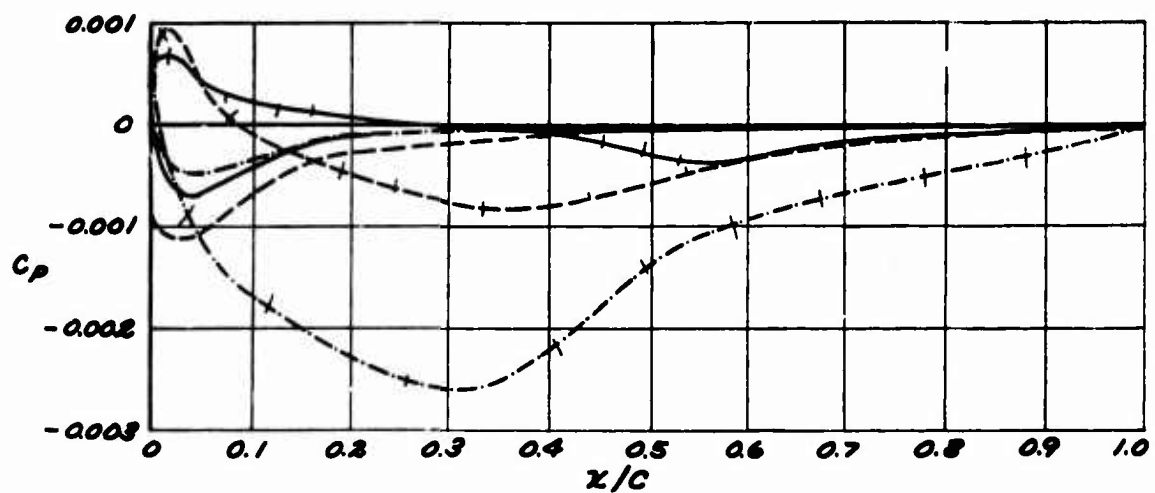


Figure 19-j. Shroud Pressure Distribution - Forward Motion, 4500 RPM, 20 MPH.

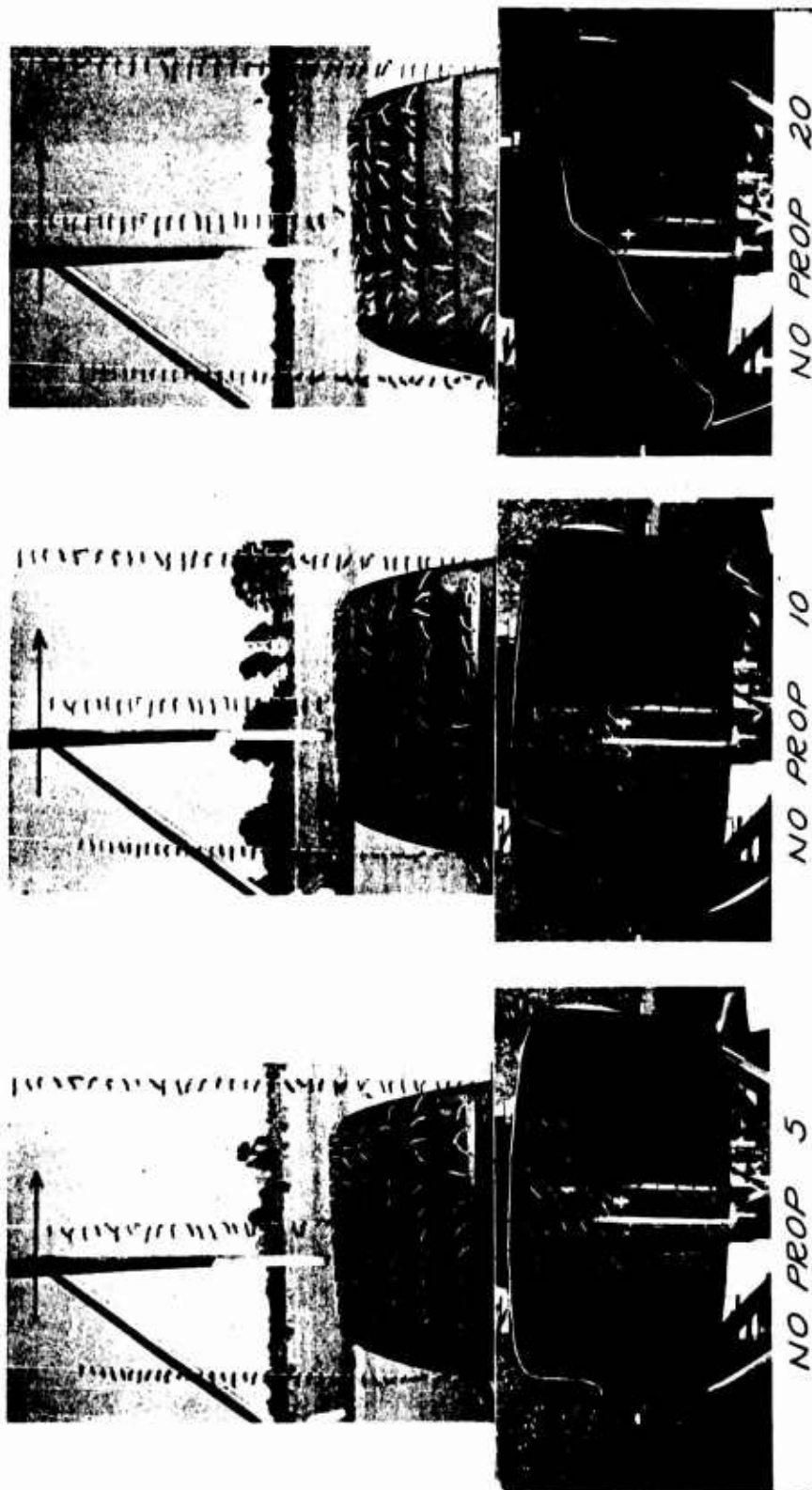


Figure 20. Tuft Patterns - Forward Motion.

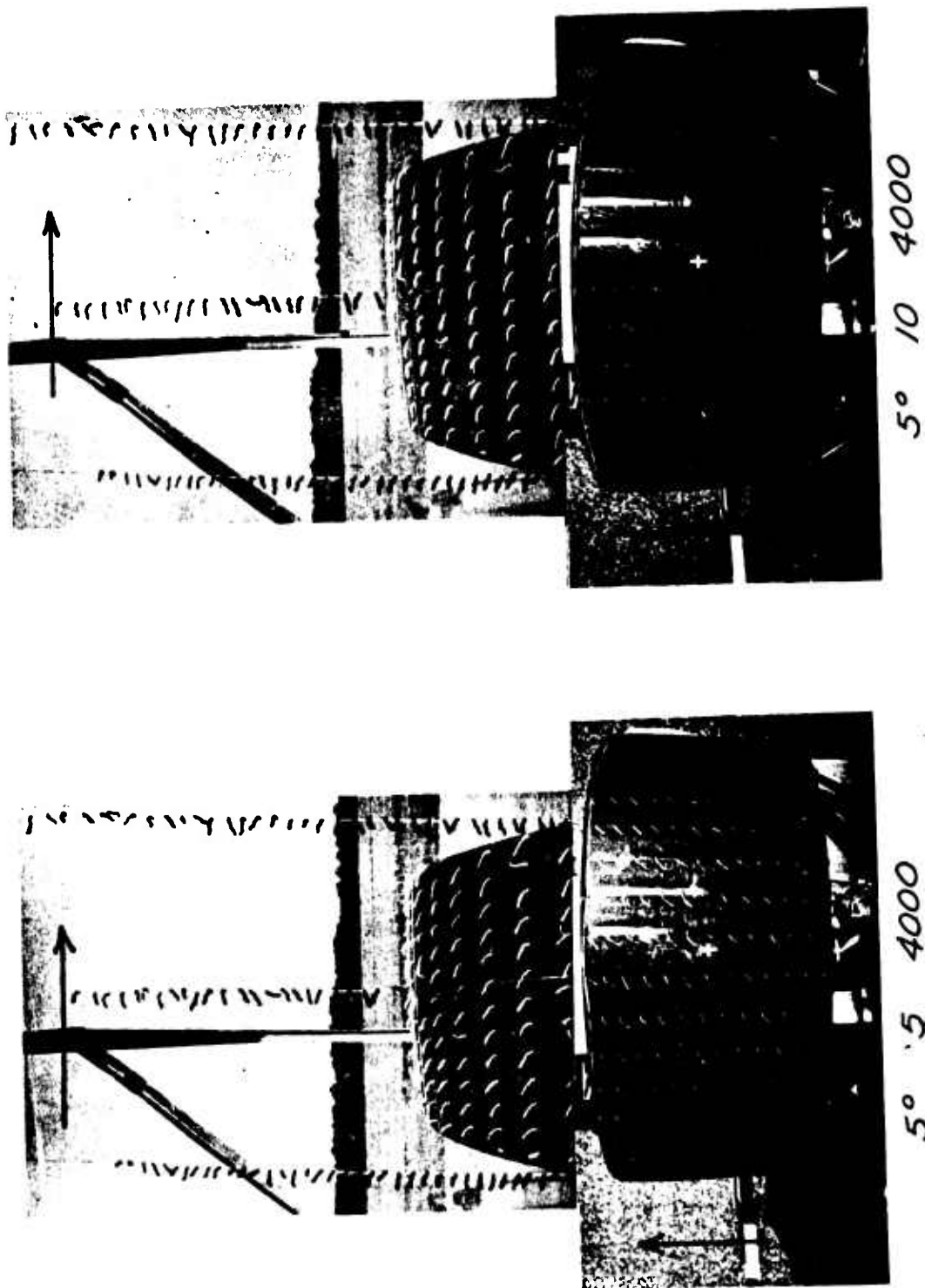
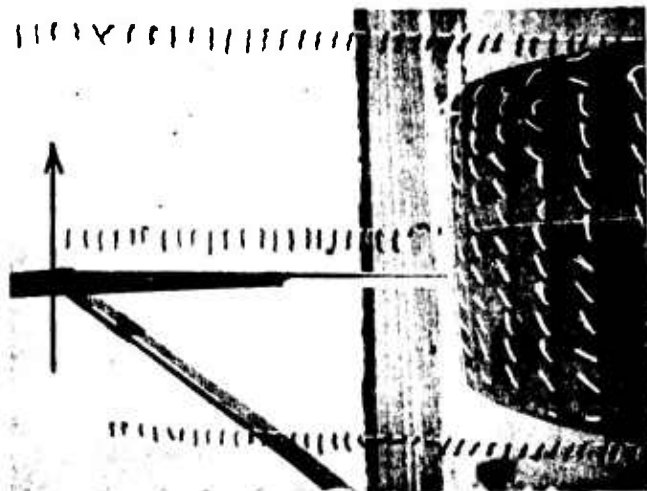
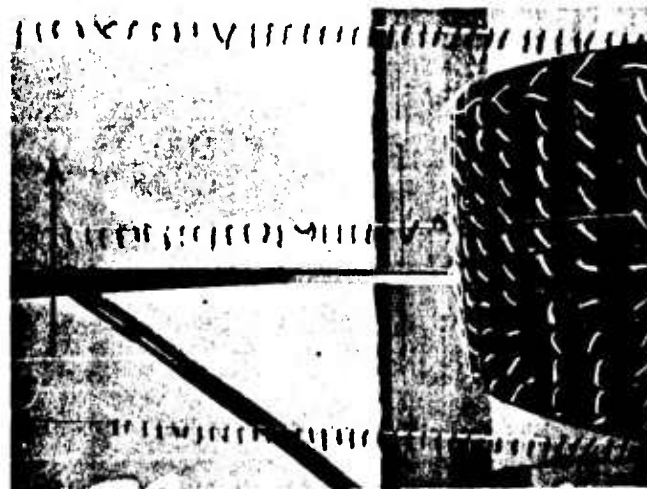


Figure 20 (Cont.). Tuft Patterns - Forward Motion.



5° 30 4000



5° 20 4000

Figure 20 (Cont.). Tuft Patterns - Forward Motion.

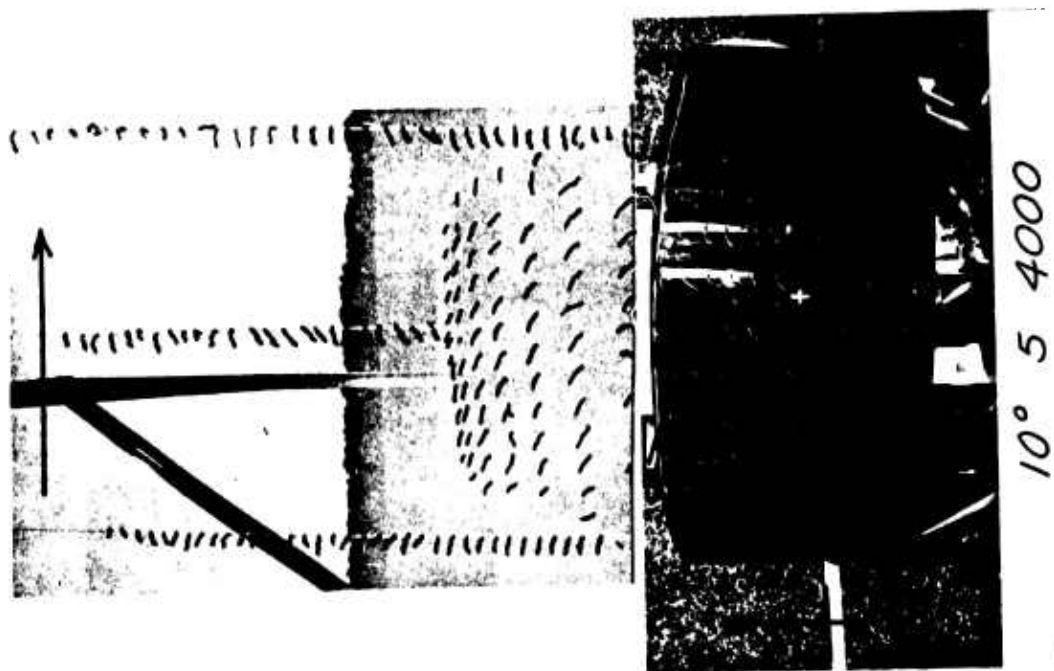
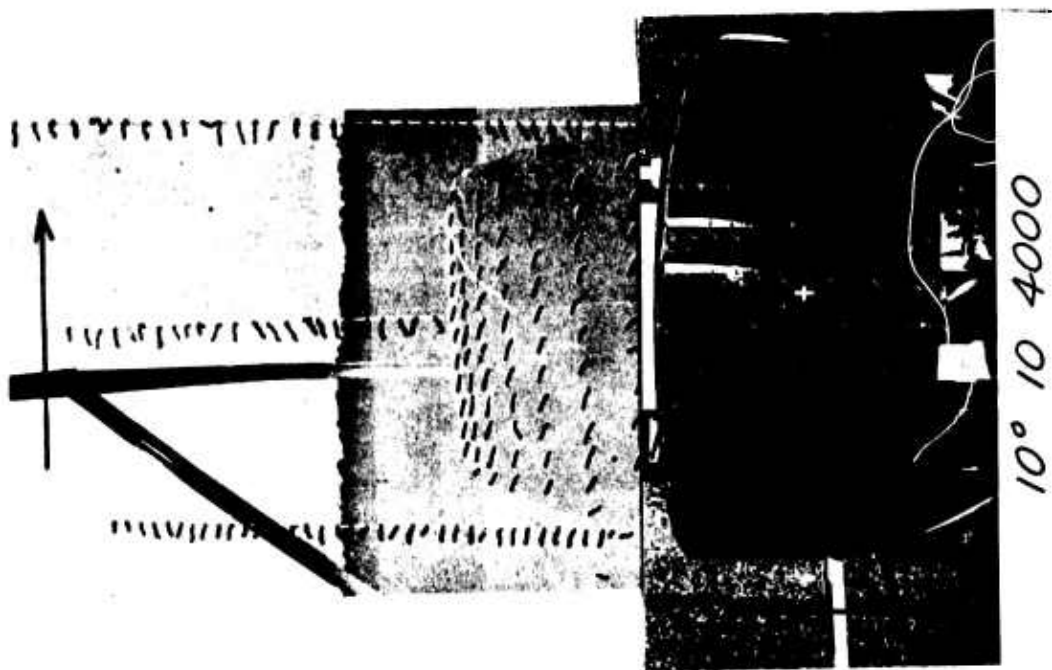


Figure 20 (Cont.). Tuft Patterns - Forward Motion.

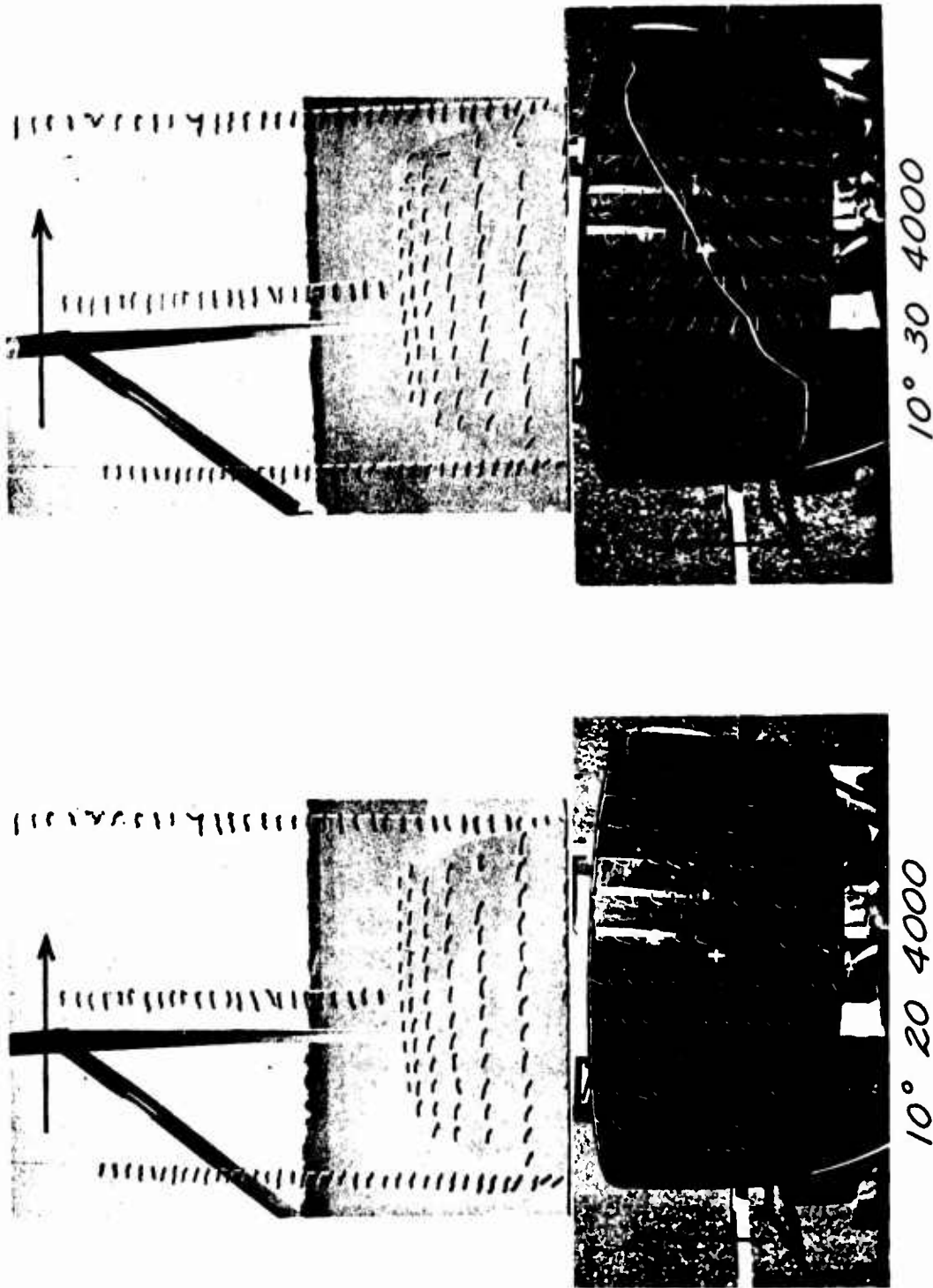


Figure 20 (Cont.). Tuft Patterns - Forward Motion.

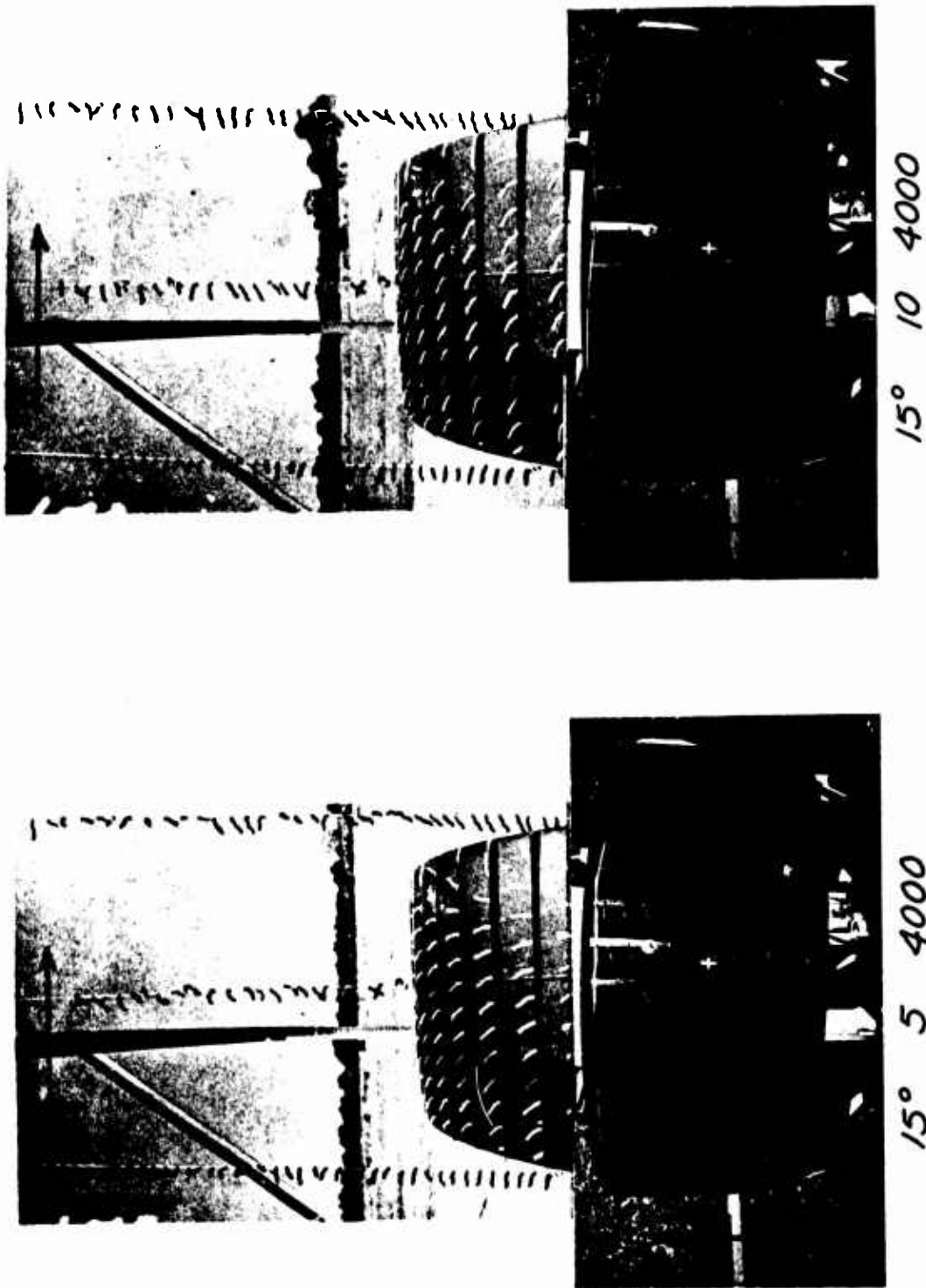


Figure 20 (Cont.). Tuft Patterns - Forward Motion.

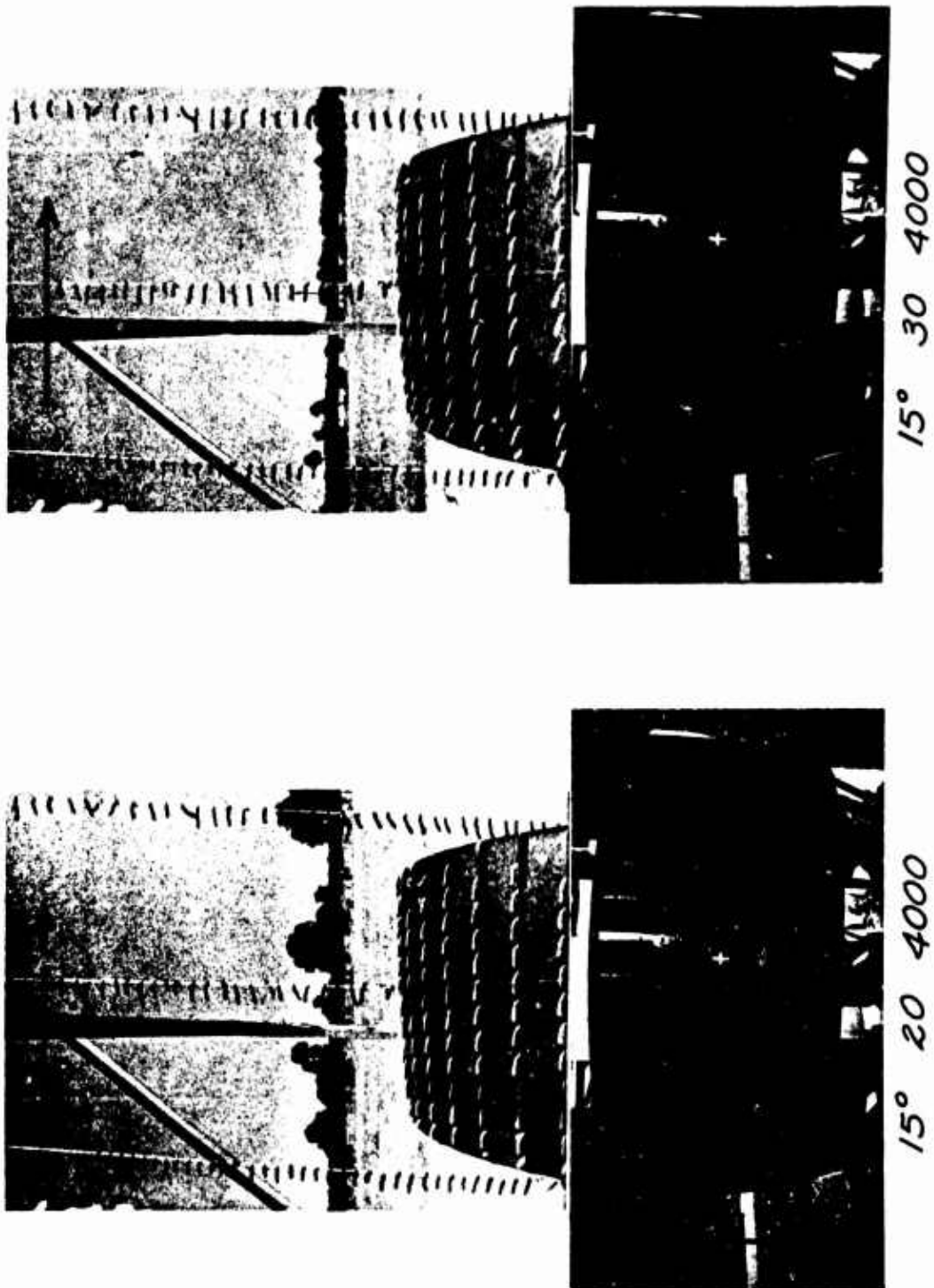


Figure 20 (Cont.). Tuft Patterns - Forward Motion.

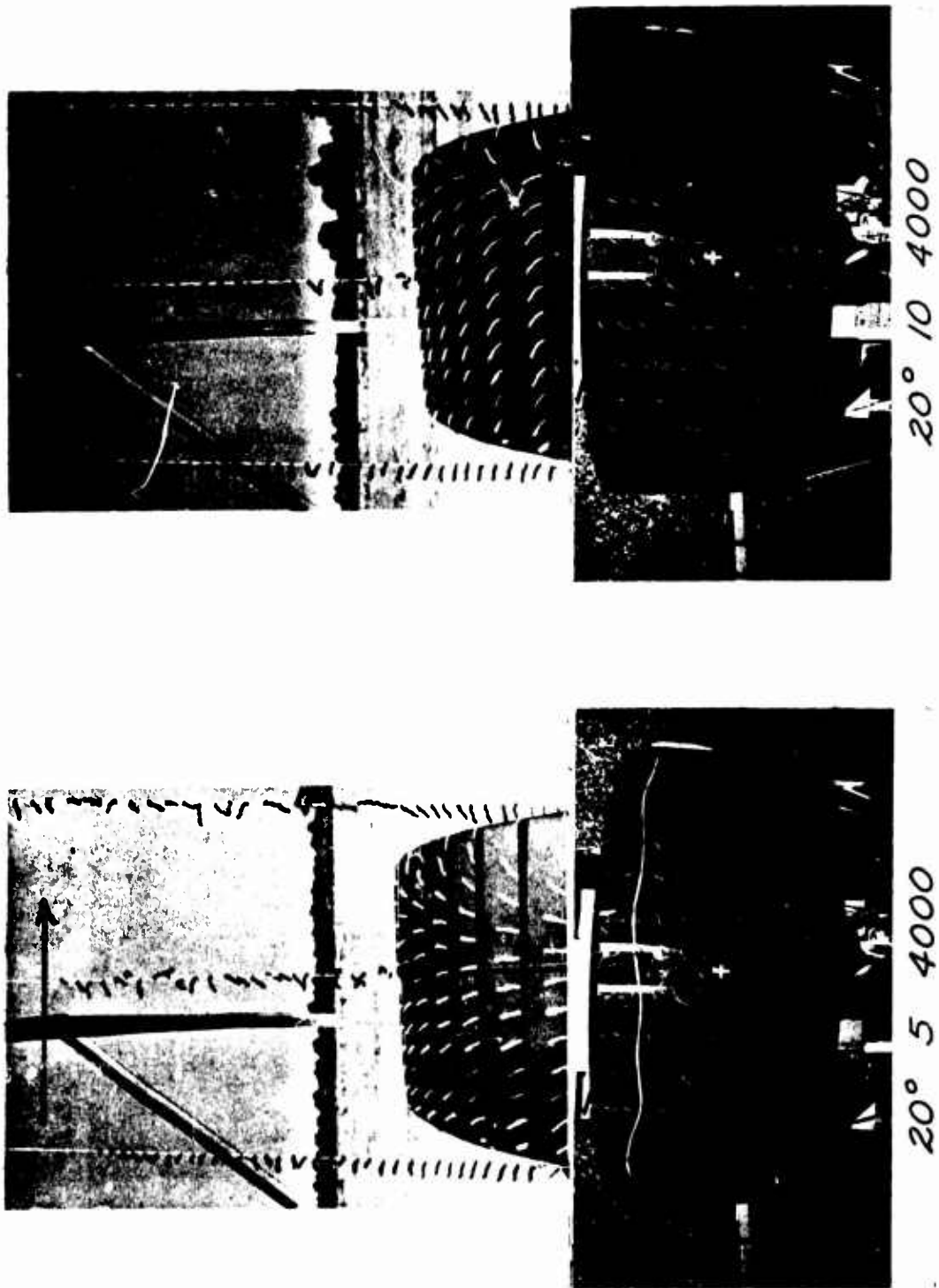


Figure 20 (Cont.). Tuft Patterns - Forward Motion.

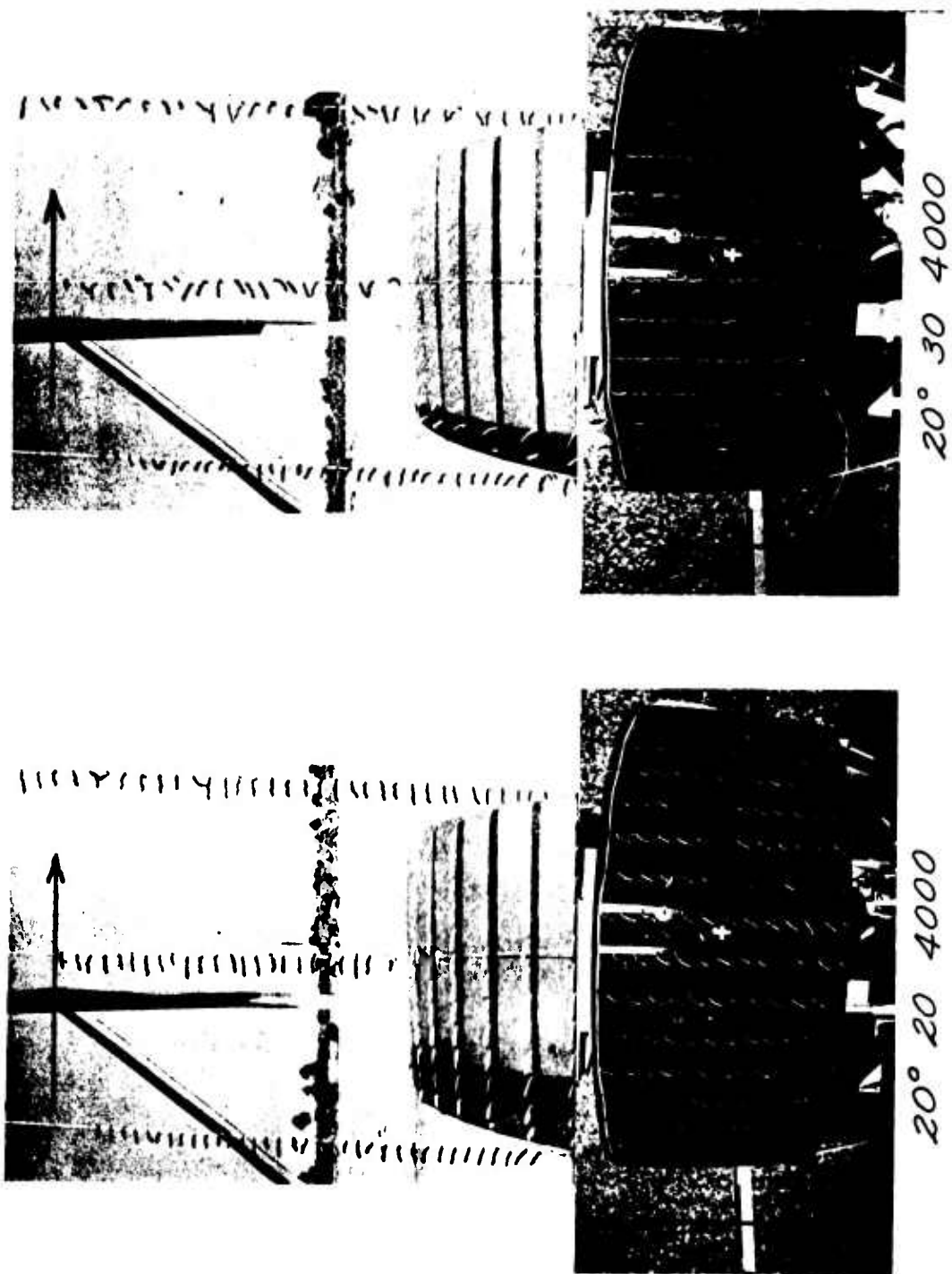


Figure 20 (Cont.). Tuft Patterns - Forward Motion.

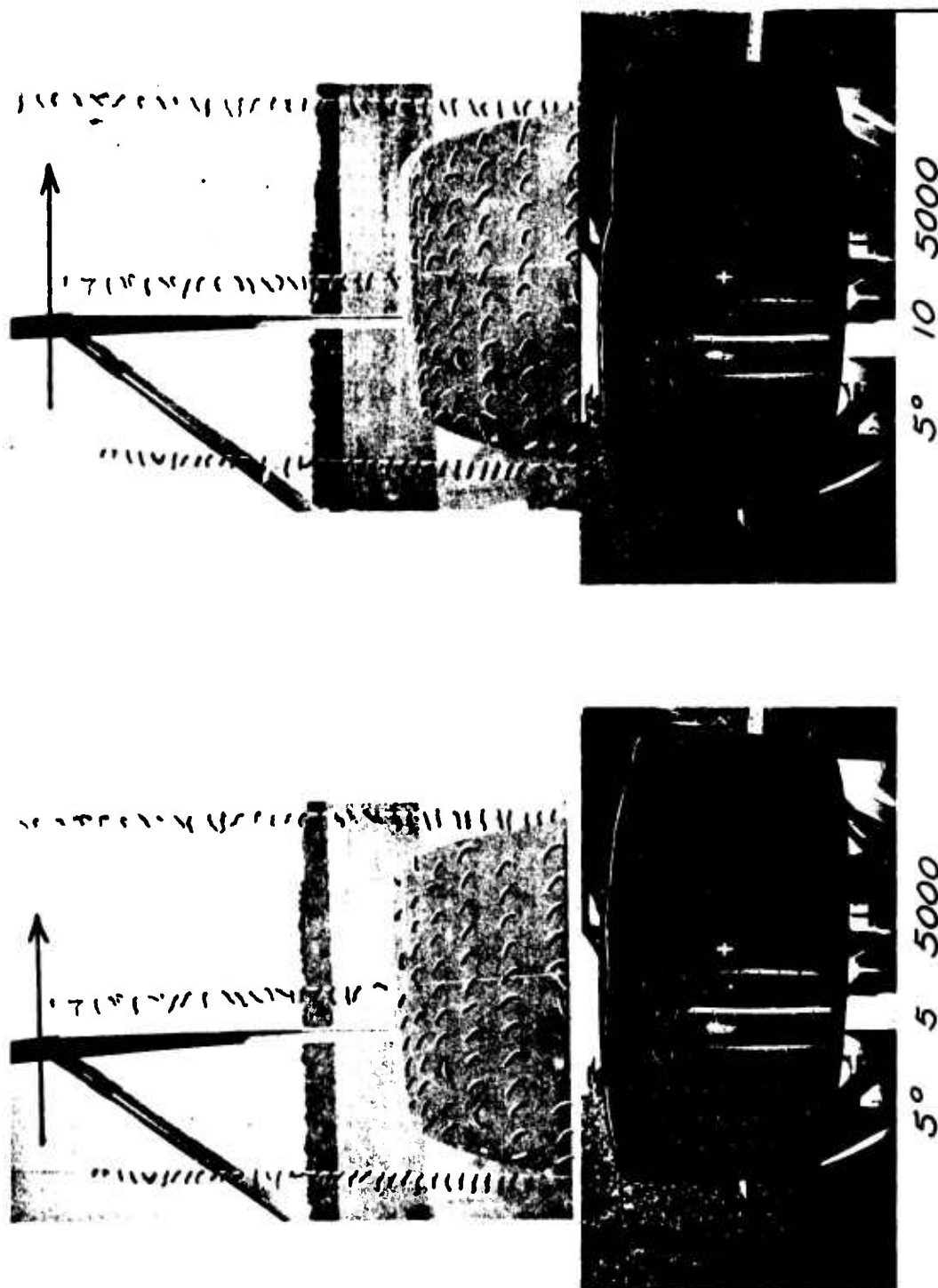


Figure 20 (Cont.). Tuft Patterns - Forward Motion.

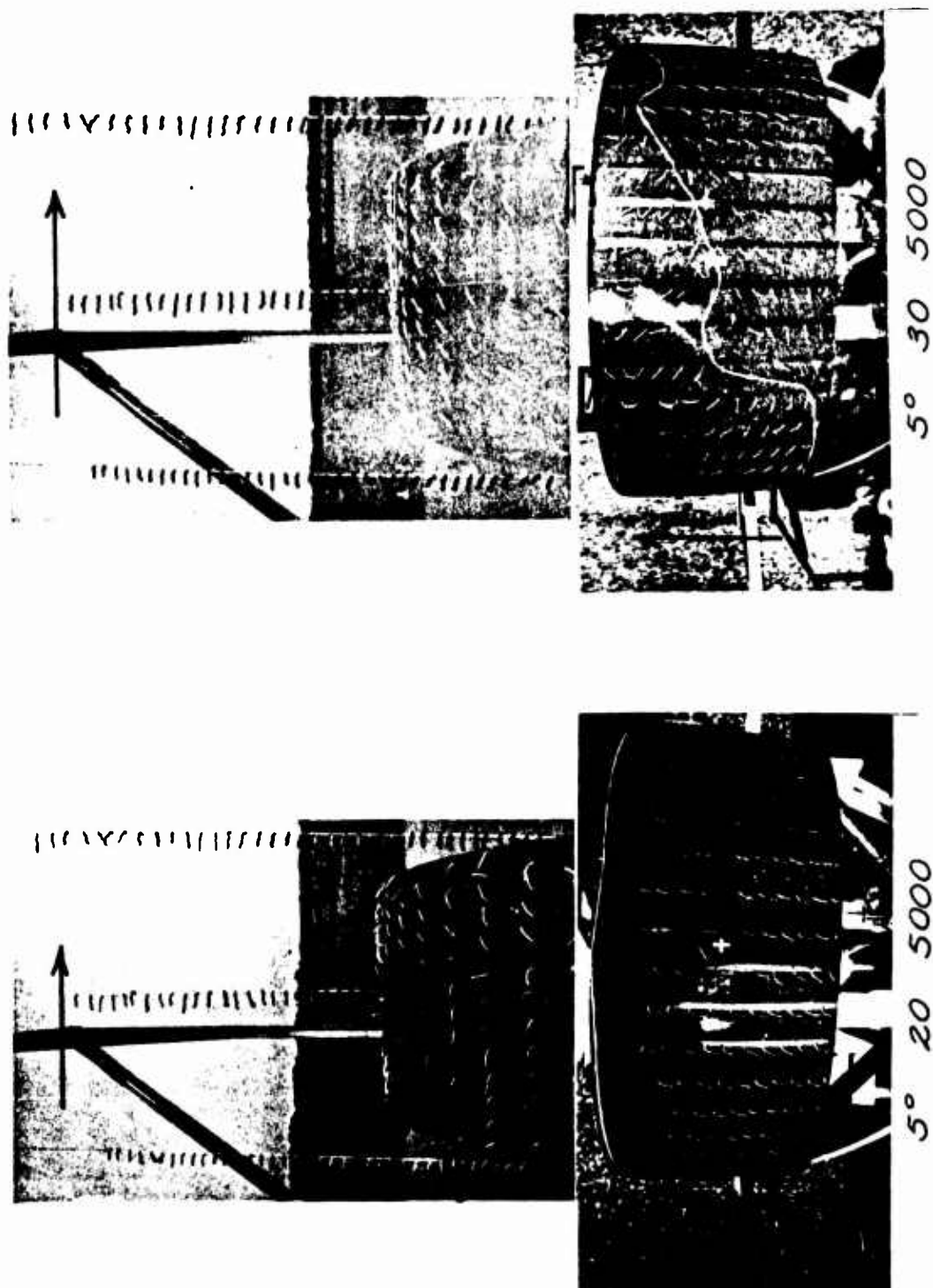


Figure 20 (Cont.). Tuft Patterns - Forward Motion.

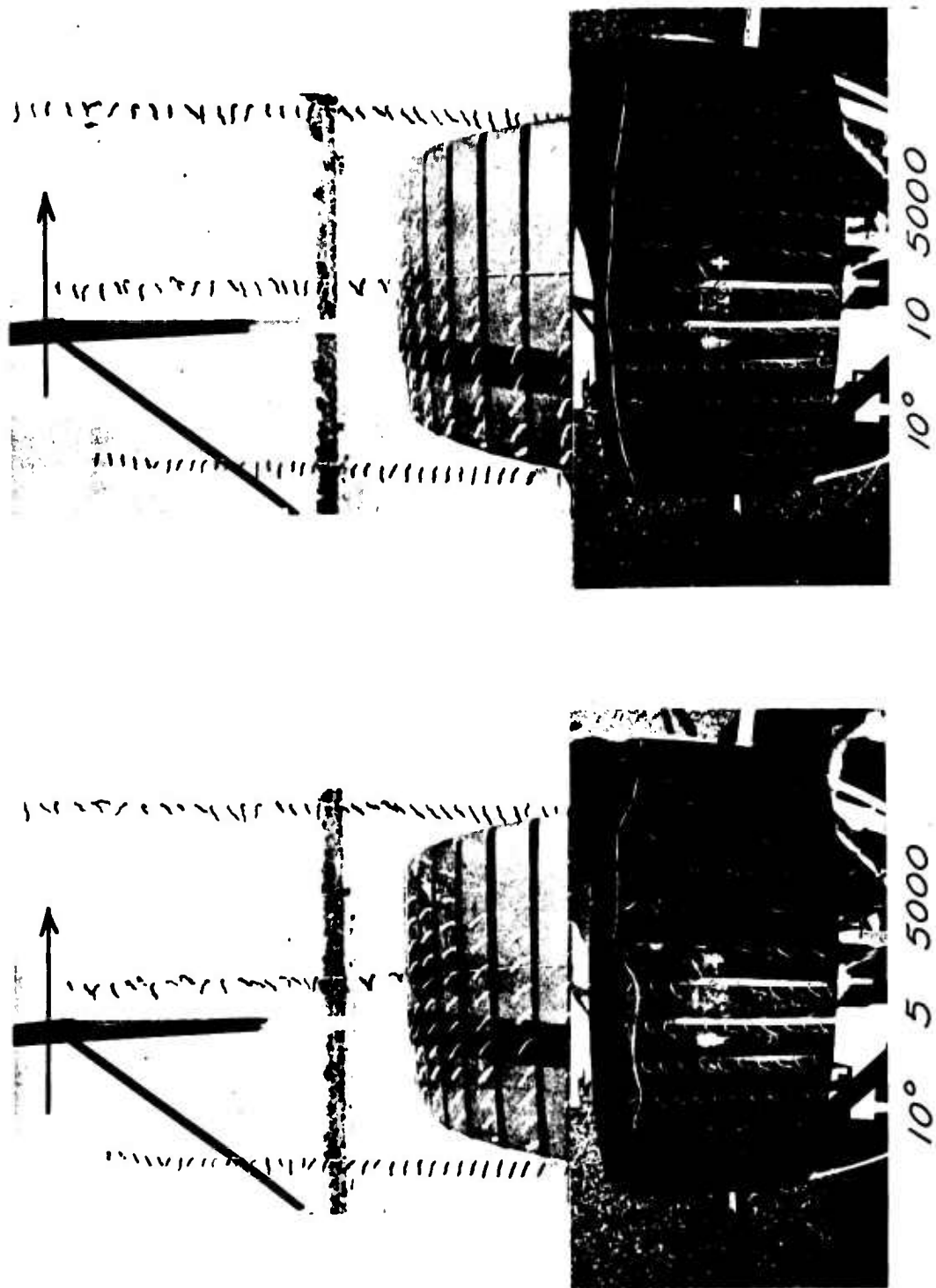
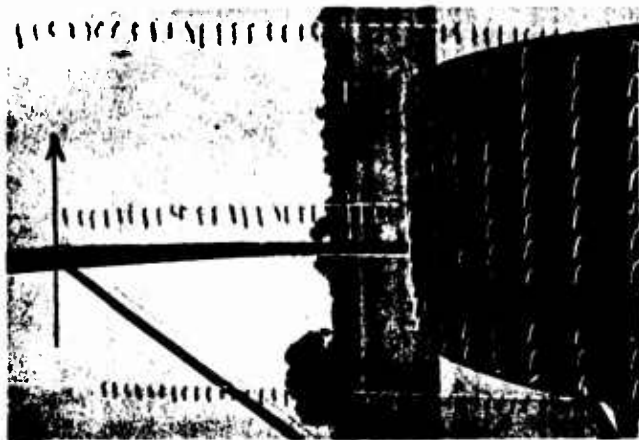
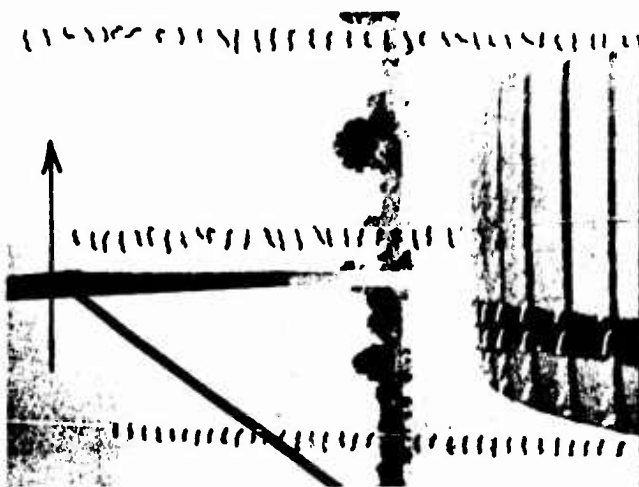


Figure 20 (Cont.). Tuft Patterns - Forward Motion.



10° 30 5000



10° 20 5000

Figure 20 (Cont.). Tuft Patterns - Forward Motion.

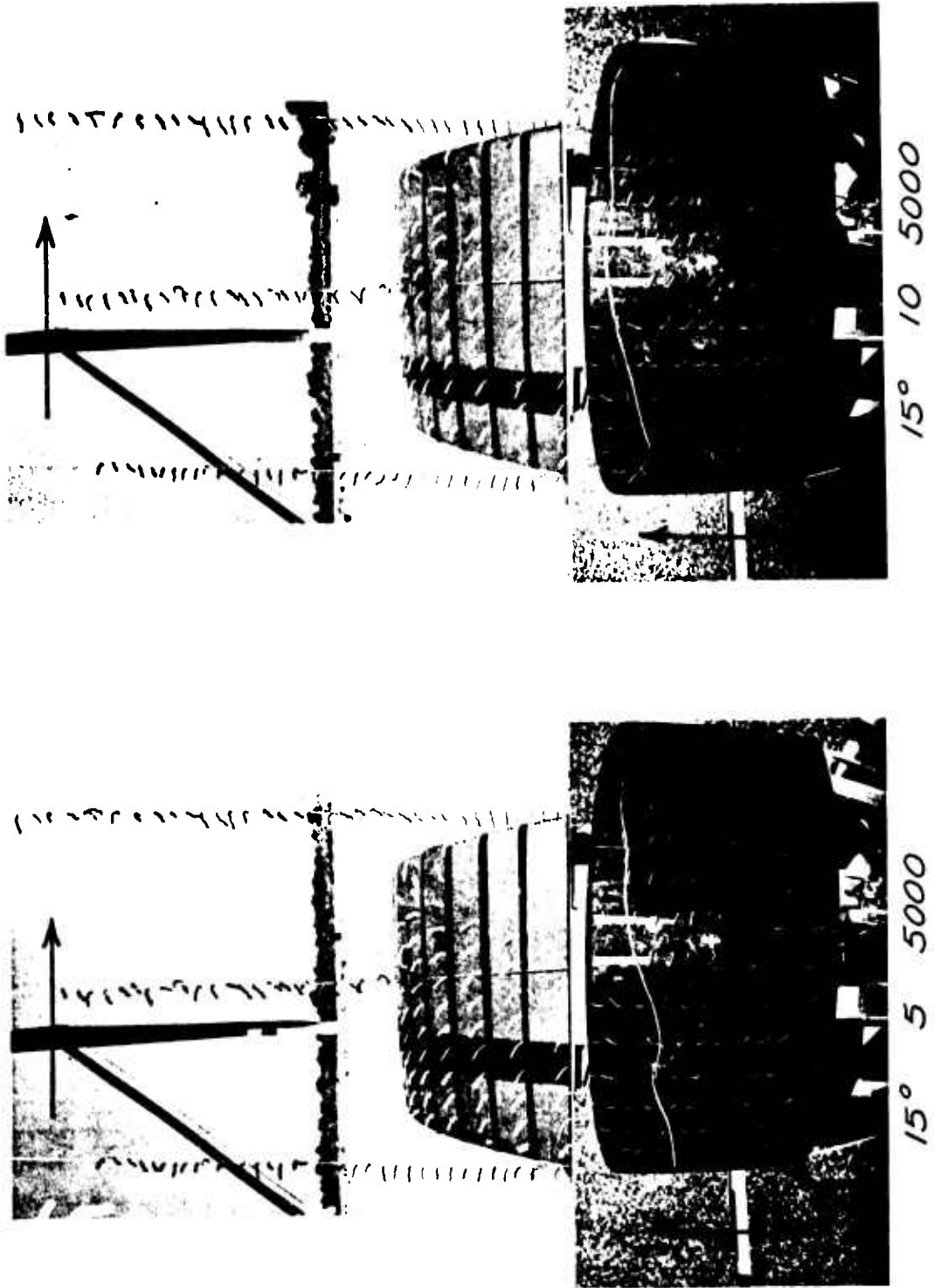


Figure 20 (Cont.). Tuft Patterns - Forward Motion.

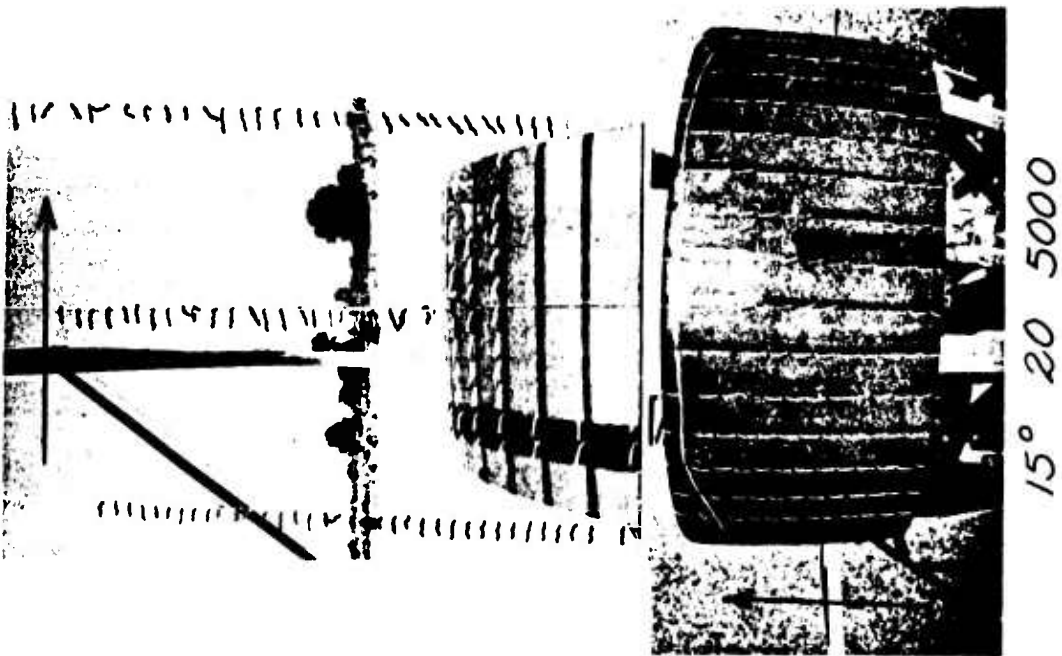


Figure 20 (Cont.). Tuft Patterns - Forward Motion.

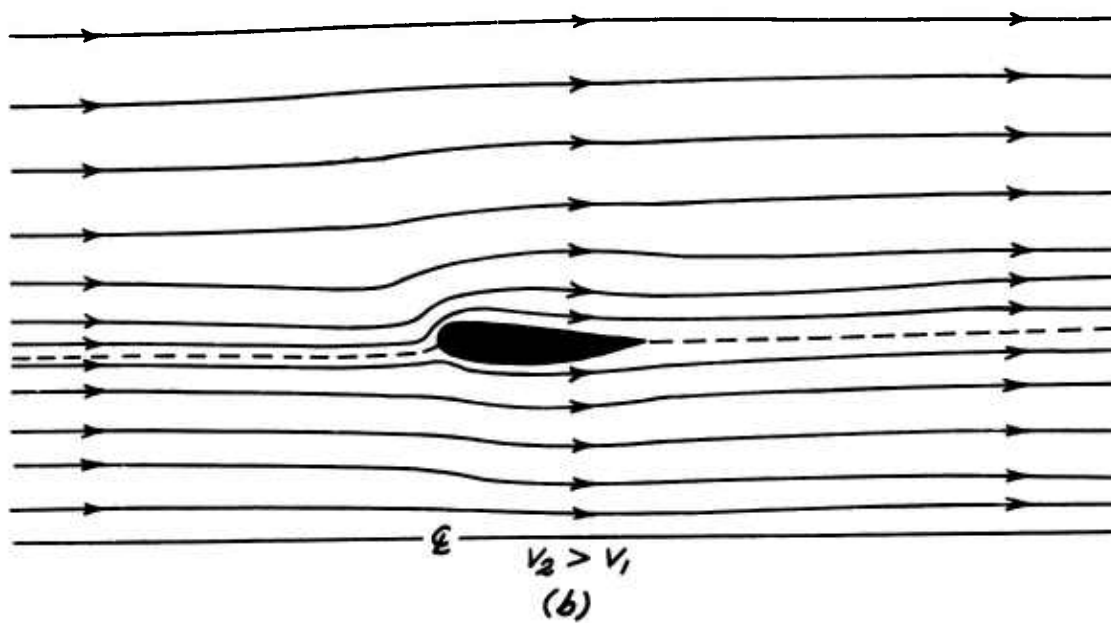
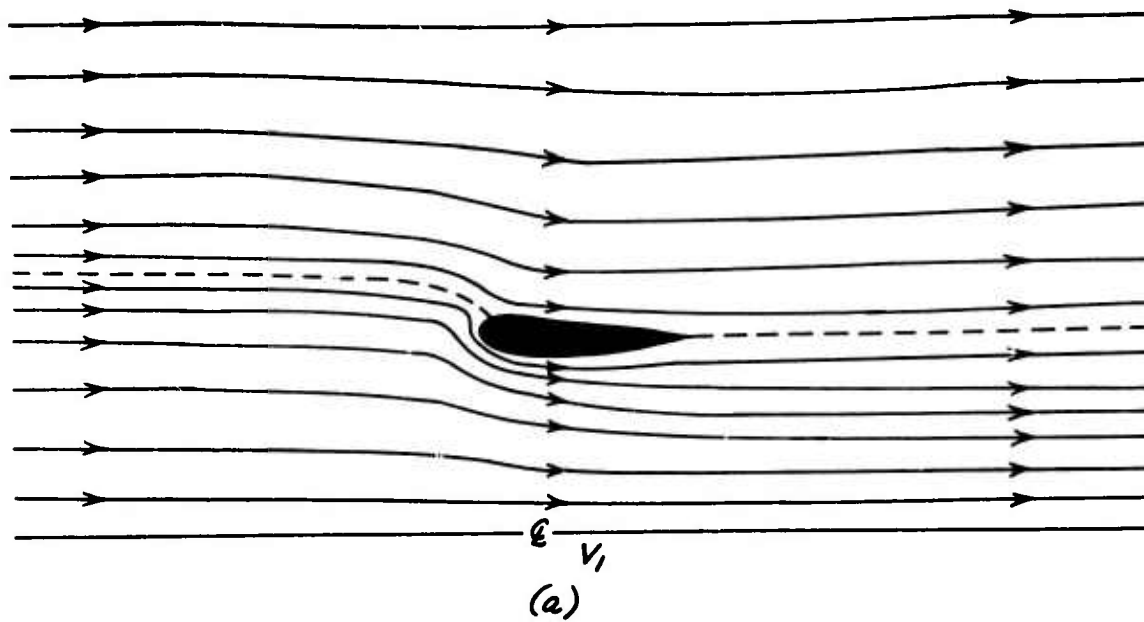


Figure 21. Flow Patterns - Forward Motion.

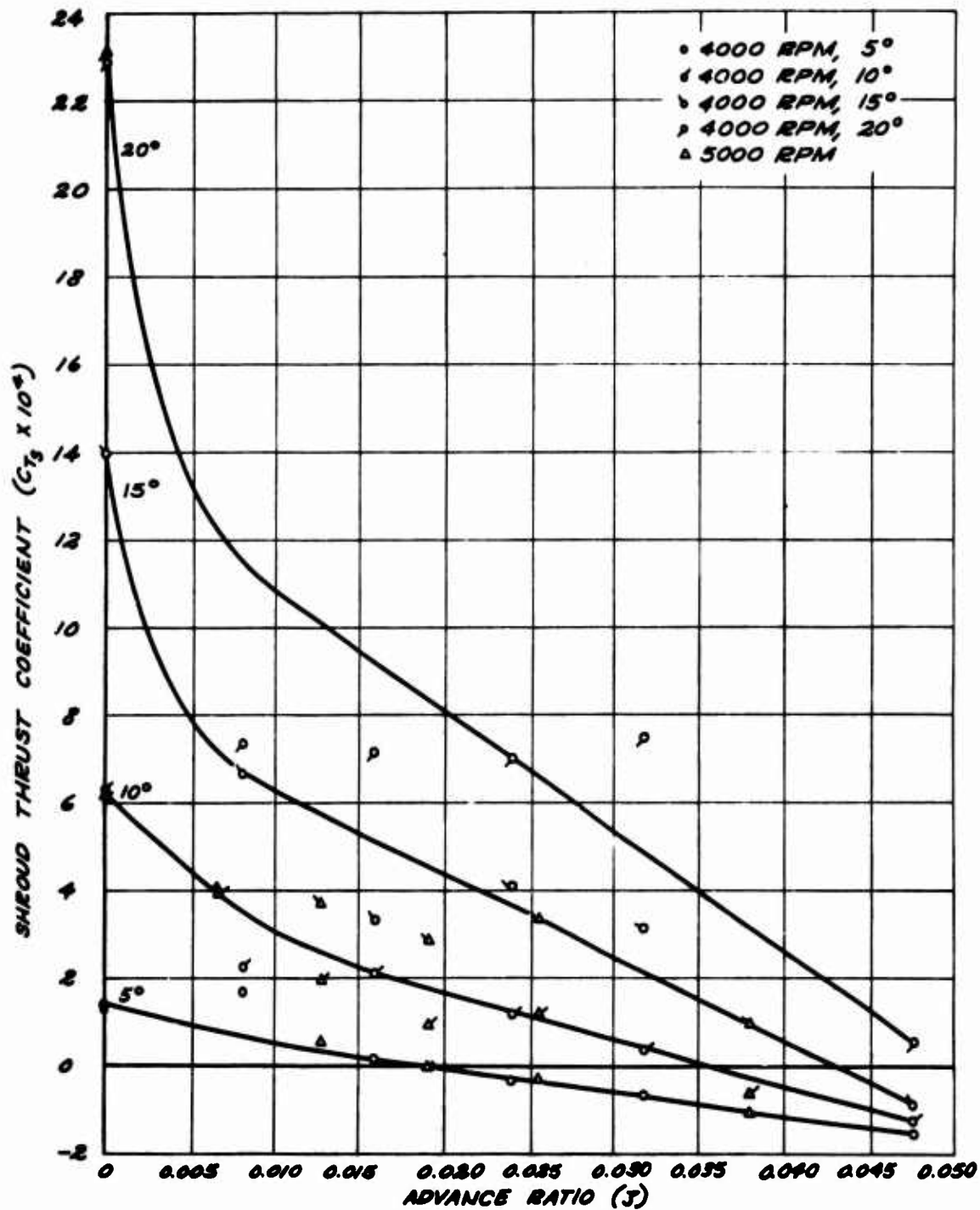


Figure 22. Shroud Thrust - Forward Motion.

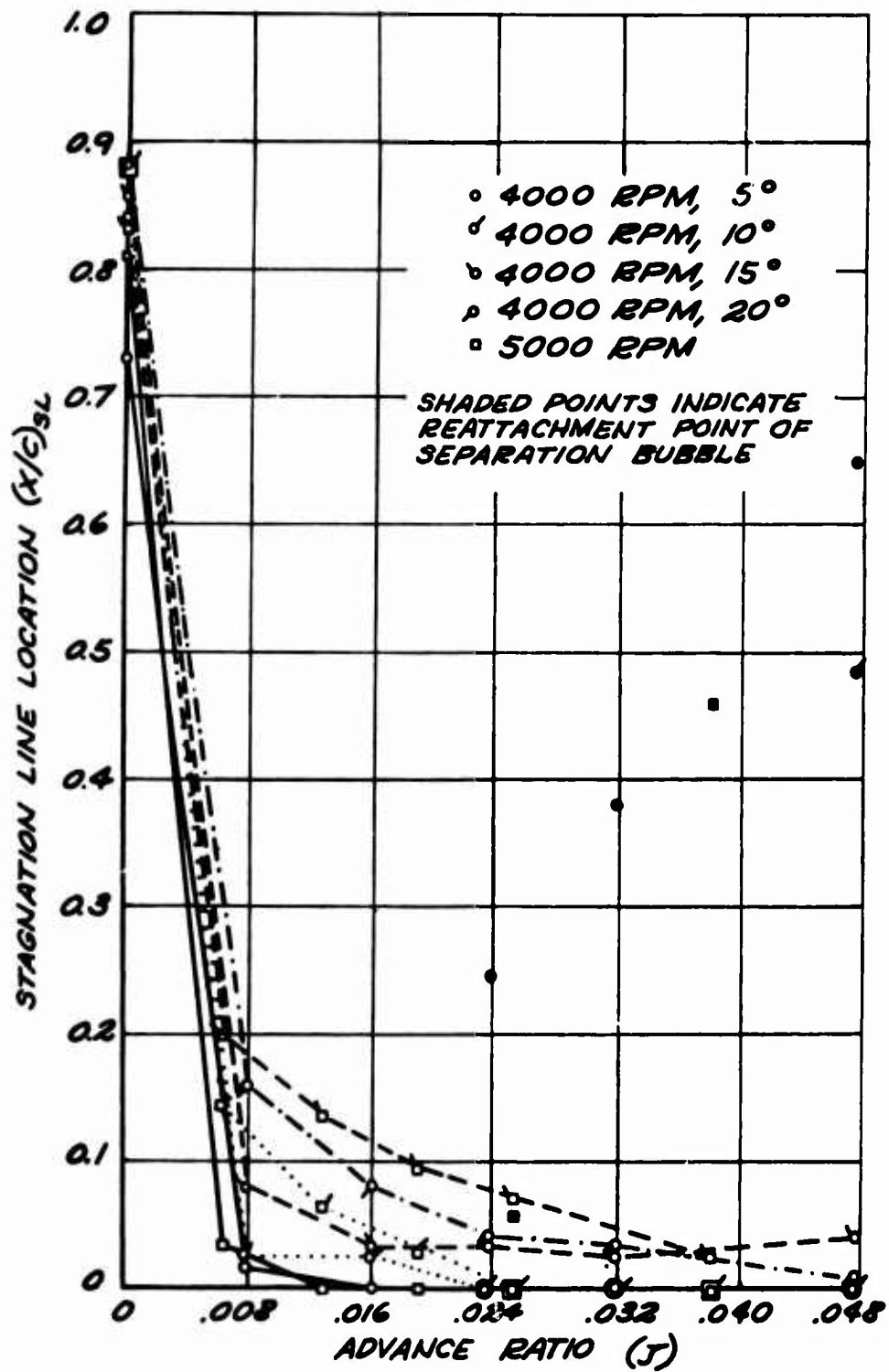


Figure 23. Stagnation Line Location - Forward Motion.

TABLE
PRESSURE DISTRIBUTION TYPES - REARWARD MOTION

5°

Speed MPH RPM	5	10	15	20	25	30
4000	B	B	C	C	C	C
4500	B	B	B		C	C
5000	C	B	B	C	C	C

10°

Speed MPH RPM	5	10	15	20	25	30
4000	A	B	B	B	C	C
4500	A	A	B	B	B	C
5000	A	A	B	B	B	C

15°

Speed MPH RPM	5	10	15	20	25	30
4000	A	A	A	A	B	B
4500		A	A	B	B	B
5000	A	A	A	A	B	A

BIBLIOGRAPHY

1. Greenberg, M. D., and Ordway, D. E., The Ducted Propeller in Static and Low-Speed Flight, TAR-TR 6407, Therm Advanced Research, Inc., Ithaca, New York, October 1964.
2. Kaskel, A. L., Ordway, D. E., Hough, G. R., and Ritter, A., A Detailed Numerical Evaluation of Shroud Performance for Finite Bladed Ducted Propellers, TAR-TR 639, Therm Advanced Research, Inc., Ithaca, New York, December 1963.
3. Ordway, D. E., and Greenberg, M. D., General Harmonic Solutions for the Ducted Propeller, TAR-TR 613, Therm Advanced Research, Inc., Ithaca, New York, August 1961.
4. Ordway, D. E., Sluyter, M. M., and Sonnerup, B. O. U., Three-Dimensional Theory of Ducted Propellers, TAR-TR 602, Therm Advanced Research, Inc., Ithaca, New York, August 1960.
5. Roberts, Seán C., The MARVEL Project, Part C: An Investigation of the Shrouded Propeller Propulsive System on the MARVELETTE Aircraft, Mississippi State University Research Report, TRECOM Technical Report 64-41, U. S. Army Transportation Research Command (now, U. S. Army Aviation Materiel Laboratories), Fort Eustis, Virginia, August 1964.

Unclassified

Security Classification

DOCUMENT CONTROL DATA - R&D		
(Security classification of title, body of abstract and indexing annotation must be entered when the overall report is classified)		
1. ORIGINATING ACTIVITY (Corporate author) Mississippi State University Aerophysics Department State College, Mississippi		2a. REPORT SECURITY CLASSIFICATION Un-Classified
		2b. GROUP
3. REPORT TITLE AN EXPERIMENTAL INVESTIGATION OF THE EFFECT OF FORWARD AND REARWARD MOTION ON THE THRUST OF A SHROUDED PROPELLER		
4. DESCRIPTIVE NOTES (Type of report and inclusive dates)		
5. AUTHOR(S) (Last name, first name, initial) Thompson, Joe F., Jr.		
6. REPORT DATE September 1966	7a. TOTAL NO. OF PAGES 94	7b. NO. OF REFS 5
8a. CONTRACT OR GRANT NO. DA 44-177-AMC-892(T)	9a. ORIGINATOR'S REPORT NUMBER(S) USAAVLABS Technical Report 66-65	
a. PROJECT NO. Task 1P125901A14203	9b. OTHER REPORT NO(S) (Any other numbers that may be assigned this report) Aerophysics Research Report No. 65	
c.		
d.		
10. AVAILABILITY/LIMITATION NOTICES Distribution of this document is unlimited.		
11. SUPPLEMENTARY NOTES		12. SPONSORING MILITARY ACTIVITY U. S. Army Aviation Materiel Laboratories Fort Eustis, Virginia
13. ABSTRACT <p>Experimental evidence of the existence of a stagnation line between the leading and trailing edges of the outer surface of the shroud of a shrouded propeller in the static condition, in rearward motion, and in forward motion is presented. This stagnation line on the outer surface, which is a result of viscous interaction between the propeller slipstream and the external flow, causes a reduction in shroud circulation below that calculated by distributed singularities methods which assume a stagnation line at the trailing edge only. Shroud thrust decreases as the distance between this stagnation line and the trailing edge increases. It is shown that in rearward motion, such as is the case for a VTOL aircraft landing, the stagnation line moves forward from the vicinity of the trailing edge to the vicinity of the leading edge as vehicle speed increases. This forward movement of the stagnation line results in a significant loss in thrust, which can be correlated with the stagnation line location. Shroud pressure distribution, stagnation line location, and shroud thrust are presented for all three cases of motion at several propeller pitch angles, propeller rotational speeds, and vehicle linear speeds. It is shown that the flow pattern about the shroud is rather complicated in rearward motion, involving two coaxial ring-vortices surrounding the shroud.</p>		

DD FORM 1473
1 JAN 64

Unclassified

Security Classification

KEY WORDS	LINK A		LINK B		LINK C	
	ROLE	WT	ROLE	WT	ROLE	WT

INSTRUCTIONS

1. ORIGINATING ACTIVITY: Enter the name and address of the contractor, subcontractor, grantee, Department of Defense activity or other organization (*corporate author*) issuing the report.

2a. REPORT SECURITY CLASSIFICATION: Enter the overall security classification of the report. Indicate whether "Restricted Data" is included. Marking is to be in accordance with appropriate security regulations.

2b. GROUP: Automatic downgrading is specified in DoD Directive 5200.10 and Armed Forces Industrial Manual. Enter the group number. Also, when applicable, show that optional markings have been used for Group 3 and Group 4 as authorized.

3. REPORT TITLE: Enter the complete report title in all capital letters. Titles in all cases should be unclassified. If a meaningful title cannot be selected without classification, show title classification in all capitals in parenthesis immediately following the title.

4. DESCRIPTIVE NOTES: If appropriate, enter the type of report, e.g., interim, progress, summary, annual, or final. Give the inclusive dates when a specific reporting period is covered.

5. AUTHOR(S): Enter the name(s) of author(s) as shown on or in the report. Enter last name, first name, middle initial. If military, show rank and branch of service. The name of the principal author is an absolute minimum requirement.

6. REPORT DATE: Enter the date of the report as day, month, year; or month, year. If more than one date appears on the report, use date of publication.

7a. TOTAL NUMBER OF PAGES: The total page count should follow normal pagination procedures, i.e., enter the number of pages containing information.

7b. NUMBER OF REFERENCES: Enter the total number of references cited in the report.

8a. CONTRACT OR GRANT NUMBER: If appropriate, enter the applicable number of the contract or grant under which the report was written.

8b, 8c, & 8d. PROJECT NUMBER: Enter the appropriate military department identification, such as project number, subproject number, system numbers, task number, etc.

9a. ORIGINATOR'S REPORT NUMBER(S): Enter the official report number by which the document will be identified and controlled by the originating activity. This number must be unique to this report.

9b. OTHER REPORT NUMBER(S): If the report has been assigned any other report numbers (*either by the originator or by the sponsor*), also enter this number(s).

10. AVAILABILITY/LIMITATION NOTICES: Enter any limitations on further dissemination of the report, other than those imposed by security classification, using standard statements such as:

- (1) "Qualified requesters may obtain copies of this report from DDC."
- (2) "Foreign announcement and dissemination of this report by DDC is not authorized."
- (3) "U. S. Government agencies may obtain copies of this report directly from DDC. Other qualified DDC users shall request through _____."
- (4) "U. S. military agencies may obtain copies of this report directly from DDC. Other qualified users shall request through _____."
- (5) "All distribution of this report is controlled. Qualified DDC users shall request through _____."

If the report has been furnished to the Office of Technical Services, Department of Commerce, for sale to the public, indicate this fact and enter the price, if known.

11. SUPPLEMENTARY NOTES: Use for additional explanatory notes.

12. SPONSORING MILITARY ACTIVITY: Enter the name of the departmental project office or laboratory sponsoring (*paying for*) the research and development. Include address.

13. ABSTRACT: Enter an abstract giving a brief and factual summary of the document indicative of the report, even though it may also appear elsewhere in the body of the technical report. If additional space is required, a continuation sheet shall be attached.

It is highly desirable that the abstract of classified reports be unclassified. Each paragraph of the abstract shall end with an indication of the military security classification of the information in the paragraph, represented as (TS), (S), (C), or (U).

There is no limitation on the length of the abstract. However, the suggested length is from 150 to 225 words.

14. KEY WORDS: Key words are technically meaningful terms or short phrases that characterize a report and may be used as index entries for cataloging the report. Key words must be selected so that no security classification is required. Identifiers, such as equipment model designation, trade name, military project code name, geographic location, may be used as key words but will be followed by an indication of technical context. The assignment of links, rules, and weights is optional.